MECHANISMS OF SILENCING THE BREAST TUMOR SUPPRESSOR GENE SINGLE-MINDED 2

A Dissertation

by

TANYA GUSTAFSON

Submitted to the Office of Graduate Studies of
Texas A&M University
in partial fulfillment of the requirements for the degree of

DOCTOR OF PHILOSOPHY

May 2009

Major Subject: Toxicology

MECHANISMS OF SILENCING THE BREAST TUMOR SUPPRESSOR GENE SINGLE-MINDED 2

A Dissertation

by

TANYA GUSTAFSON

Submitted to the Office of Graduate Studies of
Texas A&M University
in partial fulfillment of the requirements for the degree of

DOCTOR OF PHILOSOPHY

Approved by :

Co-Chairs of Committee,	Weston W. Porter
	Keith E. Murphy
Committee Members,	Stephen H. Safe
	Shashi Ramaiah
	Kevin A. Hahn
Chair of Intercollegiate Faculty,	Robert Burghardt

May 2009

Major Subject: Toxicology

ABSTRACT

Mechanisms of Silencing the Breast Tumor Suppressor Gene Single-minded 2.

(May 2009)

Tanya Gustafson, B.A., Tufts University

Co-Chairs of Advisory Committee: Dr. Weston Porter
Dr. Keith Murphy

In order to design patient-tailored medicine and better predict patient response to treatment and outcome, the mechanisms of altered gene expression in cancer cells must be understood. Recently, Single-minded 2 (SIM2) has been shown to be a breast tumor suppressor gene that is down-regulated in approximately 72% of breast cancers, and reintroduction of SIM2 into highly metastatic cancer cells decreases their proliferative rate and their ability to grow on soft agar. SIM2 is a member of the basic helix-loop-helix Per-Arnt-Sim (bHLH/PAS) family of transcription factors, which includes genes responsible for maintenance of circadian rhythms (CLOCK and BMAL) and for sensing hypoxia (HIF-α) and environmental contaminants (AHR). Here we have shown that SIM2 undergoes progressive epigenetic changes that correlate with loss of expression during breast cancer progression in a cell line model. In addition, NFκB, C/EBPβ and the Notch intracellular domain (NICD) act as repressors of SIM2 transcription. Each is able to bind to the SIM2 promoter, demonstrated by chromatin immunoprecipitation assay, with the NICD acting through a novel CBF1-independent mechanism. NFκB is a central mediator of SIM2 regulation as it facilitates repression by C/EBPβ and leads to

deacetylation of histone 3 associated with the SIM2 promoter, contributing to epigenetic changes observed during cancer progression. SIM2, however, also antagonizes NFκB signaling through inhibiting specific NFκB target genes including the ATP-binding cassette transporter, ABCB5, and through direct interaction with NFκB. SIM2, through this antagonism of NFκB, increases cancer cell susceptibility to antineoplastic drugs, including doxorubicin and 5-fluorouracil.

To my husband, Bruce L. Ngo

ACKNOWLEDGEMENTS

I would like to thank my advisor, Dr. Weston Porter, for his support throughout this journey. I would like to thank my committee members, Dr. Stephen Safe, Dr. Shashi Ramaiah, Dr. Kevin Hahn, and a special thanks to Dr. Keith Murphy for encouraging me to apply for the Howard Hughes Medical Institute Predoctoral Fellowship, which supported this research. I also thank Dr. Rick Metz for all his help and patience and Brian Laffin for help with the protein work. Also, thanks go to our collaborators, Dr. Steffi Oesterreich, Dr. Cynthia Zahnow and Drs. Brian and Alana Welm. I would like to send a special thanks to Dr. Yanan Tian and Sui Ke for the NFκB constructs. Last but not least, I would like to thank Keelan Anderson, who gave above and beyond what was expected of her and was a great help to me.

NOMENCLATURE

5-aza-dC	5-aza-2'-deoxcytidine
5-FU	5-fluorouracil
5X NFκB-luc	5 NFκB binding sites upstream of the luciferase gene
ABC	ATP-binding cassette
AcH3	Acetylated histone 3
AP-1	Activator protein-1
AHR	Aryl hydrocarbon receptor
ARNT	Aryl hydrocarbon receptor nuclear translocator
bHLH	Basic helix-loop-helix
CAR	Constitutive active/androstane receptor
CBF1	C-promoter binding factor 1
C/EBPβ	CCAAT/enhancer binding protein, beta
ChIP	Chromatin immunoprecipitation
c-IAP	Cellular inhibitors of apoptosis
CME	Central midline element
CYP	Cytochrome P450
DAPT	N-[N-(3,5-difluorophenacetyl)-l-alanyl]-S-phenylglycine t-butyl ester
DMBA	7,12-dimethylbenz[a]anthracene
DMEM	Dulbecco's modified Eagle's medium

DNMT	DNA methyltransferase
DOX	Doxorubicin
DR5	Death receptor 5
DSL	Delta/Serrate/lag-2
E	Embryonic day
EGF	Epidermal growth factor
EGFR	Epidermal growth factor receptor
ERK1/2	Extracellular signal-regulated kinases 1 and 2
HDAC	Histone deacetylase
HIF-α	Hypoxia-inducible factor, alpha subunit
HP1	Heterochromatin protein 1
HRE	Hypoxia response element
HSP90	Heat shock protein 90
IFNβ	Interferon β
IκB	Inhibitor of kappaB
IκB-SR	Inhibitor of kappaB super-repressor
IKK	Inhibitor of kappaB kinase
LAP	Liver-enriched activating protein
LIP	Liver-enriched inhibiting protein
MAPK	Mitogen-activated protein kinase
MDR1	Multi-drug resistance gene 1
MMTV	Mouse mammary tumor virus

MTT	3-(4,5-dimethylthiazol-2-yl)-2,5-diphenyltetrazolium bromide
NFκB	Nuclear factor-kappaB
NICD	Notch intracellular domain
PAS	Per-Arnt-Sim
PDTC	Pyrollidine dithiocarbamate
PI3K	Phosphatidylinositol 3′-kinase
PLZF-RARα	Promyelocytic leukemia zinc finger-retinoic acid receptor alpha fusion
PML-RARα	Promyelocytic leukemia-retinoic acid receptor alpha fusion
SAHA	Suberoylanilide hydroxamic acid
SIM1	Single-minded 1
SIM2	Single-minded 2
SIM2s	Single-minded 2, short isoform
Su(H)	Suppressor of hairless
TACE	TNFα-converting enzyme
TCDD	2,3,7,8-Tetrachlorodibenzo-*p*-dioxin
TEB	Terminal end buds
TGFα	Transforming growth factor, alpha
TSA	Trichostatin A
XRE	Xenobiotic response element
Zip	Leucine zipper

TABLE OF CONTENTS

CHAPTER Page

CHAPTER Page

LIST OF FIGURES

FIGURE Page

LIST OF TABLES

CHAPTER I

INTRODUCTION

The American Cancer Society estimated 1,399,790 new cancer cases and 564,830 cancer deaths in the United States in 2006. Breast cancer continues to be the second leading cause of cancer-related death in women in the United States despite improvements in early detection and treatment. Most pharmacological approaches for treating cancer are designed to attack the cells after they have become malignant. These treatments carry serious side effects, and many cancer types still recur after treatment. In the mid-1970's, Dr. Mike Sporn and coworkers proposed that intervention via a pharmacological approach, to either inhibit or delay cancer progression, would provide an alternative for treating this disease (1). This concept, termed chemoprevention, focuses on disrupting the step-wise progression of a cell from a normal to an invasive state by blocking the initial stages of cancer formation; however, for this idea to be successful, novel therapeutic approaches and targets are needed. Patient-tailored medicine, or the use of specific treatments based on genetic, genomic and/or proteomic analyses of an individual patient, has the potential to greatly reduce the suffering and mortality associated with breast cancer. The efficacy of such an approach depends upon our understanding of basic mammary gland biology and how these processes are deregulated during tumorigenesis. Recent advances in targeted medicine in breast

---

This dissertation follows the style of Cancer Research.

cancer treatment focus on inhibition of oncogenic signaling and reactivation of tumor suppressor genes (2). Loss of tumor suppressor gene expression occurs through multiple mechanisms including mutations, chromosomal rearrangements, gene deletions, DNA methylation, histone modification and direct transcriptional repression (3-5). With the knowledge of which genes are altered in an individual's cancer, and by what mechanisms, an oncologist can tailor his or her treatment approach to maximize efficacy while decreasing untoward effects.

The bHLH/PAS family of proteins

The bHLH superfamily contains diverse transcriptional regulators that function in gene expression networks in many fundamental biological processes. The basic region functions in DNA binding and the helix-loop-helix motif is a dimerization domain. Both are necessary for the formation of functional DNA binding complexes. bHLH proteins can be divided into three subfamilies: those with the bHLH domain only; those with a bHLH domain contiguous with a leucine zipper (Zip); and those with a bHLH domain contiguous with a Per-Arnt-Sim (PAS) domain (6). Both bHLH and bHLH/Zip families recognize the classic E-box core enhancer sequence CANNTG. The bHLH/PAS family form heterodimers that recognize sequences that diverge from the prototypical E-box, such as xenobiotic response elements (XRE), TNGCGTG, hypoxia response elements (HRE), TACGTGC, and central midline elements (CME), TACGTG (6). The PAS domain, which consists of two adjacent degenerate repeats of approximately 130 amino acids, is important in mediating the specificity of the

dimerization (6). The bHLH/PAS family of transcription factors includes genes responsible for maintaining circadian rhythms (CLOCK and BMAL), and sensing hypoxia (HIF-α) and environmental contaminants (AHR) (6). Activation of signaling occurs when one bHLH/PAS protein is converted into a form that is able to dimerize with another bHLH/PAS protein, namely ARNT. DNA binding and modulation of gene expression via interaction with the transcriptional machinery then occurs (6). The AHR, the most well characterized member of this family, mediates the molecular response to 2,3,7,8-tetrachlorodibenzo-*p*-dioxin (TCDD) and other related halogenated aromatic hydrocarbons, which act as AHR ligands. In the absence of ligand AHR is associated with heat shock protein 90 (HSP90) in the cytoplasm. The AHR binds ligand within its PAS domain, and this leads to translocation of the AHR/HSP90 complex to the nucleus where HSP90 is exchanged for ARNT (6). The AHR/ARNT heterodimer activates transcription from XREs. The HIF-α proteins function similarly but are regulated by oxygen levels. In normoxia, the HIF-α proteins are actively degraded by the ubiquitin-proteasome system. Under hypoxic conditions, the proteins involved in targeting the HIF-α proteins for degradation are inactive, and the HIF-α proteins accumulate. They also dimerize with ARNT in the nucleus and activate gene expression from HREs (6).

The Single-minded proteins

SIM1 and SIM2 are unique members of the bHLH/PAS family because they function as transcriptional repressors (6, 7). They are the mammalian orthologs of the *Drosophila* single-minded (sim) gene, which is a master regulator of central midline

development (8). In *Drosophila* mutations in sim are embryonic lethal, due to fusion of the longitudinal axon bundles and collapse of the axon scaffold (9). Ectopic expression of *Drosophila* sim is sufficient to direct cells of the lateral central nervous system to display central midline cell morphology and gene expression patterns (10). In *Drosophila* the mechanism of sim activity is similar to that of the mammalian AhR. Sim is bound by hsp90 in the cytoplasm, which facilitates its heterodimerization to tango, the *Drosophila* homolog of mammalian Arnt (Figure 1). The sim::tango heterodimer localizes to the nucleus and binds to and activates transcription from CMEs. Target genes, which fail to be expressed in sim mutant embryos in the central midline, include breathless, slit, toll, spitz and engrailed (11). This group of genes, in turn, regulates axon

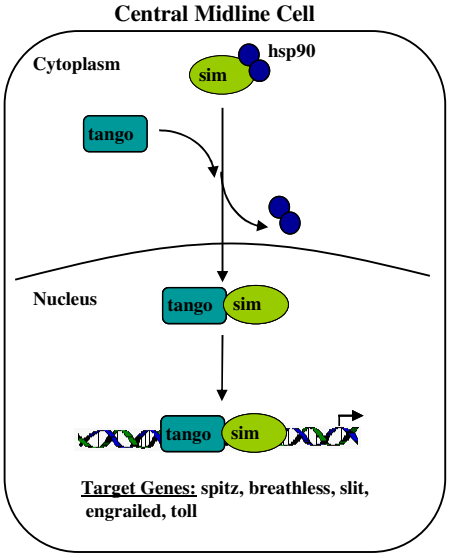

Figure 1
Model of sim activity in *Drosophila* central midline. *Drosophila* sim is bound by hsp90 in the cytoplasm which facilitates its interaction with tango. The sim::tango heterodimer translocates to the nucleus and binds to CMEs to activate transcription of target genes spitz, breathless, slit, engrailed and toll.

growth and midline crossover. For example, mutations in slit result in a phenotype very similar to that of sim mutants, displaying collapse of axon tracts onto the midline. Slit is the ligand for robo, which is a cell surface protein expressed on central nervous system axons (12). Interaction between slit and robo functions to prevent midline crossing in *Drosophila* axons (12). Spitz, a homolog of transforming growth factor, alpha (TGFα), activates the *Drosophila* epidermal growth factor receptor and is required for midline glial survival (13). Through these gene targets, sim functions as the master regulator of central nervous system development in *Drosophila*.

In *Drosophila* sim is regulated by several activating and repressive factors, which localize its expression to a single row of cells. Sim-expressing cells make up the mesectoderm layer, lying between mesoderm and neuroectoderm (Figure 2). In mesectoderm, sim is transcriptionally activated by factors dorsal, twist and notch/suppressor of hairless. In neighboring mesoderm cells, sim is transcriptionally repressed by snail.

Mammalian Sim genes also play a role in development of portions of the central nervous system. Murine Sim1 is necessary for development of the paraventricular and supraoptic nuclei of the hypothalamus, while Sim2 mutants have a normal hypothalamus (14). Sim1 and Sim2 can heterodimerize with Arnt (15), but Sim1 dimerization with Arnt2 is important for development of the hypothalamus (16). SIM2 is located in the Down Syndrome critical region of human chromosome 21 and has been implicated in some of the abnormalities associated with Down Syndrome (17). SIM2 is expressed in human fetal brain regions, which correspond to key regions for cognitive processes.

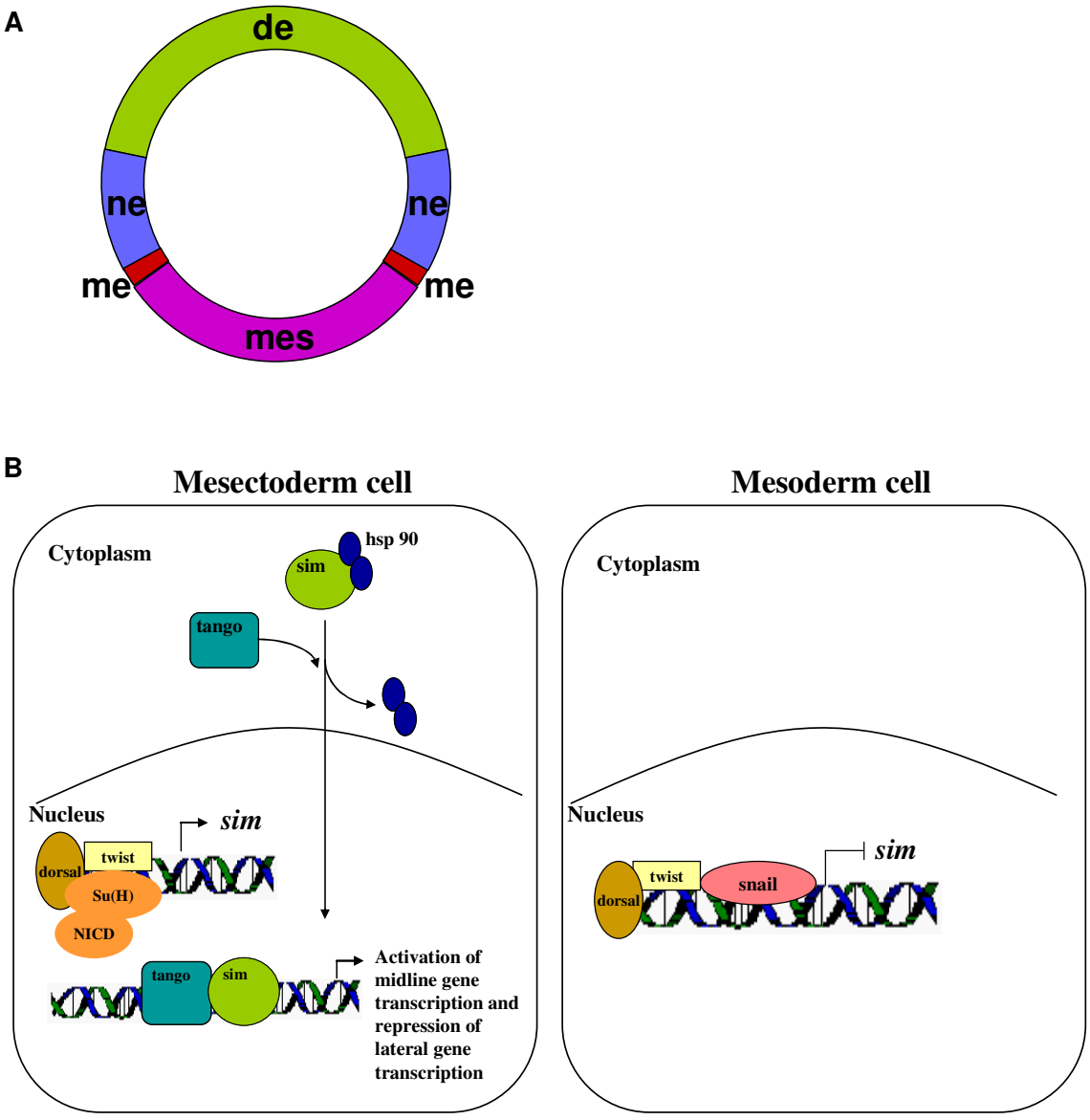

Figure 2
Regulation of sim expression in *Drosophila* embryo. (A) Cross-section of *Drosophila* embryo showing localization of cell layers. de = dorsal ectoderm; ne = neuroectoderm; me = mesectoderm; mes = mesoderm. (B) Regulation of sim in mesectoderm and mesoderm cells. In mesectoderm sim is activated by dorsal, twist and notch. This leads to formation of the sim::tango heterodimer, which leads to activation of midline gene transcription and repression of lateral gene transcription. In neighboring mesoderm cells, snail represses sim transcription.

SIM2 is expressed in pyramidal and granular cell layers of the hippocampus, in cortical cells and in cerebellar external granular and Purkinje cell layers. These SIM2-expressing brain regions correspond to altered structures in Down Syndrome patients (17). Overexpression of Sim2 under the control of the β-actin promoter results in mice with superficially normal skeletal, brain and heart structures, but mild learning and memory deficits, exhibited by a defect in context-dependent fear conditioning and a mild defect in the Morris water maze test, consistent with a role in the pathogenesis of Down Syndrome (18). Murine Sim2 is also expressed in several tissues outside the CNS, including lung, kidney, skeletal muscle, and mammary gland (19). Homozygous deletion of Sim2 results in various defects that cause perinatal lethality. Defects include cleft secondary palate, malformations of the tongue and pterygoid processes of the sphenoid bone, rib protrusions, abnormal intercostal muscle attachments, diaphragm hypoplasia and pleural mesothelium tearing. These abnormalities result in breathing difficulty and death, usually within 3 days of birth (14, 20).

SIM2 short (SIM2s), a splice variant of SIM2 which lacks the carboxyl Pro/Ala-rich repression domain encoded by exon 11, is the predominant form of SIM2 expressed in mammary tissues. In a murine model, the effects of Sim2s on transcriptional regulation through hypoxia, xenobiotic and central midline response elements differ from those of the full length Sim2, although Sim2 and Sim2s both interact with Arnt to mediate their effects (19). Sim2s is less repressive on HREs compared to the full length Sim2 but is equally effective at repression of TCDD-induced gene expression. Additionally, Sim2s is more effective at activating expression from a CME compared to

Table 1
Observed and expected site-specific number of cancer cases among 2814 individuals with Down Syndrome. Individuals with Down Syndrome have an overall low risk of solid tumors and a markedly lower risk of breast cancer (24).

Site	Observed	Expected
Buccal cavity	0	1.04
Digestive system	4	6.52
Respiratory system	1	4.96
Breast	0	7.32
Female genital organs	4	5.68
Male genital organs	4	2.82
Urinary tract	4	2.97
Skin	2	8.14
Other	1	4.75
Secondary sites	3	0.92
Non-Hodgkins lyphoma	0	1.41
Hodgkin's disease	0	0.92
All Solid Tumors	24	47.77

the full length Sim2 (19). SIM2 has also been shown to have tumor suppressor activity in the breast (21). This is consistent with epidemiological data showing women with Down Syndrome have an extremely low risk of breast cancer compared to a matched control group of women (22-24) (Table 1). SIM2 levels are decreased in approximately 72% of breast cancers, and its expression inversely correlates with relative invasiveness of breast cancer derived cell lines (21). Reintroduction of SIM2s into highly metastatic cancer cells decreases their proliferative rate, anchorage-independent growth and invasive potential (21). Matrix metalloprotease-3, a known mediator of breast cancer metastasis, is directly regulated and silenced by SIM2s (21, 25, 26). In order to develop

effective therapeutic strategies targeting tumor suppressor gene inactivation during cancer progression, it is vital that processes leading to aberrant gene silencing are understood. Therefore, understanding mechanisms contributing to SIM2 silencing in breast tissues may provide valuable therapeutic tools to increase survival and reduce morbidity in breast cancer patients.

Mouse models of breast cancer

The mouse is a particularly useful model for mammary gland biology because most development occurs postpartum. The mammary gland develops in well-defined stages: embryonic, prepubertal, pubertal, pregnant, lactating and involuting (27). The gland cycles through the pubertal (virgin), pregnant, lactating and involution stages repeatedly with each successful pregnancy (Figure 3). The gland consists of epithelium derived from ectoderm as well as stroma derived from mesoderm of the embryo (27). In the mouse the first morphological signs of mammary structures are lens-like placodes that form around embryonic day 11 (E11). By E12, these placodes have grown into bulb-shaped buds that invaginate the underlying dermis (28). In the female mouse, at embryonic day 16 (E16), cells begin to proliferate at the tip of the mammary bud, which leads to elongation of the primary duct. It grows towards what will become the mammary fat pad. The duct invades the fat pad at E17 and forms a small ductal tree. Thus, at birth fifteen to twenty branched ducts are present (27). The fat pad differentiates in an independent process, forming immediately around the epithelium. It differentiates from more deeply placed subcutaneous mesenchymal cells. The first

appearance of the fat pad precursor tissue is E14 in mice (27). At the onset of puberty, at approximately 4 weeks of age, terminal end buds (TEB) develop at the ends of ducts in females beginning the ductal phase of mammary development (29). These are sites of intense DNA synthesis that elicits ductal elongation. Ovarian hormones are released during this time, inducing the terminal end buds to grow into the fat pad. This results in a minimally branched mammary ductal "tree" characteristic of the mature virgin gland (27). During pregnancy, lateral buds, which develop along the mature ducts, experience outgrowth along with alveolar buds, resulting in lobuloalveolar structures. This lobuloalveolar development is caused by hormonal stimuli during pregnancy, including elevated estrogen, progesterone and prolactin levels. At weaning the gland undergoes involution, regressing to the virgin state in a process involving apoptosis (27).

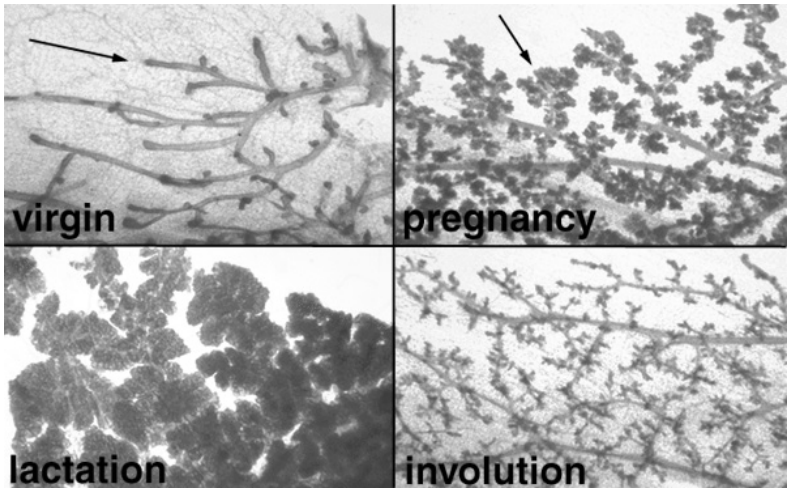

Figure 3
Developmental stages of the mouse mammary gland. Mouse mammary gland goes through virgin, pregnant, lactating and involuting stages repeatedly with each successful pregnancy. Arrows point to a terminal end bud in the virgin gland and a lobuloalveolar unit in the pregnant gland (29).

The development of transgenic mouse models has greatly contributed to our understanding of breast cancer over the past several years. In particular HRAS and c-MYC transgenic mice have provided key insights into multiple mechanisms of mammary tumorigenesis (30). Ras is a small G-protein that links growth factor/receptor interaction to transcription of genes involved in cell cycle progression (Figure 4) (31). For example, epidermal growth factor (EGF) binding to epidermal growth factor receptor (EGFR) causes its dimerization. The intrinsic tyrosine kinase activity of EGFR allows autophosphorylation, which recruits and activates Ras through SH2-domain proteins, which bind phosphorylated tyrosines. Ras activates Raf-1, which, in turn, phosphorylates MEK1/2, which activates extracellular signal-regulated kinases 1 and 2 (ERK1/2) (31). ERK1/2 regulates transcription factors c-MYC, c-FOS, c-JUN and C/EBPβ through phosphorylation (32). c-MYC dimerizes with MAX to regulate target genes which promote cell cycle progression, including cyclin D1 and cyclin D2 (33). Activator protein-1 (AP-1) is a ubiquitous transcription factor formed by Fos and Jun family members (31).

The oncogenic potential of Ras signaling was identified through recognition of the Harvey and Kirsten murine sarcoma virus oncogenes. In addition, an early model of mammary tumorigenesis through the use of the chemical carcinogen 7,12-dimethyl-benz[a]anthracene (DMBA) results in a high rate of mutations in Hras (31). In human cancer, HRAS is mutated in up to 20% of total cases. Although mutations in HRAS are rare in breast cancers (34), HRAS is significantly activated in approximately 50% of breast tumors (35). HRAS plays an important role in HER2-overexpressing breast

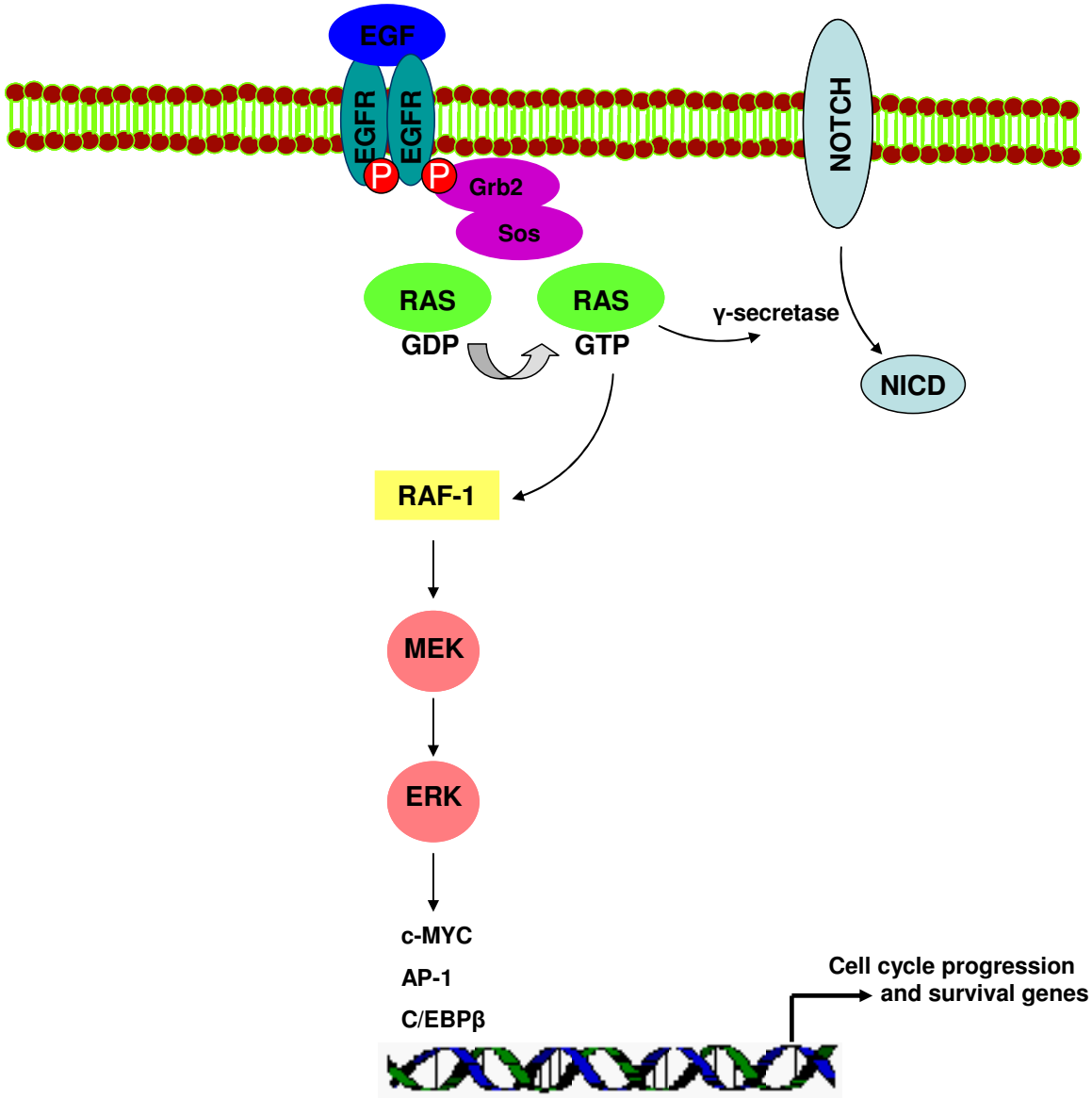

Figure 4
Ras signaling pathway. Growth factor binds to receptor tyrosine kinase, which autophosphorylates. Phosphorylated tyrosines are recognized by SH2-domain proteins and recruit Ras, which exchanges GDP for GTP. Ras-GTP leads to a kinase signaling cascade. This results in activation of transcription factors, including c-MYC, AP-1 and C/EBPβ, which contributes to cell cycle progression and survival. Activated Ras also enhances γ-secretase activity, leading to increased activated Notch.

cancers, which represents 30% of cases (36). HER2 is a member of the epidermal growth factor receptor family. It heterodimerizes with other family members, including EGFR, to initiate Ras signaling. HRAS-induced tumors are characterized by activation of mitogen-activated protein kinase (MAPK) signaling and are cyclin D1-dependent (37, 38). By activating potent oncogenic pathways, HRAS overexpression, driven by the MMTV promoter, can induce mammary tumors in mice in as little as 5 weeks of age (39, 40). These tumors are estrogen receptor negative and can be histologically classified as papillary transitional cell carcinomas (Figure 5A) (29). Metastasis to the lungs is common (41). The transforming potential of c-MYC was first identified in humans through Burkitt's lymphoma, in which the causative mutation in 90% of cases is a reciprocal translocation that moves c-MYC from chromosome 8 to a position close to the enhancers of the antibody heavy chain genes on chromosome 14 (31). c-MYC contributes to normal mammary gland development (42) and is amplified in 15-20% and overexpressed in approximately 70% of breast cancers (43). c-MYC overexpression, driven by the MMTV promoter, causes spontaneous mammary adenocarcinomas in mice that have a longer latency compared to HRAS tumors, occurring within 4 to 8 months (30). These tumors are also estrogen receptor negative, as are most transgenic mouse models of breast cancer, excluding the p53 knockout model (41). c-MYC tumors are acinar adenocarcinomas and also produce metastases to the lungs (Figure 5B) (29). Interestingly, c-MYC is the most dominant transgene; combination of c-MYC and HRAS, or any transgene or knockout, results in tumors with the c-MYC phenotype (41). Doxycycline-inducible systems have demonstrated that HRAS- and c-MYC-induced

tumors can remain dependent on oncogene expression for growth. However, some tumors fail to regress after doxycycline withdrawal or recur after a variable period of latency, indicating changes have occurred in the cell that have not reversed (44, 45).

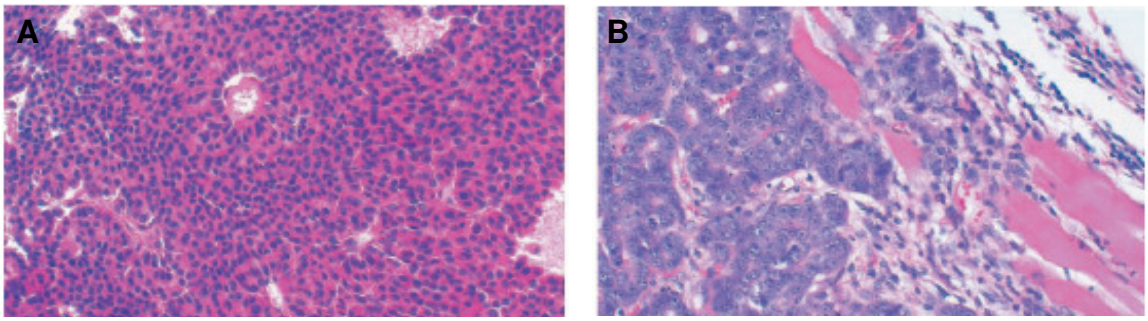

Figure 5
Histology of HRAS and c-MYC transgenic mouse mammary tumors. (A) HRAS-induced tumors are papillary transitional cell carcinomas, organized around blood vessels. (B) c-MYC-induced tumors are acinar adenocarcinomas that retain a more glandular structure (29).

Notch and C/EBPβ, effectors of Ras signaling

Notch and C/EBPβ have recently been shown to be activated by Ras signaling and to be critical for Ras-mediated tumorigenesis (46, 47). Canonical Notch signaling is initiated by interaction of the Notch transmembrane receptor with Delta/Serrate/lag-2 (DSL) transmembrane ligands on neighboring cells (Figure 6). Notch is first cleaved by TNFα-converting enzyme (TACE) in the extracellular domain. The transmembrane domain is then cleaved by γ-secretase activity of a multiprotein complex including Presenilins, Nicastrin, APH-1 and PEN-2, releasing the active intracellular domain

(NICD). The NICD then translocates to the nucleus and interacts with CSL transcription factors (CBF1 in humans), displacing corepressors and recruiting coactivators. Thus, target genes in the Hairy/Enhancer of Split family, including HES1, HEY1 and HEY2, are activated (48).

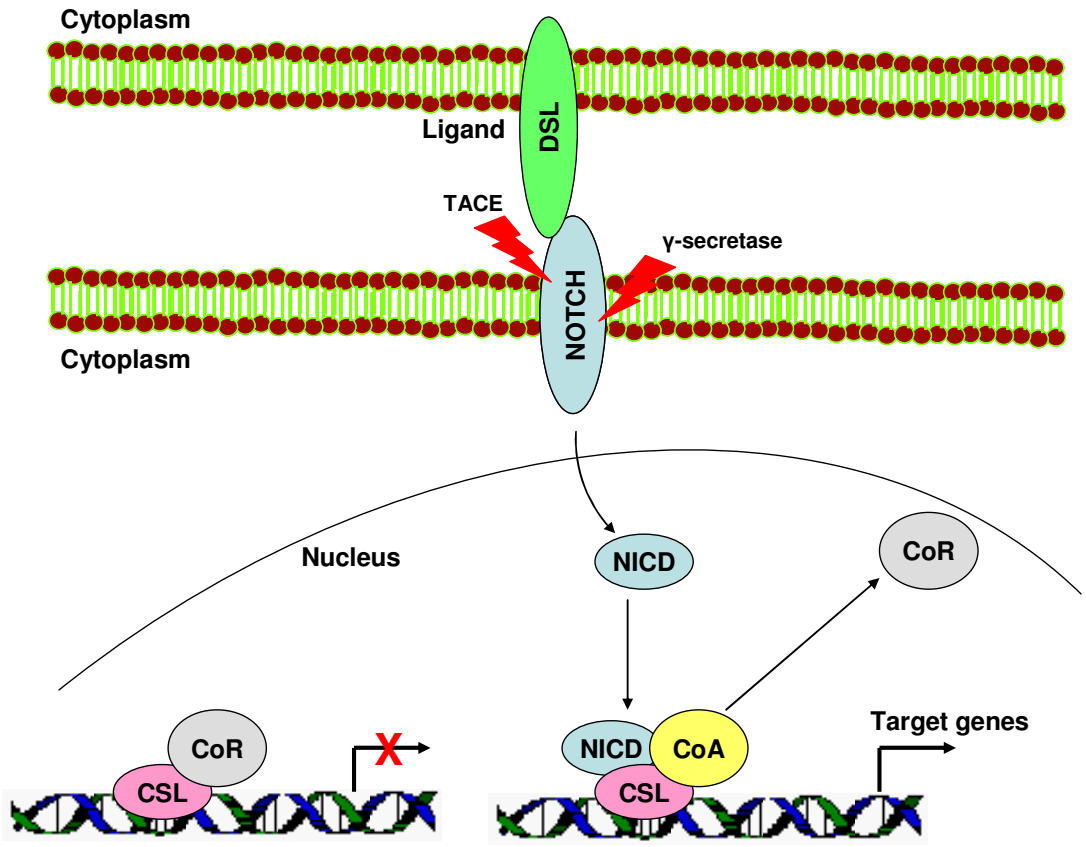

Figure 6
Notch pathway. Canonical Notch signaling is initiated by interaction of the Notch transmembrane receptor with Delta/Serrate/lag-2 (DSL) transmembrane ligands on neighboring cells. Notch is first cleaved by TACE in the extracellular domain. The transmembrane domain is then cleaved by γ-secretase activity of a multiprotein complex including Presenilins, Nicastrin, APH-1 and PEN-2, releasing the active intracellular domain (NICD). The NICD then translocates to the nucleus and interacts with CSL transcription factors (CBF1 in humans), displacing corepressors and recruiting coactivators. Thus, target genes in the Hairy/Enhancer of Split family, including HES1, HEY1 and HEY2, are activated.

However, the NICD has been shown to interact with other transcription factors including MEF2C (49), NFκB (50) and HIF-1α (51), and there is significant evidence for the importance of CBF1-independent Notch function for maintaining cell fate (52). Notch was first identified as an oncogene through studies involving MMTV. The mouse Notch homolog, Int-3, is a common integration site for MMTV that leads to mammary tumorigenesis (53). A translocation placing a truncated, activated form of NOTCH1 under control of the T-cell receptor-beta locus is responsible for approximately 1% of human T-cell acute lymphoblastic leukemia cases; however, activating mutations in NOTCH1 are present in up to 50% of cases (54). Increased Notch signaling has also been demonstrated in a variety of human breast carcinomas (55). However, Notch plays the opposite role in keratinocytes as a tumor suppressor by promoting differentiation. In a mouse model, loss of Notch1 results in a substantially increased susceptibility to skin tumors induced by the carcinogen DMBA (56). HRAS activates Notch signaling by increasing γ-secretase activity (Figure 4), which is required to maintain the transformed phenotype in human fibroblast cells (46), and Hras-mediated oncogenesis in mouse mammary glands is inhibited by introduction of the Notch antagonist Deltex (57). Recently, Notch has been shown to contribute to cancer cell survival by inhibiting p53 activity, and there is an ongoing effort to identify other tumor suppressor genes targeted for inactivation by Notch signaling (58).

C/EBPβ is overexpressed in breast, ovarian and colorectal tumors (59). A single intronless C/EBPβ mRNA can produce three different proteins: full length liver-enriched activating protein 1 (LAP1), liver-enriched activating protein 2 (LAP2) and the

dominant negative liver-enriched inhibiting protein (LIP). Alternative translation or cleavage events can lead to production of these alternate isoforms in the cell. The full length isoform, translated from the first AUG, contains three N-terminal transactivation domains and two regulatory domains, which interact with the transactivation and DNA-binding domains to inhibit their activities. LAP2, translated from the second AUG, lacks the first 23 N-terminal amino acids but contains intact transactivation domains (59). This difference between LAP1 and LAP2 allows LAP1 but not LAP2 to interact with the SWI/SNF chromatin remodeling complex to mediate activation of certain myeloid genes in cooperation with Myb (60). The LIP isoform is translated from the third AUG and lacks the N-terminal transactivation domains. In neonatal liver, LIP can be generated through cleavage of LAP1 by calpain-type proteases activated by C/EBPα (59). In the liver, the LAP isoforms function primarily as a transcriptional activators, and LIP functions as an antagonist of LAP activity by competing for DNA binding sites as a homodimer or a LAP/LIP heterodimer (61). C/ebpβ$^{-/-}$ mice are viable but display immune system defects, abnormal brown adipose tissue function, skin irregularities and female infertility (59). Lack of C/ebpβ in the mammary gland leads to impaired ductal morphogenesis, resulting in enlarged ducts with decreased branching (62). C/EBPβ plays an important role in the early immune response by inducing expression of acute phase proteins, like serum amyloid A, in response to stimulation of cells by specific interleukins, in conjunction with NFκB (63). C/EBPβ also regulates the early steps of adipocyte differentiation and is a key inducer of PPARγ, which is the central coordinator of the adipogenesis process (64). The role of C/EBPβ in the mammary gland is less

well-defined but seems to be involved in the proliferation of the gland during pregnancy, as that is when it is most highly expressed (61). Also, C/EBPβ regulates expression of beta-casein, an important protein in milk (65). Both LAP2 and LIP isoforms have been shown to be involved in transformation of mammary epithelial cells (66, 67). Overexpression of LAP2 has been shown to confer anchorage-independent growth and invasiveness on MCF10A cells in culture (66), and overexpression of LIP in mammary glands of transgenic mice causes increased mammary intraepithelial neoplasias and carcinomas (67). C/ebpβ was also identified as an important mediator of Ras-induced tumorigenesis in a mouse skin carcinogenesis model known to cause Hras mutations. In these studies, C/ebpβ$^{-/-}$ mice were completely protected from tumorigenesis following 7,12-dimethylbenz[a]anthracene and 12-O-tetradecanoylphorbol 13-acetate treatments (47). Ras-initiated MAPK activity leads to phosphorylation of C/EBPβ on threonine-235, which contributes to its activation (68). C/EBPβ also has been shown to cooperate with Cyclin D1 to mediate oncogenesis (69). Both Notch and C/EBPβ pathways, therefore, represent significant mediators of mammary tumorigenesis induced by activation of Ras.

Epigenetic gene regulation in cancer

Epigenetic gene regulation is another crucial mechanism in cancer development (70). CpG islands are genomic regions about one kilobase in length that have a high GC content, are rich in CpG dinucleotides and are normally hypomethylated (71). The 5-methylation of cytosines within CpG islands in gene promoters is associated with gene

silencing and can promote cancer by inactivating tumor suppressor genes (72). In contrast, pericentromeric DNA is compacted into heterochromatin and normally contains methylated CpG dinucleotides. Cancer cell genomes are relatively hypomethylated relative to normal cells, especially in repetitive regions. It is thought that loss of methylation at pericentromeric regions contributes to the genomic instability phenotype of tumor cells (71). Three functional DNA methyltransferases have been identified in mammals: DNMT1, DNMT3A, and DNMT3B (73). DNMT1 is a maintenance methylase with high affinity for hemimethylated DNA. DNMT3A and DNMT3B are responsible for *de novo* methylation. DNMT1 is expressed in proliferating cells, with different somatic and oocyte protein isoforms. DNMT3A and DNMT3B are highly expressed in embryonic stem cells but are expressed at low levels in normal adult somatic cells (73). DNMT1 and DNMT3B have been shown to be overexpressed in breast cancer at the protein and mRNA levels, respectively, and contribute to hypermethylation of tumor suppressor gene promoters (74, 75). The pathways of methylation differ between these two genes, as DNMT1 is associated with global hypermethylation, whereas DNMT3B is targeted to fewer CpG's, suggested by antisense depletion studies (76).

Posttranslational modification of histone proteins, the building blocks that package DNA into repeated nucleosomes, affects both chromatin folding and association with non-histone regulatory proteins (77). Increased histone acetylation is associated with gene activation, whereas histone deacetylation represses gene transcription. Histones have also been shown to be methylated (on arginines and lysines),

phosphorylated (on threonines and serines), ubiquitinated (on lysines), sumoylated (on lysines), ADP ribosylated (on glutamates) and deiminated (on arginines), within their N-terminal tails (78). Each of these modifications contributes to regulation of transcription by affecting contact between histones in adjacent nucleosomes and between histones and DNA (Table 2) (78, 79). For example, dimethylation of lysine 9 of histone 3 is catalyzed by the histone methyltransferase Suv39h at silent gene promoters. This modified residue is recognized by heterochromatin protein 1 (HP1), which condenses the chromatin through internucleosome dimerization (80).

Table 2
Classes of modifications identified on histones. Histones are modified at specific residues within their N-terminal tails. Each of the modifications contributes to the regulation of transcription by affecting contact between histones in adjacent nucleosomes and between histones and DNA (78,79).

Chromatin Modifications	Residues Modified	Effect on Transcription
Acetylation (lysines)	H3 (9, 14, 18, 56), H4 (5, 8, 13, 16), H2A, H2B	Activation
Methylation (lysines)	H3 (4, 36, 79) H3 (9, 27), H4 (20)	Activation Repression
Methylation (arginines)	H3 (17, 23), H4 (3)	Activation
Phosphorylation (serines/threonines)	H3 (3, 10, 28), H2A, H2B	Activation
Ubiquitylation (lysines)	H2B (120) H2A (119)	Activation Repression
Sumoylation (lysines)	H2A (126), H2B (6/7)	Repression
ADP ribosylation (glutamates)	H2B (2)	Undefined
Deimination (arginines to citrullines)	H3, H4	Repression
Proline Isomerization (cis to trans)	H3 (30-38)	Activation or Repression

Mammalian histone deacetylases (HDACs) can be classified into three classes based on their homology to yeast proteins: class I consists of HDAC 1, 2, 3 and 8 which are homologous to yeast Rpd3 deacetylase; class II consists of HDAC 4-7 and 9-11 which are homologous to yeast Hda1 deacetylase; and class III consists of SIRT 1-7 which are homologous to yeast Sirt2 family (81). These enzymes deacetylate specific residues in the N-terminal tails of histones as well as in other promoter-bound transcription factors. The most direct evidence for the role of HDAC activity in cancer comes from acute promyelocytic leukemias caused by promyelocytic leukemia-retinoic acid receptor alpha (PML-RARα) or promyelocytic leukemia zinc finger (PLZF)-RARα fusions. The PML or PLZF portion of the fusion recruits HDACs, which the RARα targets to retinoic acid-inducible genes, resulting in repression of transcription and lack of differentiation (82). HDAC inhibitors can induce differentiation of tumor cells, cause cell cycle arrest, initiate apoptosis and enhance tumor sensitivity to other chemo- and radiotherapy, and many inhibitors are currently undergoing extensive clinical trials with some success in cancer treatment (Table 3) (81, 83). For example, suberoylanilide hydroxamic acid (SAHA) was approved for phase II and phase III clinical trials for the treatment of hematological malignancies. Clinical trials with trichostatin A (TSA) have been suspended, however, due to excessive cardiotoxicity and instability *in vivo* (81).

Epigenetic events occur during all stages of tumorigenesis and represent an alternative to deletions or mutations for inactivating tumor suppressor genes (70). The tumor suppressors CDH1 and $p16^{INK4a}$ have been shown to be epigenetically silenced in cancer. Loss of E-cadherin is associated with an epithelial-mesenchymal transition,

Table 3
Natural and synthetic HDAC inhibitors. Many classes of HDAC inhibitors have been identified (81). Some of these are undergoing clinical trials for the treatment of cancer in humans, with some success (83).

GROUP	EXAMPLE	CLINICAL TRIALS
Hydroxamic acid-derived compounds	Trichostatin A (TSA)	Discontinued due to cardiotoxicity and instability *in vivo*
	Suberoylanilide hydroxamic acid (SAHA)	Phase II and Phase III ongoing
	Azelaic bis-hydroxamic acid (ABHA)	None
	Pyroxamide	Phase I completed
Cyclic tetrapeptides	Depsipeptide (FK228, FR901228)	Phase I and Phase II ongoing
	Trapoxin A	None
Short-chain fatty acids	Valproic acid	Phase I and Phase II ongoing
	Butyrate	Phase I completed
Synthetic pyridyl carbamate derivative	MS-275	Phase I and Phase II ongoing
Synthetic benzamide derivatives	CI-994 (N-acetyldinaline)	Phase II ongoing
Ketones	Trifluoromethyl ketone	None

which is a more invasive phenotype (84). Loss of p16 is among the most frequently observed molecular lesions in human cancer and is reported to be hypermethylated in 31% of breast cancers (85). A growing number of tumor suppressor genes are being identified which demonstrate a correlation between silencing and the epigenetic modifications of promoter hypermethylation and hypoacetylation, including genes

involved in DNA repair (BRCA1), cell cycle regulation (RB1), cell-cell adhesion (TIMP-3) and hormonal regulation (ER and RARβ2) (86, 87).

Problem of chemoresistance

Continued efforts to understand these mechanisms of gene repression are necessary because despite improvements in early detection and treatment, breast cancer is still the second leading cause of cancer-related death in United States women. Resistance to chemotherapeutic agents is a leading cause of treatment failure, affecting up to 90% of patients with metastatic cancer (88). In 1973 it was recognized that reduced drug accumulation was a major factor in chemoresistance, and this led to the discovery of the ATP-binding cassette (ABC) family of transporters (89). There are 49 known human ABC genes that function in transport of a variety of endogenous and exogenous substances (90). The first discovered and most well-characterized ABC transporter is ABCB1, commonly called multi-drug resistance gene 1 (MDR1). *In vitro* p-glycoprotein, encoded by MDR1, confers resistance to vinca alkaloids, anthracyclines, colchicines, epipodophyllotoxins, and paclitaxel (Table 4) (90). MDR1 is often highly expressed in kidney, liver and colon cancers, but only expressed in leukemias, lymphomas and multiple myelomas after chemotherapy and relapse (91). MDR1 and another member of the ABC family ABCG2 have also been used to identify "stem cell" populations due to their role in exclusion of Hoechst 33342 dye, which leads to formation of a distinct "side population" (92). ABCG2 was first identified as a gene overexpressed in MCF7 cells that confers resistance to mitoxantrone, doxorubicin and

Table 4
ABC transporters and their substrates and inhibitors. Many ABC genes function in the export of antineoplastic drugs and, thus, contribute to resistance of cancer cells. Inhibitors are being extensively studied to overcome the problem of drug resistance in cancer (91).

ABC Transporter	Substrates	Inhibitors
ABCB1	vinca alkaloids, anthracyclines, colchicines, epipodophyllotoxins, and paclitaxel	verapamil, PSC833, cyclosporine
ABCG2	mitoxantrone, gefitinib, erlotinib, doxorubicin, daunorubicin, etoposide, camptothecins	imatinib mesylate, fumitremorgin C
ABCC1	anthracyclines, methotrexate, camptothecins, vinca alkaloids	MK571, benzbromarone
ABCB5	5-fluorouracil, doxorubicin	unknown
ABCC2	cisplatin, doxorubicin, methotrexate	MK571
ABCC6	anthracyclines	unknown

daunorubicin, hence its common name breast cancer resistance protein 1 (92). ABCC1 is another prominent member of the ABC family, discovered in a small-cell lung cancer cell line showing multi-drug resistance without overexpressing ABCB1. ABCC1 confers a resistance profile similar to that of MDR1, including vinca alkaloids and anthracyclines (91). The discovery of ABCC1 stimulated the search for homologues, leading to the discovery of several closely related ABC transporters, including ABCC2

and ABCC6. ABCC2 contributes to resistance to cisplatin, doxorubicin and methotrexate, while ABCC6 primarily has activity on anthracyclines (91). ABCB5 is a recently identified ABC transporter due to its use in identification of progenitor cells (93). It has also been shown to have a role in 5-fluorouracil and doxorubicin resistance in melanoma cell lines (94, 95). There is an ongoing effort to inhibit these efflux pumps in order to overcome drug resistance in cancer (90). Several effective modulators of MDR1 are available, including verapamil, cyclosporine and the cyclosporine derivative PSC833 (91). These drugs are undergoing clinical trials to be used in a variety of cancers to combat chemoresistance (83). Only a few inhibitors of ABCC1 have been described, including the leukotriene D4 receptor agonist MK571; however, it has limited application *in vivo* due to low bioavailability and toxic side effects (91). ABCG2 inhibitors have also been identified. Fumitremorgin C is a mycotoxin isolated from *Aspergillus fumigatus*, which reverses multi-drug resistance mediated by ABCG2 *in vitro* but is too toxic for *in vivo* use (91). A surprising inhibitor of ABCG2 was found to be the tyrosine kinase inhibitor imatinib mesylate (Gleevec) (91, 96). ABCG2 can transport other small molecule tyrosine kinase inhibitors, such as erlotinib and gefitinib as substrates; however, imatinib mesylate potently reverses ABCG2-mediated resistance to camptothecins but is not exported as a substrate (96). Understanding how members of the ABC family are regulated will aid this ongoing search for inhibitors to overcome the growing problem of drug resistance in cancer.

Role of Nuclear Factor-κB in cancer and chemoresistance

NFκB plays a major role in mediating chemoresistance, as inhibition of NFκB signaling has been shown to enhance antineoplastic-induced apoptosis (97). NFκB/Rel is a family of transcription factors, which includes five members: p105/p50, p100/p52, p65, RelB and c-Rel. The NFκB/Rel family is characterized by the presence of the Rel homology domain, which mediates DNA binding, dimerization and nuclear localization. The most abundant heterodimer is between p65 and p50 (98, 99). In the canonical pathway (Figure 7A), the p65/p50 dimer is maintained in the cytoplasm by inhibitor of kappaB, alpha (IκBα). Upon stimulation of cells by proinflammatory cytokines or pathogen-associated molecules, the inhibitor of kappaB kinase (IKK) complex, the IKKβ subunit predominantly, phosphorylates IκBα, leading to its degradation by the proteasome. NFκB p65/p50 is then free to translocate to the nucleus and to bind to promoters of a variety of target genes. A noncanonical pathway is activated by ligand-binding to a subset of TNF family receptors, including LTβR, BAFF and CD40L (Figure 7B). This leads to processing of the p100 precursor into p52 mediated by NFκB-inducing kinase (NIK) and IKKα. The p52/RelB dimer then translocates to the nucleus to selectively activate genes involved in the adaptive immune response (98).

Although now the role of NFκB in linking inflammation and cancer is well established, NFκB was initially described over 20 years ago as a nuclear factor in B cells that bound a site in the immunoglobulin κ enhancer (100). It was shortly discovered that NFκB is involved in the response to many immunological stimuli, both exogenous like

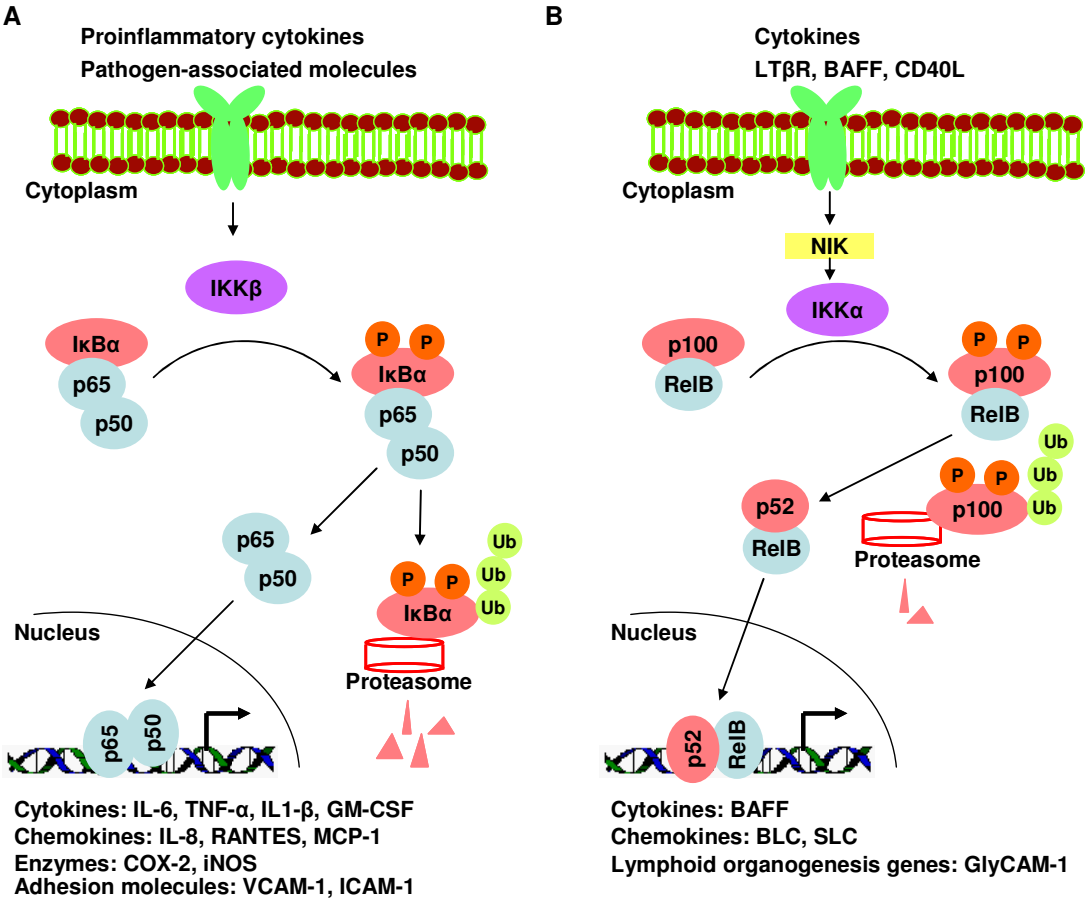

Figure 7
NFκB signaling. (A) In the canonical pathway, the p65/p50 dimer is maintained in the cytoplasm by inhibitor of kappaB, alpha (IκBα). Upon stimulation of cells by proinflammatory cytokines or pathogen-associated molecules, the inhibitor of kappaB kinase (IKK) complex, the IKKβ subunit predominantly, phosphorylates IκBα, leading to its degradation by the proteasome. NFκB p65/p50 is then free to translocate to the nucleus and to bind to promoters of a variety of target genes (96). (B) The noncanonical pathway is activated by ligand-binding to a subset of TNF family receptors, including LTβR, BAFF and CD40L. This leads to processing of the p100 precursor into p52 mediated by NFκB-inducing kinase (NIK) and IKKα. The p52/RelB dimer then translocates to the nucleus to selectively activate genes involved in the adaptive immune response (98).

lipopolysaccharide and endogenous like TNFα. NFκB is extensively post-translationally modified, through phosphorylation, acetylation and dephosphorylation. Different phosphorylation states can determine whether NFκB recruits co-activators or co-

repressors to target genes (101). Also, NFκB is able to interact with other transcription factors which determine specificity of promoter or enhancer binding. C/EBPβ, Jun, Fos, CREB and Sp1 are some of the transcription factors which interact with NFκB on various promoters. The most well characterized cooperation occurs on the interferon β (IFNβ) enhancer. IFNβ is induced specifically in response to viral infection by the cooperation of NFκB, a Jun/ATF2 heterodimer, IRF proteins and HMG-1 because only viral infection induces the full complement of proteins required for IFNβ enhancer binding and activation (101). NFκB also involves epigenetic modifications in its regulation of gene transcription. NFκB has been shown to directly interact with HDAC1 through the Rel homology domain of p65. HDAC2 can interact with this complex through its association with HDAC1 (102). Acetylation status of several NFκB target gene promoters has been shown to be an important mechanism of their regulation, including IL-8 and death receptor 5 (DR5) (102, 103).

In many contexts, NFκB can induce genes that promote cell survival, thus contributing to cancer progression. NFκB can induce the expression of cellular inhibitors of apoptosis (c-IAP) and members of the anti-apoptotic Bcl-2 family (104). NFκB exerts a large part of its regulatory role upon apoptosis through p53. NFκB can induce expression of HDM2, the E3 ubiquitin ligase that induces p53 proteolysis. Also, the NFκB p65 subunit antagonizes p53 transactivation through sequestration of p300 and CBP co-activators (101). These effects of NFκB contribute to its cancer-promoting ability; however, NFκB can function in the opposite capacity through cooperation with p53. Both NFκB and p53 can bind to response elements in the pro-apoptotic DR5

promoter to activate its expression. In addition, NFκB can directly up-regulate p53 expression, leading to sensitization to apoptosis (101). Through this extensive crosstalk between NFκB and p53 pathways, NFκB has the potential to exert an agonistic or antagonistic effect on tumor progression in a context-dependent manner.

Inhibition of apoptosis is one mechanism by which cancer cells decrease the effectiveness of chemo- and radio-therapy. Also, inflammation and infection have long been known to negatively affect xenobiotic metabolism. NFκB plays a large role in this process, antagonizing AHR to suppress induction of cytochrome P450 1A1 (CYP1A1) and CYP1A2 and interfering with glucocorticoid receptor-mediated transactivation of constitutive active/androstane receptor (CAR) leading to downregulation of CYP3A4, glutathione S-transferases, and UDP-glucuronosyltransferases (105). In addition, NFκB induces MDR1 expression in colon cancer cells, contributing to drug resistance, and, recently, it has been shown that NFκB regulates ABCA1 expression in macrophages (106, 107). The interactions between NFκB and ABC transporters provide additional mechanisms to be targeted to combat drug resistance in cancer.

Mechanisms of silencing SIM2

In these studies, epigenetic mechanisms, oncogenic transformation and transcriptional repressors, NFκB, NOTCH1 and C/EBPβ, have been shown to contribute to silencing the breast tumor suppressor gene SIM2 in cancer cells. SIM2 undergoes progressive epigenetic changes during cancer progression in a cell line model that correlate with loss of expression. By overexpressing DNMT1 in a normal breast

epithelial cell line, we have shown that *de novo* methylation of the SIM2 promoter contributes to but is not sufficient for complete silencing. Overexpression of HRAS and c-MYC oncogenes was used as a model to identify alternate pathways of SIM2 repression. Using the normal immortalized human breast epithelial cell line MCF10A, stable overexpression of HRAS or c-MYC was found to down-regulate SIM2 expression. SIM2 mRNA levels were preferentially reduced by HRAS, although both HRAS and c-MYC lead to an observed reduction in protein levels. In *Drosophila* sim is regulated by dorsal, twist, snail and notch signals to narrow its expression to a single row of cells in the embryo (108). Also, NOTCH1, dorsal homolog NFκB, and C/EBPβ transcription factors can be activated by HRAS (46, 68, 109). Each is able to bind to the SIM2 promoter, with the NICD acting through a novel CBF1-independent mechanism. NFκB is a central mediator of SIM2 regulation as it facilitates the repression by C/EBPβ and leads to deacetylation of histone 3 in the SIM2 promoter, contributing to epigenetic changes observed during cancer progression. SIM2, however, also antagonizes NFκB signaling through inhibiting specific NFκB target genes including the ATP-binding cassette transporter, ABCB5, and through direct interactions with NFκB. SIM2, through this antagonism of NFκB, increases cancer cell susceptibility to antineoplastic drugs, including doxorubicin and 5-fluorouracil. We expect that SIM2 silencing plays an important role in progression of a subset of human breast cancer, which is supported by analysis of SIM2 expression by immunohistochemistry (21). Elucidating oncogenic pathways and factors involved in SIM2 silencing contributes to the characterization of the molecular basis for specific subsets of cancer and thus facilitates development of

targeted therapies for human breast cancer. In addition, we expect that the antagonism between SIM2 and NFκB may be exploited to develop new treatment strategies countering antineoplastic drug resistance.

CHAPTER II

MATERIALS AND METHODS

Cell line maintenance and drug treatment

MCF7 and MDA435 cells were maintained in DMEM supplemented with 10% fetal bovine serum and 1% penicillin and streptomycin. MCF10A cells were maintained in DMEM/F-12 supplemented with 5% fetal bovine serum, 1% penicillin and streptomycin as well as 20 ng/ml epidermal growth factor, 0.5 µg/ml hydrocortisone, 100 ng/ml cholera toxin and 10 µg/ml insulin. For the treatment with the epigenetic-altering drugs, 10 µM 5-aza-2'-deoxcytidine (5-aza-dC) or vehicle was added to fresh media every 24 hours for 3 days. Trichostatin A (TSA) at 500 nM or vehicle was added for the last 24 hours. For inhibition of NFκB, cells were treated with 300 µM pyrollidine dithiocarbamate (PDTC) for 4 hours. Stably transduced MCF10A and MDA435 cells were grown in the presence of 1µg/ml puromycin. C/ebpβ$^{-/-}$ cells (provided by C. Zahnow) were maintained in DMEM/F-12 supplemented with 2% fetal bovine serum, 1% penicillin and streptomycin, 5 ng/ml epidermal growth factor and 5 µg/ml insulin. Stably transduced C/ebpβ$^{-/-}$ cells were grown in the presence of 1.5 µg/ml puromycin. All cells were grown in 5% CO_2 at 37^{o}C.

Construction of plasmids

HRAS and c-MYC constructs were provided by Brian and Alana Welm. HRAS was amplified with primers 5′-ATG ACG GAA TAT AAG CTG GT-3′ and 5′-TCA GGA GAG CAC ACA CTT G-3′ and cloned onto pCR2.1 TOPO (Invitrogen) and subcloned into *EcoRI* sites in pLPCX (Clontech). The NICD was amplified with primers 5′-ATG TAC GTG GCG GCG-3′ and 5′-TTA CTT GAA GGC CTC CGG-3′ and cloned onto pCR2.1 TOPO and subcloned onto pcDNA3 using *EcoRI* restriction sites. CBF1 was amplified with primers 5′-ATG GCG TGG ATT AAA AGG A-3′ and 5′-TTA GGA TAC CAC TGT GGC TGT-3′ and cloned onto pCR2.1 TOPO and subcloned into pcDNA3 with *KpnI* and *XhoI*. The HES1 promoter was amplified with primers 5′-TTG ATT GAC GTT GTA GCC TCC-3′ and 5′-TGT TAT CAG CAC CAG CTC CG-3′ and cloned onto pCR Blunt II TOPO (Invitrogen) and subcloned onto pGL2 Basic (Promega) using *KpnI* and *XhoI* restriction sites. Vectors (pBABEpuro or pEFIRESpuro backbones) containing human and mouse C/EBPβ isoforms were graciously provided by C. Zahnow and were subcloned as necessary onto pcDNA3 or pLPCX with *EcoRI*. Human LIP was amplified with primers 5′-ATG GCG GCG GGC TTC CC-3′ and 5′-CTA AGC GTA TGC TGG GAC GTC GTA TG-3′ and cloned onto pCR2.1 TOPO and subcloned into pcDNA3 using *EcoRI*. The full length SIM2 promoter was amplified in two pieces with primers (5′-ATC TGG GTA ATC CCT TTC AAG CC-3′ and 5′-CCT GAG CTC CGA GCA ACC-3′) and (5′-GTG GAC AGC GGA GGT GCT-3′ and 5′-CCA AAC CAA ACC AGA ATG C-3′). Each piece was cloned onto pCR2.1 TOPO. The former fragment was subcloned onto pGL2 Basic into *KpnI*

and *XhoI* restriction sites. The latter fragment was then subcloned into *SacI* and *XhoI* restriction sites to obtain the full length SIM2 promoter on pGL2 Basic. To generate SIM2 deletion constructs, forward primers (5′-GGA CAG GCA GGG GGA GAG C-3′, 5′-CCT TCC TGG CGC AGG GGA GG-3′, 5′-ACT GCT CCA CGG CTC TGC A-3′, 5′-TCT GCT CAA GCC GCT GCA-3′ or 5′-ATC TGG GTA ATC CCT TTC AAG CC-3′) were combined with reverse primers (5′-CCT GAG CTC CGA GCA ACC-3′ or 5′-GGG AGG ATC GAG CCT TCC GAG GGT-3′). Fragments were cloned onto pCR2.1 TOPO and sucloned into *KpnI* and *XhoI* restriction sites of pGL2 Basic. The region from -1380 to -1167 was deleted by digestion of the -1380 to +220 fragment on pCR2.1 TOPO with *EcoRV* and *PvuII*, and that fragment was then subcloned onto pGL2 Basic into the *SmaI* site. DNMT1 full length cDNA was cloned initially onto pCR2.1 TOPO cloning vector. An N-terminally truncated form, DNMT1ΔN, was generated by cleavage with *XbaI* and cloned onto the retroviral vector pLPCX. The ABCB5 promoter was amplified with primers 5′-CTC AGT AGA AAG ATT GCC TGC-3′ and 5′-CAA AGG AGT AAA CTG ACA GTC-3′ and cloned onto pCR Blunt II TOPO and subcloned onto pGL2 Basic using *XhoI* and *HindIII* restriction sites. The NFκB p65 and IκB-SR expression vectors and 5X NFκB-luc vector were graciously provided by Dr. Yanan Tian and Sui Ke. IκB-SR was amplified with primers 5′-ATG TTC CAG GCG GCC GAG-3′ and 5′-TCA TAA CGT CAG ACG CTG GC-3′, cloned onto pCR2.1 TOPO and subcloned onto pLPCX using *EcoRI* restriction sites. IKKβ was amplified with primers 5′-CCG ACA GAG TTA GCA CGA CAT-3′ and 5′-ACA TCA TGA GGC

CTG CTC CA-3′, cloned onto pCR2.1 TOPO and subcloned onto pLPCX using *HindIII* and *NotI* restriction sites. Cloning of SIM2s was described previously (21).

RNA isolation and real time RT-PCR

RNA was isolated using a Qiaquick RNeasy Mini kit with Qiashredder columns (Qiagen) and DNase digested. One µg of RNA was reverse transcribed with Superscript II Reverse Transcriptase (Invitrogen) with an oligo $d(T)_{12-18}$ primer. Relative quantitative PCR was performed using Sybr Green master mix and cDNA-specific primers. TBP was used as the internal standard. Data were collected using SDS software, and analyzed by the $\Delta\Delta C_T$ method. Primers used for real time RT-PCR are shown in the table below (Table 5).

Table 5
Primers for real time RT-PCR.

Target Gene	Forward Primer	Reverse Primer
SIM2	AGACAAAGCTGAGAACAAACCCTTA	CCGCATTCCAGTTTGTCCAT
TBP	TGCACAGGAGCCAAGAGTGAA	CACATCACAGCTCCCCACCA
DNMT1	GCGATGTGGCGTCTGTGA	CTGCCACCAAATTTAACCATGTC
Sim2	TCACGTCTTCAGCAGCAAGAA	AGAAGCGTGCCACCTCACA
CEBPB	GCCAAGAAGACCGTGGACAA	TGCGCACGGCGATGT
Cebpb	AAGCTGAGCGACGAGTACAAG	GTCAGCTCCAGCACCTTGTG
HES1	AGGCGGCTAAGGTGTTTGG	TTGGGAATGAGGAAAGCAAACT
HEY1	TGACCGTGGATCACCTGAAA	GCGTGCGCGTCAAAGTAAC
HEY2	TCGCCTCTCCACAACTTCAGA	GAATCCGCATGGGCAAAC
ABCB5	CCTGATTCTGAGTATTGCTCCAGTACT	TTGGCAAATCCAGTCATTGC
ABCG2	GCGACCTGCCAATTTCAAAT	CGTCAGAGTGCCCATCATAA
ABCC1	GATCGTCAAGTCCCCACAGAA	GTAGGGCCCAAAGGTCTTGTATAA
ABCB1	GTCCCAGGAGCCCATCCT	CCCGGCTGTTGTCTCCATA
ABCC6	GCTTGGATTCGCCCTCATAG	GGCGTTCCCTGTTGGATTT
ABCC2	ACCCTCAGTCTTAGCAGGTGTTG	AATGGTCTTACTCTTGGTGGACAGT

5′ RACE

Five µg of RNA was reverse transcribed with Superscript II Reverse Transcriptase (Invitrogen) with a primer to the SIM2 promoter: 5′-CCT GAG CTC CGA GCA ACC-3′. The product was purified over a Qiaquick PCR purification column (Qiagen). The TdT tailing reaction of the cDNA was performed with dATP for 1 hour at 37^{o}C. Two rounds of PCR were performed, first with 5′-GGG AGG ATC GAG CCT TCC GAG GGT-3′ and 5′-GAT CAG GAC GTT CGT TTG AGT TTT TTT TTT TTT TTT T-3′. The second round again utilized the former primer and 5′-GAT CAG GAC GTT CGT TTG AG-3′.

Bisulfite sequencing

DNA was isolated and digested with *HindIII*. After purifying through a Qiaquick PCR purification column, DNA is eluted in 0.1XTE. DNA is then treated with a denaturation buffer (0.3 N NaOH, 0.23 mg/ml shSSDNA, 8.4 mM EDTA, 6.7 mM Tris-Cl) at 98^{o}C for 5 minutes. DNA is deaminated with saturated sodium metabisulfite containing 1 mM hydroquinone at 50^{o}C for 6 hours. DNA is then purified through a Qiaquick PCR purification column and eluted in 50µl of water. DNA is desulfonated in 0.36 N NaOH and 0.17 mg/ml shSSDNA at 37^{o}C for 15 minutes. DNA is precipitated by ethanol/ammonium acetate and resuspended in 0.1xTE. The region around the SIM2 transcriptional start site was amplified with 5′-GTT TAT TTT GTG ATT TTG GTT TAG-3′ and 5′-AAA TAA CCC TTC TAC CCT TTC TAT CC-3′, and the region encompassing the ATG start site was amplified with 5′-GTT AAG ATT AGG AGG

GAG AAG GAA A-3′ and 5′-CCA AAC CAA ACC AAA ATA CAC TAA C-3′ using *Taq* polymerase (Invitrogen). PCR products were then cloned onto pCR2.1-TOPO and transformed into chemically competent DH5α *E. coli* (Invitrogen). Plasmid was isolated from individual colonies and evaluated for containing an appropriately sized insert. Plasmids were sequenced using the M13 (-20) forward primer or the M13 reverse primer on an ABI Prism™ 3730*xl* DNA sequencer by Seqwright (Houston, TX).

Chromatin immunoprecipitation

ChIP assays were carried out as described by the manufacturer (Upstate Cell Signaling) with a few modifications. Briefly, cells were fixed with 1% formaldehyde for 10 minutes. Crosslinking was stopped by addition of 125 mM glycine. Cells were washed in the presence of protease inhibitors (Complete tablets, Roche), pelleted at 2000 rpm for 4 minutes at 4^{o}C and resuspended in SDS lysis buffer with protease inhibitors (Complete tablets, Roche). Aliquots of 200 µl (1x10^{6} cells) were sonicated for 10 pulses of 10 seconds each to shear chromatin to between 200 and 1500 bp. The supernatant was collected and diluted in ChIP dilution buffer to an appropriate amount. After pre-clearing twice with salmon sperm DNA/protein A agarose-50% slurry in TE/Na azide/0.1% BSA, the supernatant was incubated overnight with antibody at 4^{o}C. Antibodies used were anti-acetyl histone H3 (5 µg, Upstate), anti-HP1α, clone 15.19s2 (2.9 µg, Upstate), normal rabbit IgG (1 µg, Upstate), anti-RNA polymerase II, clone CTD4H8, (9.4 µg, Upstate), anti-DNMT1 (5 µg, Abcam), anti-Sim2 (10 µg, Chemicon), anti-NFκB p105/p50 (10 µg, Abcam), anti-C/EBPβ (20 µg, Santa Cruz), anti-CBF1 (4

µg, Upstate), anti-Notch1 (10 µl, Abcam) and anti-HA tag (5 µg, Abcam). The salmon sperm DNA/protein A agarose-50% slurry was then used to collect the antibody complexes for 1 hour at 4°C. Agarose was pelleted at 1000 x *g* at 4°C for 1 minute and washed consecutively with low salt immune complex wash buffer, high salt immune complex wash buffer, lithium chloride immune complex wash buffer and TE buffer. The protein complex was eluted with 1% SDS, 0.1 M $NaHCO_3$, and the crosslinking was reversed in 200 mM NaCl at 65°C for 4 hours. Ethanol was added to precipitate the DNA, which was then resuspended in TE and digested with proteinase K for 1-2 hours at 45°C. DNA was purified using the Qiaquick PCR purification kit. PCR was performed with primers to the transcriptional start site region (5′-GCC CAC CCT GTG ACC CTG-3′ and 5′-AAG TGA CCC TTC TGC CCT TTC-3′), primers to the ATG start site region (5′-GCC AAG ACC AGG AGG GAG-3′ and 5′-CCA AAC CAA ACC AGA ATG C-3′), primers to the ABCB5 promoter (5′-TCC TCA ATT TAT GTG TGG CTG-3′ and 5′-TTA GCC AAA AGG CCG AGA A-3′) and primers to the luciferase gene (5′-TAG AGG ATG GAA CCG CTG GA-3′ and 5′-TCA CGA TCA AAG GAC TCT GGT-3′).

Chromatin accessibility assay

The assay was based on a protocol described previously with some modifications (110). Briefly, cells were collected and lysed in 1X Reporter Lysis buffer (Promega). The cells were washed twice before resuspension in 100µl 1X NEBuffer 2 for 10^7 nuclei. 10^6 nuclei were incubated with 0 or 275 U of *MspI* for 1 hour at 37°C. Reaction was stopped by addition of 0.2mg/ml proteinase K and 0.6% SDS. DNA was extracted

with phenol:chloroform:isoamyl alcohol, ethanol/sodium acetate precipitated and resuspended in water. A constant amount of DNA was ligated to a linker. The linker was made by first phosphorylating the reverse oligo: 5′-CGG CTC AAA CGA ACG TCC TGA TC-3′ with T4 kinase (Invitrogen). The phosphorylated oligo was then annealed to its complement: 5′-GAT CAG GAC GTT CGT TTG AGC-3′ (AP2-Msp1) to generate a linker with *MspI* overhangs. After the ligation, two rounds of PCR were performed. For the transcriptional start site, the first set of primers was AP2-Msp1 and 5′-TCC CCC CAT TAC ACA CAC A-3′, and the second amplification was done using AP2-Msp1 with 5′-AAG TGA CCC TTC TGC CCT TTC-3′. For the ATG start site, the first set of primers was AP2-Msp1 and 5′-CGC GAT GAA GGA GAA GTC CAA GAA-3′, and the second set of primers was AP2-Msp1 with 5′-GCC AAG ACC AGG AGG GAG AAG-3′.

Western blot

Protein was isolated using RIPA buffer (25 mM Tris-HCl pH 7.6, 150 mM NaCl, 1% NP-40, 1% sodium deoxycholate, 0.1% SDS) with protease inhibitors and MG-132 added. Protein was loaded and run on an 8% acrylamide gel for 2 hours at 100 V. Protein was transferred to a PVDF membrane (Bio-Rad) at 100 mA for 2 hours. Membrane was blocked in 5% milk and probed with anti-Sim2 (1:600, Chemicon), anti-Dnmt1 (1:3000, Abcam), anti-C/EBPβ (1:2500, Santa Cruz), anti-phospho-C/EBPβ (1:1000, Cell Signaling), anti-NFκB p65 (1:1000, Abcam) or anti-β-actin (1:8000, Sigma). Membranes were washed in PBS, 0.1% Tween-20 and probed with the

appropriate secondary antibody, anti-rabbit (Bio-Rad) or anti-mouse (Santa Cruz), at 1:5000 for 45 minutes. Blots were again washed in PBS, 0.1% Tween-20 and developed with the ECL Plus Western Blotting Detection System (Amersham).

Methylation-specific PCR

Breast tumor samples were obtained from Baylor College of Medicine, under Institutional Review Board approval with informed consent obtained from all subjects. Bisulfite treatment was performed as described above. A portion of the second CpG island of SIM2 was amplified initially with primers non-selective for methylation status, 5′-GTT AAG ATT AGG AGG GAG AAG GAA A-3′ and 5′-CCA AAC CAA ACC AAA ATA CAC TAA C-3′. The product was diluted 1:50 and then amplified with a primer set specific for methylated DNA, 5′-TAA GTT GTT TTC GTT GTC GTC GG-3′ and 5′-AAA ACT CGC TAA CCG TAC GAA CT-3′, and a primer set specific for unmethylated DNA, 5′-TAA GTT GTT TTT GTT GTT GTT GG-3′ and 5′-AAA ACT CAC TAA CCA TAC AAA CT-3′.

Stable transduction

HEK-293T amphotrophic Phoenix cells were transfected with 10 μg retroviral vectors (pLPCX or pBabe) with or without insert. After 24 hours, cells were placed at 32^{o}C. Viral media was harvested 48 and 72 hours after transfection and used to infect cells. After 24 hours of resting in nonselective media, cells were selected with puromycin for 2 days.

Transient transfection

HEK293T cells were used for all transient transfections except with the ABCB5 promoter construct which was done in MDA435 cells. One hundred ng (0.1 μg) of plasmid containing transcription factor was mixed with 0.2 μg of plasmid containing promoter construct. Three μl of Genejuice (Novagen) was used per microgram of DNA. DNA and Genejuice were mixed in Opti-MEM media (Invitrogen). Protein was harvested 2 days after transfection, using Reporter Lysis Buffer (Promega). Luciferase activity and total protein were measured as described previously (21). Luciferase activities were normalized to total protein values and are represented as the means ± SE for three wells per condition. For ChIP assays, 5 μg of plasmid containing repressor and 5 μg of plasmid containing the SIM2 promoter construct were transfected into HEK293T cells or MDA435 stably tranduced (pLPCX or IκB-SR) cell lines, where indicated, on a 10 cm plate. Chromatin was harvested 2 days after transfection.

Cell proliferation/death assay

Control and SIM2-overexpressing MDA435 cells were seeded at 750,000 cells per well in 6-well plates. The next day doxorubicin (1 μM) and 5-fluorouracil (1.5 mM) were added in fresh media. Cells were counted, using a Coulter counter, in triplicate (3 wells) at the time of treatment and 24 hours intervals thereafter for 3 days. Doxorubicin was too toxic and all cells were dead by day 3, so a count could not be done.

MTT assay

For the MTT assay, 100,000 cells were seeded in media with or without antineoplastic drug in 96-well plates. The MTT Cell Growth Assay Kit (Chemicon) was used, according to manufacturer's instructions, to measure cell viability 24 to 36 hours after seeding for control and SIM2-overexpressing MDA435 cells.

Immunocytofluorescence

Cells were seeded on cover slips in 6-well plates or in 4-well chamber slides. The following day the cells were fixed in 4% paraformaldehyde and permeabilized with 0.1% Triton-X. The cells were blocked in 5% BSA for 30 minutes and then probed with anti-Sim2 (1:100 of 1μg/μl stock), anti-NFκB p105/p50 (1:100), or anti-phospho-C/EBPβ (1:100) for 1 hour at room temperature. Secondary antibody was anti-rabbit Ig-$Alexa_{488}$ or anti-rabbit Ig-$Alexa_{568}$. Cells were mounted in fluorescence mounting media with DAPI. To demonstrate morphology cells were stained with fluorescein-conjugated anti-phalloidin (1:40)

Immunohistochemistry

Tissue was deparaffinized at 62°C for 30 minutes and washed in xylenes and ethanol. Antigen retrieval was performed by microwaving at high, medium and low power for 5 minutes each in 0.01M NaCitrate, pH 6. Sections were then peroxidase blocked and then incubated in blocking solution (PBS 0.1% Tween-20 10% normal horse serum) overnight. Anti-Sim2 (Chemicon) antibody was used to probe at 1:100

dilution for 1.5 hours at room temperature. Secondary antibody, biotinylated anti-rabbit IgG (Vector Laboratories), was used at 1:250 for 45 minutes at room temperature. Specific recognition was detected using VectaStain ABC reagent and developed with freshly prepared DAB solution (Vector Laboratories). Sections were then counterstained with hematoxylin, dehydrated and mounted with Permount.

Co-immunoprecipitation

HEK293T cells were transfected with 5 μg of SIM2s and NFκB p65 expression vectors, using Genejuice as described above. Two days later, cells were fixed with 1% formaldehyde for 10 minutes. Crosslinking was stopped by addition of 125 mM glycine. Cells were washed in the presence of protease inhibitors (Complete tablets, Roche), pelleted at 2000 rpm for 4 minutes at 4^{o}C and resuspended in SDS lysis buffer with protease inhibitors and incubated on ice for 10 minutes. The mixture was spun for 10 minutes at 16000 x *g* at 4^{o}C, and the supernatant was collected and diluted in ChIP dilution buffer to an appropriate amount. After pre-clearing twice with salmon sperm DNA/protein A agarose-50% slurry in TE/Na azide/0.1%BSA, the supernatant was incubated overnight with antibody at 4^{o}C. Antibodies used were anti-Sim2 (1:100, Chemicon), normal rabbit IgG (1:1000, Upstate), and anti-NFκB p65 (1:100, Abcam). The salmon sperm DNA/protein A agarose-50% slurry was then used to collect the antibody complexes for 1 hour at 4^{o}C. Agarose was pelleted at 1000 x *g* at 4^{o}C for 1 minute and washed consecutively with low salt immune complex wash buffer, high salt immune complex wash buffer, lithium chloride immune complex wash buffer and TE

buffer. The pellet was resuspended in 50 µl of 1X SDS-PAGE loading buffer, boiled for 5 minutes and 10 µl of sample was run by SDS-PAGE. Western blotting was performed as described above, with anti-Sim2 and rabbit anti-NFκB p65 (1:1000, Abcam) primary antibodies.

Flow cytometry

MDA435 control (pLPCX) or SIM2s-overexpressing cells were treated with 10 µM doxorubicin for 30 minutes, washed with 1X phosphate buffered saline, and allowed to incubate in DMEM, supplemented with 10% fetal bovine serum, for an additional 3 hours. A 0 hour time point, without further incubation without doxorubicin, was also collected for comparison. The cells were washed, trypsinized, counted on a Coulter counter, and resuspended in buffer (10 mM HEPES/NaOH, pH 7.4, 140 mM NaCl, 2.5 mM $CaCl_2$) at one million cells per ml. Cells were analyzed on a FACSCalibur (Becton Dickinson Immunocytometry Systems) flow cytometer, equipped with a 15 mW air-cooled argon laser, using CellQuest (Becton Dickinson) acquisition software. Doxorubicin fluorescence was collected through a 585/42-nm bandpass filter, and list mode data were acquired on a minimum of 10,000 events falling within light scatter gates set to include cells. Data analysis was performed in FlowJo (Treestar, Inc.) using forward and side light scatter to gate on the cells.

CHAPTER III

RESULTS: EPIGENETIC REGULATION OF SIM2

SIM2 is epigenetically silenced in cancer cell lines

SIM2 has recently been identified as a novel tumor suppressor in the breast, and is down-regulated in a subset of breast cancers (21). Given the prevalence of epigenetic modifications of tumor suppressors in cancer, we sought to investigate the role of epigenetic mechanisms in SIM2 silencing. We used three cell lines to model stages of cancer progression. SIM2 is highly expressed in normal breast tissue and in the immortalized, nontransformed breast cell line, MCF10A (Figure 8A). Expression is partially reduced in the estrogen receptor positive MCF7 breast cancer cell line and is substantially abrogated in the estrogen receptor negative, highly invasive MDA435 cancer cell line. MCF10A and MDA435 cells were treated with two epigenetic-altering drugs, 5-aza-2'-deoxcytidine (5-aza-dC), which is a demethylating agent, and trichostatin A (TSA), which is an HDAC inhibitor (Figure 8B and 8C). The drugs had little effect on SIM2 mRNA expression in the normal MCF10A cells. In MDA435 cells, demethylation increased SIM2 mRNA expression 5.4-fold, and acetylation increased SIM2 expression 3.4-fold. Treatment with a combination of the drugs resulted in a 13.9-fold increase. This observed increase in SIM2 expression did not approach levels in the normal breast MCF10A cell line, which was approximately 3500-fold higher than untreated MDA435 levels. This pattern of increased expression after 5-aza-dC and TSA treatment is consistent with partial epigenetic silencing of SIM2 in cancer cells.

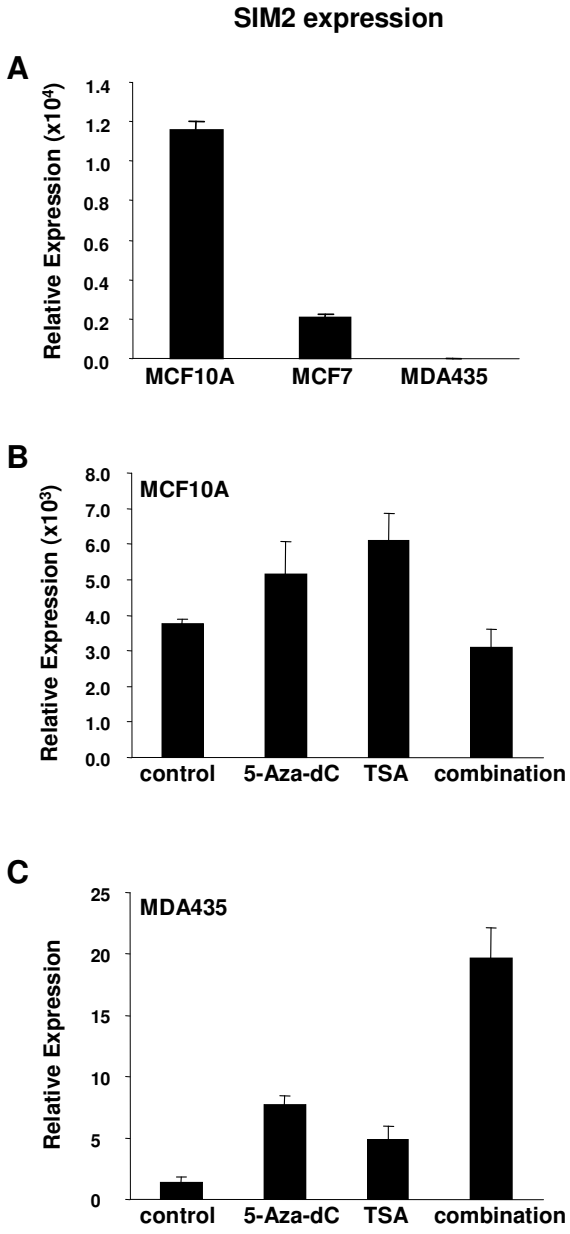

Figure 8
SIM2 is epigenetically silenced in cancer cell lines. (A) SIM2 expression in MCF10A, MCF7 and MDA435 cell lines by real time RT-PCR. (B) SIM2 expression after treatment with 5-aza-2'-deoxcytidine (5-Aza-dC) and trichostatin A (TSA) in MCF10A cells. (C) SIM2 expression after treatment with 5-Aza-dC and TSA in MDA435 cells.

Methylation within exon 1 of SIM2 correlates with expression

Because of the increase in SIM2 expression following treatment with 5-aza-dC, methylation of the SIM2 promoter was examined further. First, it was verified that MCF10A, MCF7 and MDA435 cells share the same promoter for SIM2 using 5′ RACE (Figure 9A). Analyzing the promoter using the online program MethPrimer (http://www.ucsf.edu/urogene/methprimer/index1.html) identified CpG islands in the SIM2 promoter and exon 1, and primers were designed to amplify deaminated DNA within these islands. Methylation-specific PCR, using primers designed within exon 1, was used to analyze the SIM2 promoter. SIM2 was found to be unmethylated in the MCF10A cell line, in contrast to being completely methylated in the MDA435 cell line in this region (Figure 9B). For bisulfite sequencing both the region surrounding the ATG start site in exon 1 and another around the transcriptional start site were chosen for analysis (Figure 9C). Unexpectedly, a high level of methylation was observed at the transcriptional start site in all three cell lines (Figure 9D). At the ATG start site, however, methylation level inversely correlated with expression level in the three cell lines, suggesting that methylation within exon 1 is playing a regulatory role.

Histone modifications have a role in silencing SIM2

SIM2 re-expression in MDA435 cells after TSA treatment implies that histone modification is a mechanism of SIM2 silencing. Chromatin immunoprecipitation was used to evaluate the levels of histone 3 (H3) acetylation and heterochromatin protein 1 (HP1) associated with SIM2 at the transcriptional start site and ATG start site. Presence

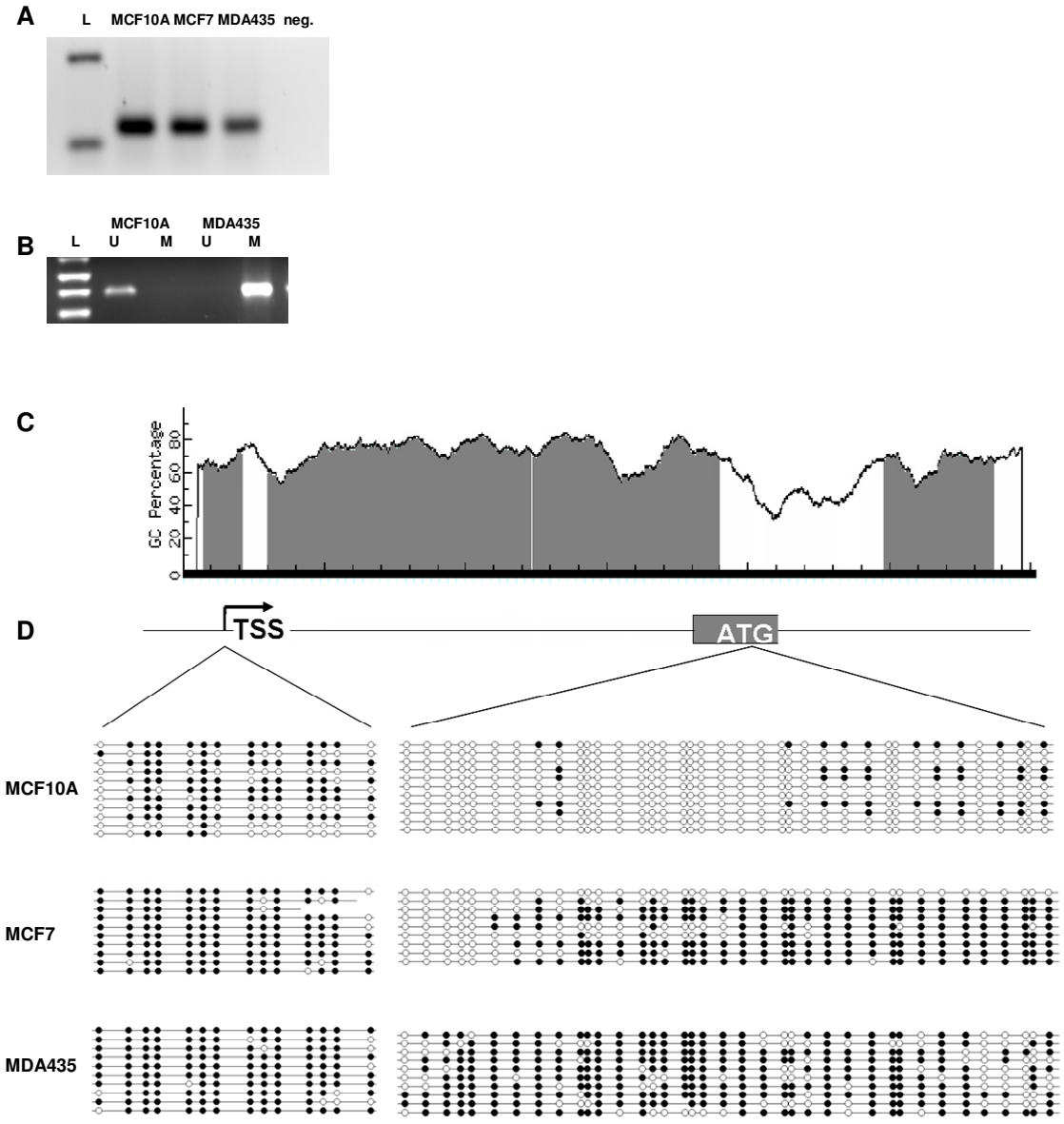

Figure 9
Methylation of SIM2 in normal breast-derived and cancer-derived cell lines. (A) 5′ RACE of SIM2 gene in MCF10A, MCF7 and MDA435 cell lines. (B) Methylation-specific PCR analysis of SIM2, using primers designed within exon 1, in MCF10A and MDA435 cell lines. (C) CpG island analysis of SIM2 promoter and 5′ end using MethPrimer. (D) Frequency of methylation of SIM2 in three cell lines, as determined by bisulfite sequencing. Circles represent CpG dinucleotides; filled-in circles indicate methylation.

of RNA polymerase II was also evaluated to determine the effect of these alterations on transcription initiation and elongation. High levels of acetylation were observed in the MCF10A and MCF7 cell lines at the transcriptional start site, but the MDA435 cell line had no acetylation of H3 (Figure 10A). HP1 showed the opposite pattern, being present at high levels in the MDA435 cell line and low to absent in the MCF7 and MCF10A cell lines at the transcriptional start site. Levels of RNA polymerase II at the transcriptional start site correlated well with expression, demonstrating the differences are due to a lack of transcriptional initiation. At the ATG start site, a similar chromatin state was observed (Figure 10B). One major exception was a lack of H3 acetylation and slightly higher levels of HP1 in MCF7 cells.

Epigenetic alterations correlate with changes in chromatin structure

Increasing DNA methylation and histone hypoacetylation in the MCF7 and MDA435 cancer cells suggests a silenced chromatin structure that is typically tightly compacted and inaccessible to various transcriptional activators but also associated with repressors that maintain the inactive state (111). As a measure of the accessibility of the SIM2 gene, nuclei isolated from MCF10A, MCF7 and MDA435 cells were treated with the restriction enzyme *MspI* (Figure 11). A PCR detection method was utilized as previously described (110). A single product indicates complete digestion and, therefore, accessibility, while multiple products and no product indicate decreased and a lack of accessibility, respectively. This assay revealed increasing changes in the SIM2 gene through increasingly malignant cancer cell lines, with the DNA being highly

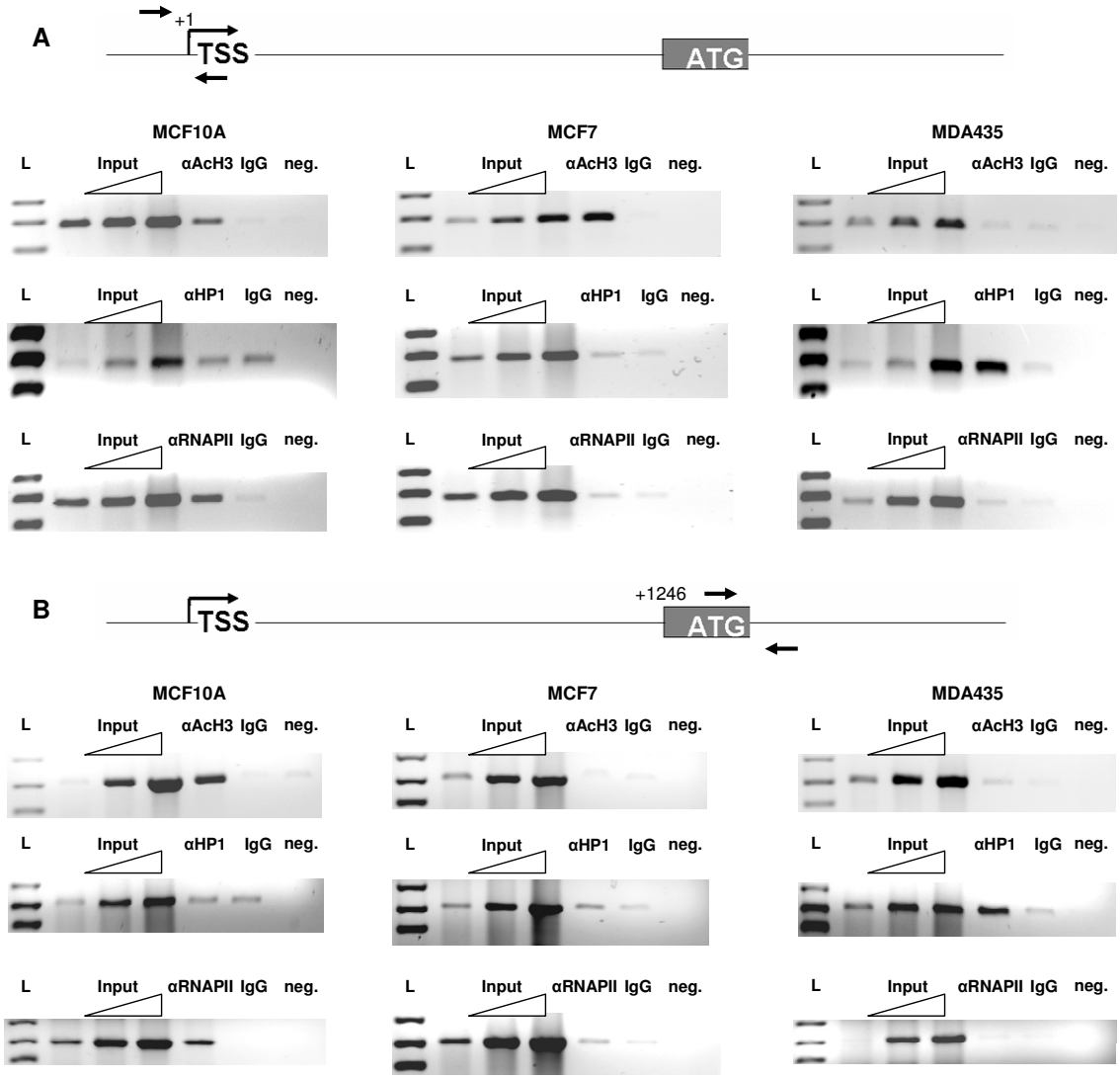

Figure 10
Chromatin immunoprecipitation analysis of SIM2. (A) ChIP analysis for acetylated histone 3 (AcH3), heterochromatin protein 1 (HP1) and RNA polymerase II (RNAPII) at the transcriptional start site of the SIM2 promoter. (B) ChIP analysis at the ATG start site. Diagrams of SIM2 promoter and primer positions are shown above for reference.

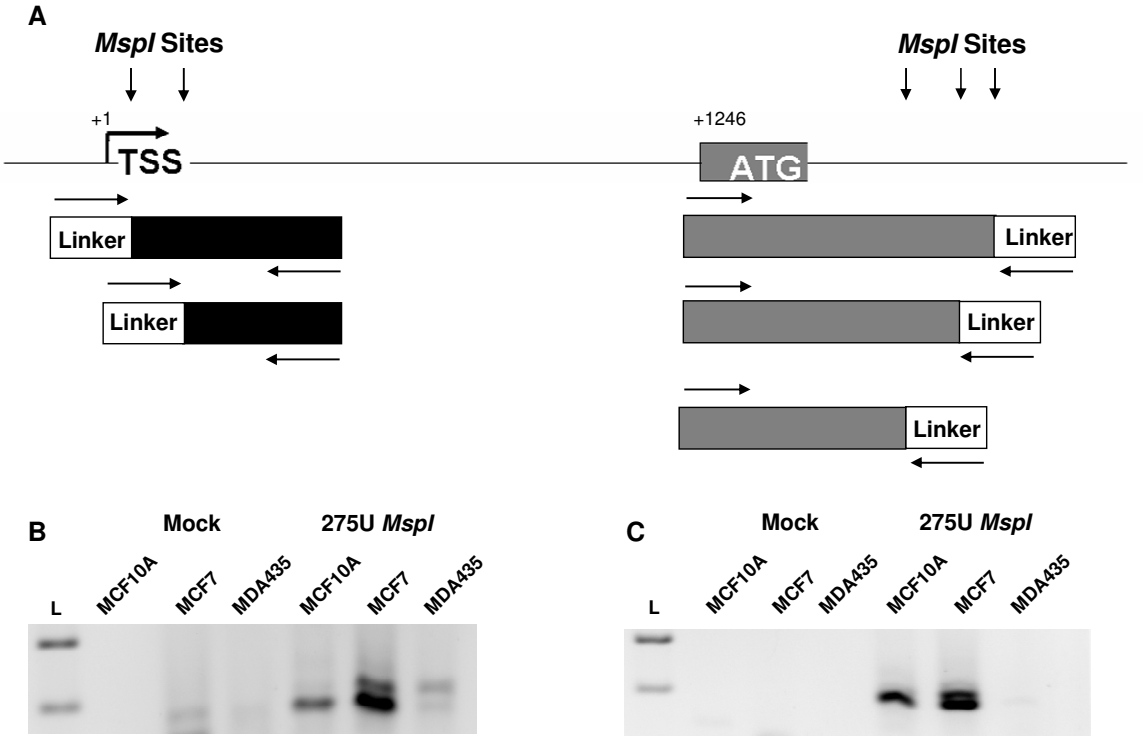

Figure 11
Chromatin accessibility assay using *MspI* restriction enzyme. (A) Diagram of *MspI*-based accessibility assay showing positions of restriction sites, linker and PCR primers on SIM2 promoter. (B) Transcriptional start site accessibility. (C) ATG start site accessibility.

accessible in the MCF10A cell line, less accessible in the MCF7 cell line and only slightly accessible in the MDA435 cell line at both the transcriptional start site and ATG start site. These results correlate well with the results of the HP1 chromatin immunoprecipitation assay.

DNMT1 overexpression contributes to SIM2 silencing

To explore the role of methylation of the SIM2 promoter that we observed in the cell lines, a truncated form of the maintenance DNA methyltransferase, DNMT1ΔN, was overexpressed in MCF10A cells. The N-terminally truncated form was used because it has previously been shown that this region encodes a destruction domain, and to achieve high expression levels, this domain must be deleted (74). DNMT1 overexpression was verified by real time RT-PCR and Western blot (Figure 12A and 12C). SIM2 expression was also analyzed by real time RT-PCR and was found to be repressed approximately 50% by passage 10 (Figure 12B). This correlated with a reduction in SIM2 protein levels by Western blot (Figure 12C). Further passaging did not lead to greater repression. By bisulfite sequencing analysis, methylation was analyzed at the ATG region in MCF10A cells stably transduced with vector control (pLPCX) and DNMT1ΔN (Figure 12D). Surprisingly, the control transduction resulted in increased methylation compared to the parent cell line. DNMT1 overexpression increased methylation levels further from 23% in the control cells to 49% in the DNMT1ΔN-transduced cells. However, we did not observe a detectable loss of acetylation of histone 3 at passage 5 or at passage 20 in the DNMT1-overexpressing MCF10A cells (Figure 12E). To confirm that DNMT1 was directly interacting with the SIM2 promoter, we performed ChIP analysis and found DNMT1 bound to the ATG region in MCF10A cells overexpressing DNMT1ΔN (Figure 12E).

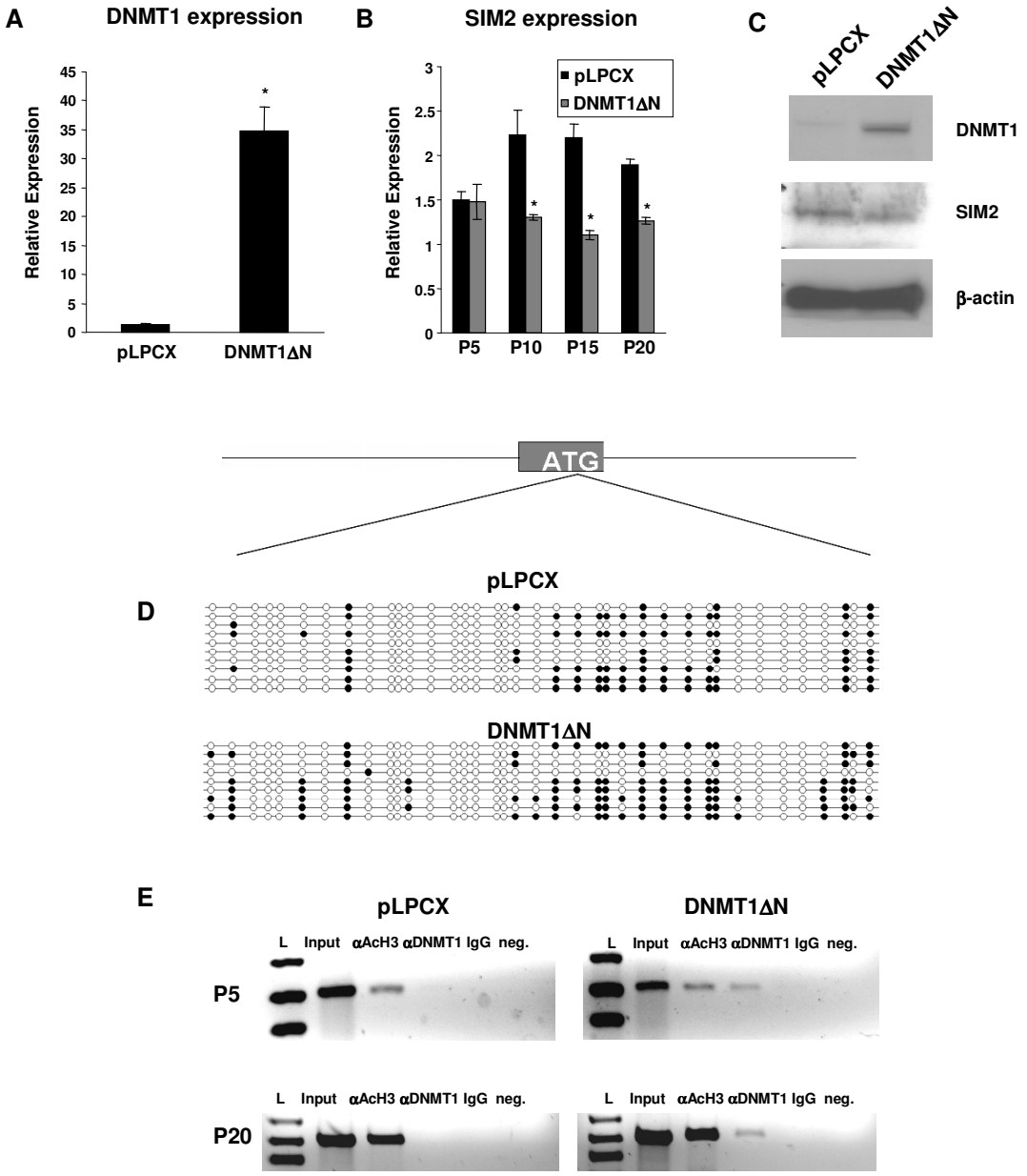

Figure 12

Overexpression of DNMT1 methylates and represses the SIM2 gene. (A) Expression of DNMT1 in MCF10A cells stably transduced with vector control (pLPCX) or DNMT1ΔN by real time RT-PCR. *Asterisk,* DNMT1 levels are significantly higher in DNMT1ΔN-transduced cells compared to control ($p = 0.001$). (B) Expression of SIM2 in MCF10A cells stably transduced with vector control (pLPCX) or DNMT1ΔN at successive passage numbers by real time RT-PCR. *Asterisk,* SIM2 levels are significantly reduced in DNMT1ΔN-transduced cells compared to control ($p \leq 0.03$). (C) Western blot for DNMT1, SIM2 and β-actin in MCF10A cells stably transduced with vector control or DNMT1ΔN. (D) Bisulfite sequencing of ATG start region in MCF10A cells stably transduced with vector control (pLPCX) or DNMT1ΔN. (E) Chromatin immunoprecipitation of acetylated histone 3 (AcH3) and DNMT1 on the SIM2 gene at the ATG start region.

Methylation of SIM2 does not correlate with expression in breast cancer

As an alternative method to analyze the role of methylation in SIM2 expression, a sampling of human breast tumor tissue was utilized. By methylation-specific PCR, SIM2 was determined to be partially methylated in 53% of breast tumors in the CpG island within exon 1 (Figure 13A). SIM2 was down-regulated in 43% of breast cancer samples; however, expression did not correlate with methylation status (Figure 13B). This result is consistent with the minimal effect of methylation on SIM2 expression seen in the MCF10A cells overexpressing DNMT1.

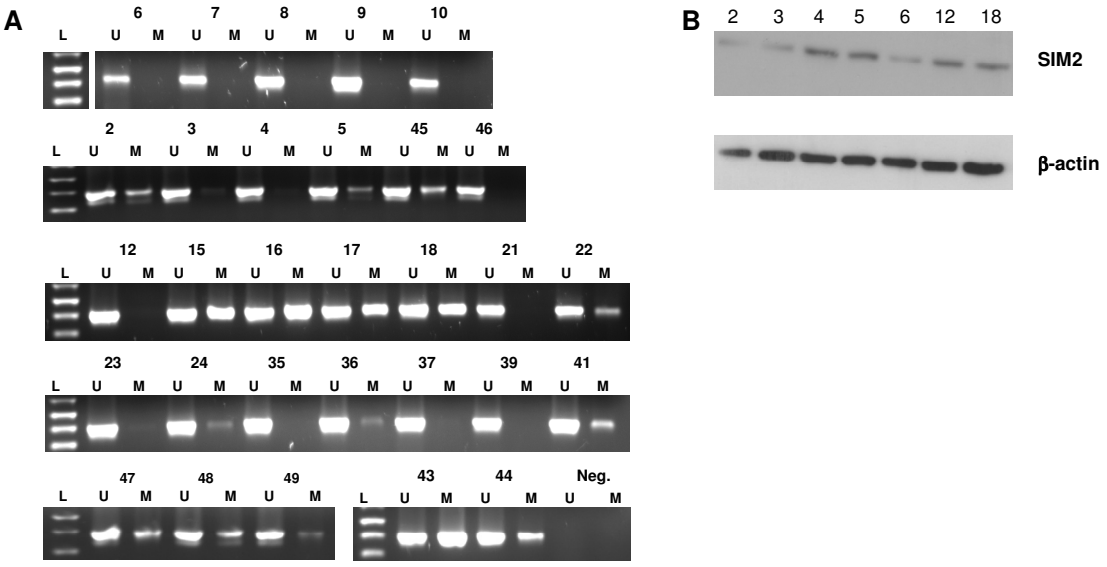

Figure 13
Methylation and expression of SIM2 in breast tumor samples. (A) Methylation-specific PCR analysis of ATG start region of SIM2. (B) Representative Western blot for SIM2 and β-actin in breast tumor samples.

CHAPTER IV

RESULTS: RAS-NOTCH-C/EBPβ PATHWAY

Oncogenic transformation decreases SIM2 expression

Since epigenetic mechanisms were not sufficient for SIM2 silencing, we sought to identify other pathways leading to SIM2 down-regulation. To model different tumor types, the normal immortalized breast cell line, MCF10A, was stably transduced with an empty vector control, an HRAS or a c-MYC expression construct. The HRAS- and c-MYC-transduced cells rapidly underwent a change in morphology. Normal MCF10A cells are large and primarily ovoid cells; however, after introduction of HRAS, the cells became small and irregularly-shaped (Figure 14A). c-MYC overexpression, on the other hand, resulted in a spindle-shaped morphology. The control MCF10A cells also retain contact inhibition, whereas HRAS- and c-MYC-overexpressing MCF10A cells easily grow over one another. HRAS-overexpression was associated with a larger decrease in SIM2 mRNA compared to c-MYC (Figure 14B), although both led to decreased protein levels as determined by Western blot (Figure 14C). The reduced SIM2 protein levels were confirmed by immunofluorescence in the HRAS-overexpressing cells (Figure 14D).

Ras activates Notch in MCF10A cells

Notch is an important mediator of RAS-induced tumorigenesis in the mammary gland (46, 57). To confirm whether Notch was activated in HRAS-overexpressing

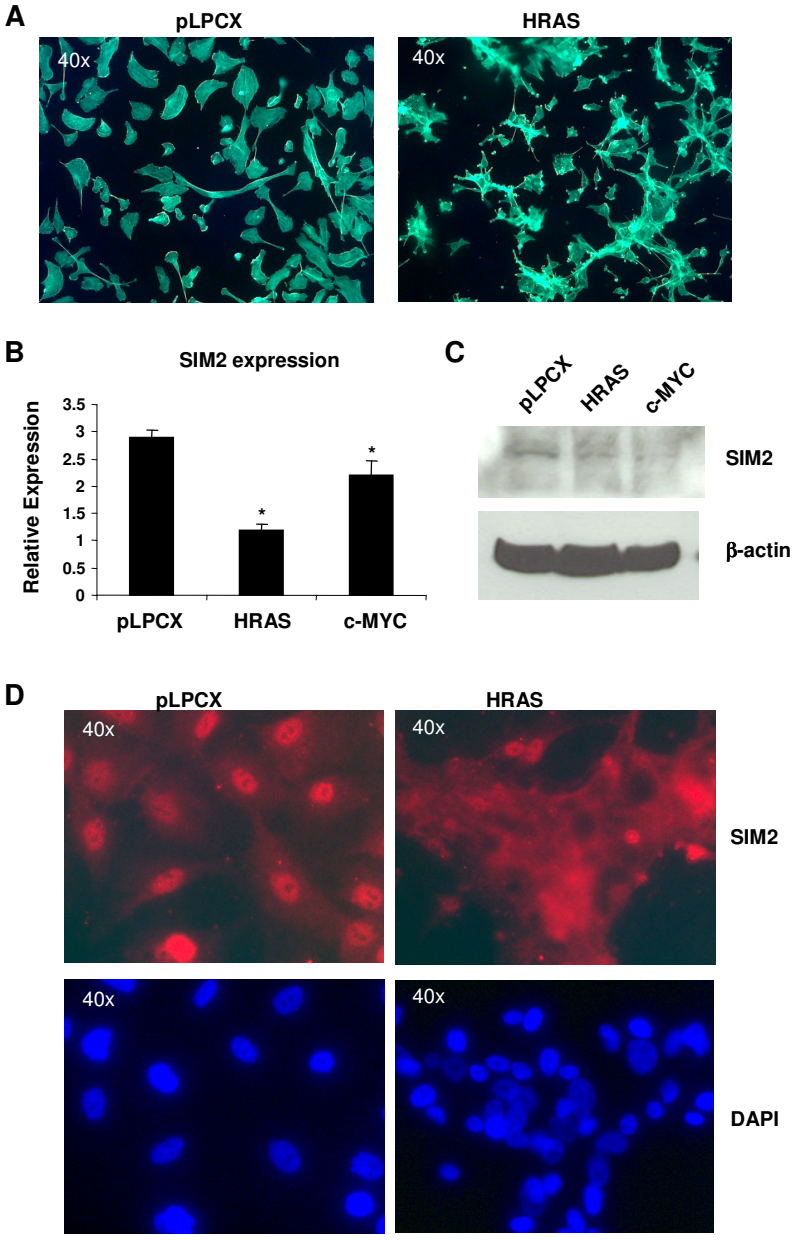

Figure 14

HRAS and c-MYC overexpression down-regulate SIM2 expression. (A) Morphology of MCF10A cells transduced with HRAS compared to vector control (pLPCX). (B) SIM2 expression in MCF10A cells stably transduced with vector only, HRAS or c-MYC by real time RT-PCR. *Asterisk*, SIM2 expression was significantly reduced in oncogene-transduced MCF10A cells compared to control (HRAS: $p = 0.0002$; c-MYC: $p = 0.04$). (C) Western blot for SIM2 protein in HRAS- or c-MYC-overexpressing MCF10A cells versus vector only control cells (pLPCX). (D) SIM2 protein immunofluorescence in HRAS-overexpressing MCF10A cells and control cells.

MCF10A cells, we evaluated the expression of several Notch target genes, including HES1, HEY1 and HEY2 (Figure 15A-C). Levels of these Notch targets were elevated in the HRAS-overexpressing cells, indicating Notch activation. To determine whether SIM2 was a Notch target, chromatin immunoprecipitation (ChIP) was used to assay Notch binding to a region near the transcriptional start site of the SIM2 promoter (Figure 15D). Interestingly, increased NOTCH1 binding to this region of the SIM2 promoter was detectable in HRAS-overexpressing cells.

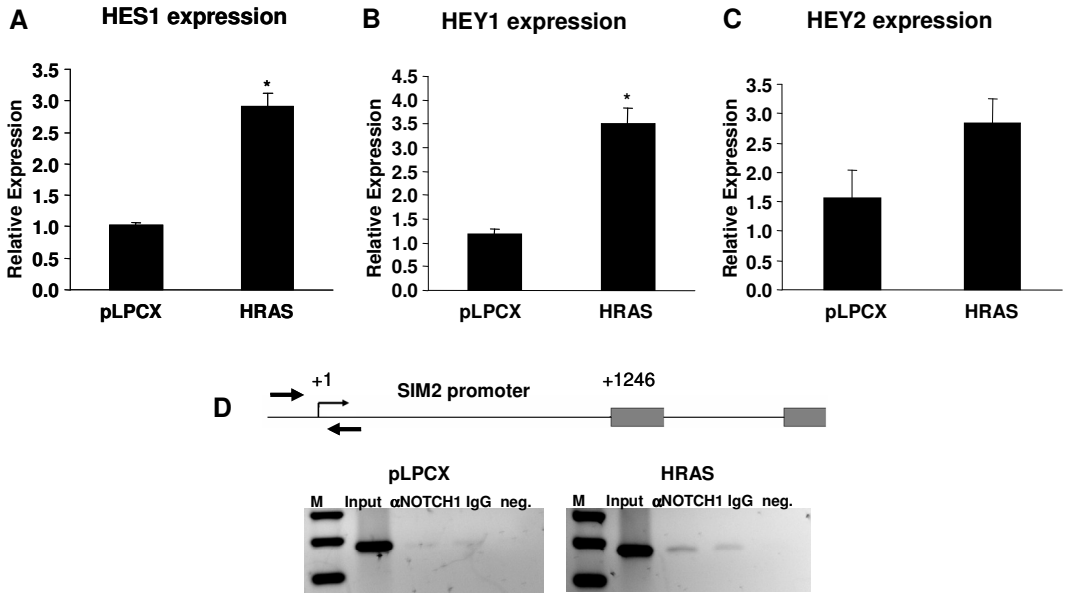

Figure 15
Notch signaling is activated in HRAS-overexpressing MCF10A cells. (A) Expression of HES1 in HRAS-overexpressing or control MCF10A cells by real time RT-PCR. *Asterisk,* HES1 levels are significantly higher in HRAS-transduced cells compared to control (p = 0.0004). (B) Expression of HEY1 in HRAS-overexpressing or control MCF10A cells by real time RT-PCR. *Asterisk,* HEY1 levels are significantly higher in HRAS-transduced cells compared to control (p = 0.001). (C) Expression of HEY2 in HRAS-overexpressing or control MCF10A cells by real time RT-PCR. Difference did not achieve significance (p = 0.053). (D) ChIP analysis for NOTCH1 on the SIM2 promoter in HRAS-overexpressing cells compared to control (pLPCX). Above, a diagram of the SIM2 promoter and primer position is shown for reference.

Notch represses SIM2 through a CBF1-independent mechanism

The association between HRAS overexpression, increased NOTCH1 binding to the SIM2 promoter and decreased SIM2 expression led us to further investigate a role for Notch signaling in SIM2 repression. An expression construct containing the coding region of activated NOTCH1 (NOTCH1 intracellular domain or NICD) was constructed and tested for the ability to activate expression from a HES1 promoter-controlled reporter. As expected (112), reporter activity was increased in cells co-transfected with either NICD or NICD plus CBF1, but not in CBF1 cells alone (Figure 16A). Transient transfections were performed using various SIM2 promoter constructs upstream of a luciferase reporter. The full length construct contained the SIM2 promoter from -1380 to +1805, relative to the transcriptional start site. Various deletion constructs of the SIM2 promoter were made and tested for activity in cells co-transfected with the NICD. Activated NOTCH1 repressed the activity of all SIM2 promoter constructs analyzed (Figure 16B). Coupled with our ChIP results, these data suggest that NICD represses SIM2 expression through direct interactions with the SIM2 promoter. This was confirmed by ChIP analysis of transiently transfected cells receiving the full length SIM2 reporter construct plus NICD or vector control (Figure 16C). The NICD was found to bind directly to the transfected SIM2 promoter, consistent with the observed binding in the HRAS-overexpressing MCF10A cells. Attempts to overexpress the NICD in MCF10A cells were unsuccessful, consistent with previous reports (113), preventing a direct evaluation of the effect of elevated Notch signaling on SIM2 expression.

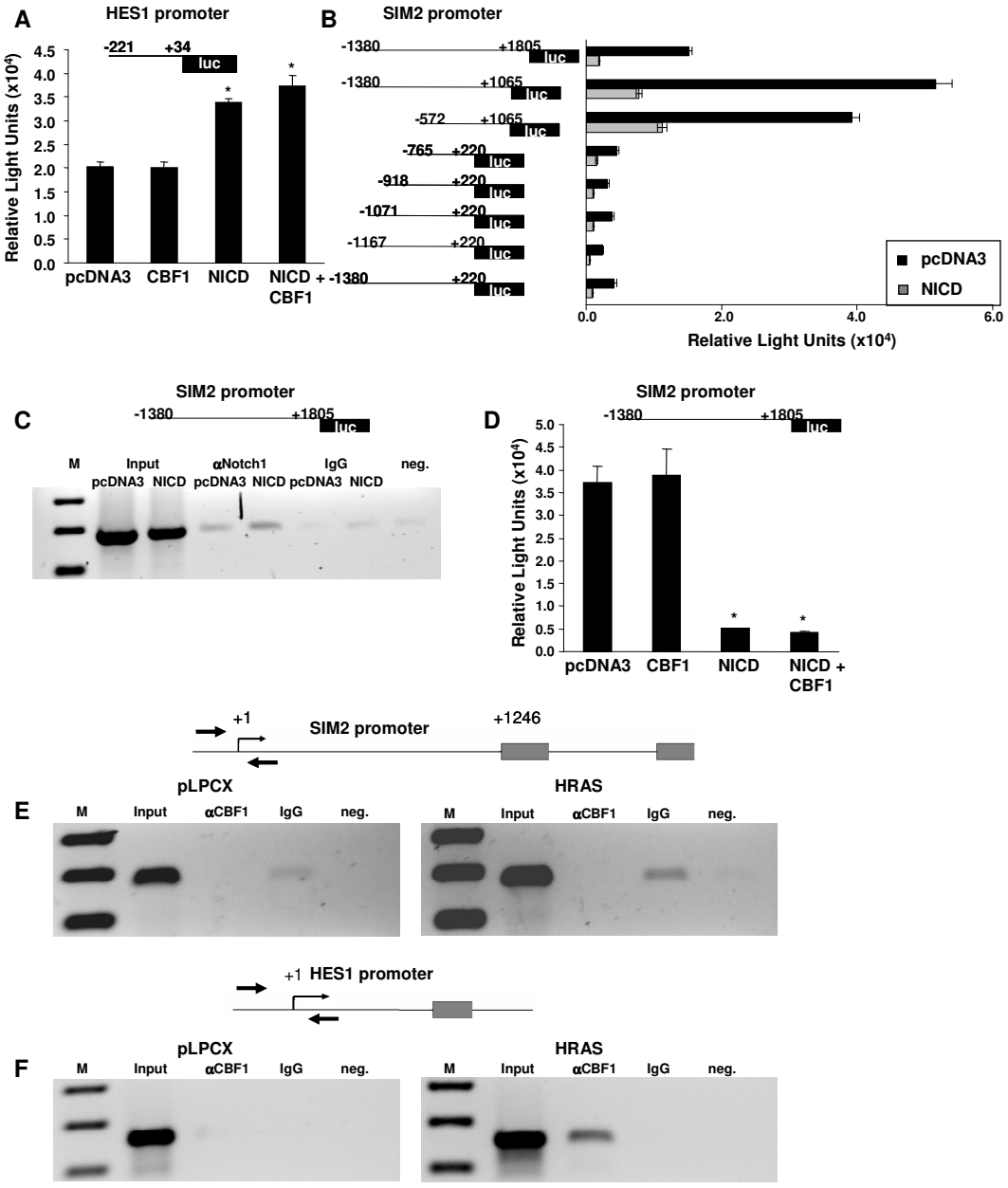

Figure 16

NICD binds and represses the SIM2 promoter through a CBF1-independent mechanism. (A) Luciferase activity of HES1 promoter co-transfected with vector control (pcDNA3), NICD, CBF1 or both. *Asterisk,* HES1 promoter activity is significantly elevated by NICD and NICD plus CBF1 compared to vector control ($p \leq 0.001$). (B) Luciferase activity after transient transfection of NICD on SIM2 promoter constructs compared to vector control (pcDNA3). (C) ChIP analysis of Notch1 on full length transfected SIM2 promoter after co-transfection with NICD or vector control. (D) Luciferase activity after transient transfection of NICD and CBF1 on full length SIM2 promoter versus vector control. *Asterisk,* SIM2 promoter activity is significantly reduced by NICD and NICD plus CBF1 compared to vector control ($p \leq 0.0008$). (E) ChIP for CBF1 on endogenous SIM2 promoter in control and HRAS-overexpressing MCF10A cells. (F) ChIP for CBF1 on endogenous HES1 promoter. Promoters are diagrammed above for reference.

Canonical Notch signaling acts through CBF1 and functions to direct developmental pathways (114). Recently, CBF1-independent mechanisms of Notch signaling that contribute to cell fate determination have been identified (52). To explore which mechanism Notch utilizes to silence SIM2 expression, we co-transfected CBF1 and the full length SIM2 promoter into HEK293T cells with and without NICD (Figure 16D). Introduction of CBF1 had no effect on SIM2 promoter activity, suggesting a CBF1-independent mechanism of SIM2 repression by NOTCH1. Further, we noted the absence of CBF1 on the SIM2 promoter in either the HRAS-overexpressing or control cells by ChIP (Figure 16E). Sufficient PCR cycles were added until a band in the IgG control was detected to make sure that no CBF1 binding was being overlooked. CBF1 was clearly detectable on the HES1 promoter in the HRAS-overexpressing cells as a positive control (Figure 16F). CBF1 was not detected on the HES1 promoter in vector control cells, most likely due to the more compacted chromatin state in the absence of HRAS-driven NOTCH1 activation (115).

C/EBPβ is activated in HRAS-overexpressing MCF10A cells

SIM2 expression was partially restored in HRAS-transformed MCF10A cells treated with N-[N-(3,5-difluorophenacetyl)-l-alanyl]-S-phenylglycine t-butyl ester (DAPT), an inhibitor of Notch proteolysis and subsequent nuclear translocation (data not shown). Since inhibition of Notch cleavage was insufficient to restore SIM2 expression to control levels, other effectors of Ras signaling seemed likely to be involved in SIM2 regulation. C/EBPβ is known to play an important role in mammary development and

has recently been shown to be a critical mediator of Ras-induced tumorigenesis (47, 62). We first evaluated the expression of C/EBPβ in the control and HRAS-overexpressing MCF10A cell lines (Figure 17A). C/EBPβ mRNA expression was slightly but significantly ($p = 0.02$) elevated in HRAS-overexpressing cells. Western analyses revealed similar levels of LAP in control and HRAS-overexpressing cells; however, increased levels of LIP were present in HRAS-overexpressing cells (Figure 17B). HRAS also mediates activation of C/EBPβ at the post-translational level (68); thus, levels of C/EBPβ phosphorylated at threonine-235 were analyzed by Western blot and immunofluorescence. These results indicated that phosphorylated C/EBPβ levels were elevated in the HRAS-overexpressing cells compared to control cells (Figure 17B and 17C).

To further investigate the role of C/EBPβ in SIM2 gene silencing in HRAS-overexpressing cells, we analyzed C/EBPβ binding to the SIM2 promoter by ChIP. Similar to NOTCH1, C/EBPβ associated with the SIM2 promoter near the transcriptional start site in HRAS-overexpressing MCF10A cells but not in control MCF10A cells (Figure 17D).

C/EBPβ represses SIM2 promoter activity

A single C/EBPβ mRNA can be translated into three different proteins: full length liver-enriched activating protein 1 (LAP1), liver-enriched activating protein 2 (LAP2) and the dominant negative liver-enriched inhibiting protein (LIP). An initial transient transfection with the full length SIM2 promoter revealed that LAP1 and LAP2

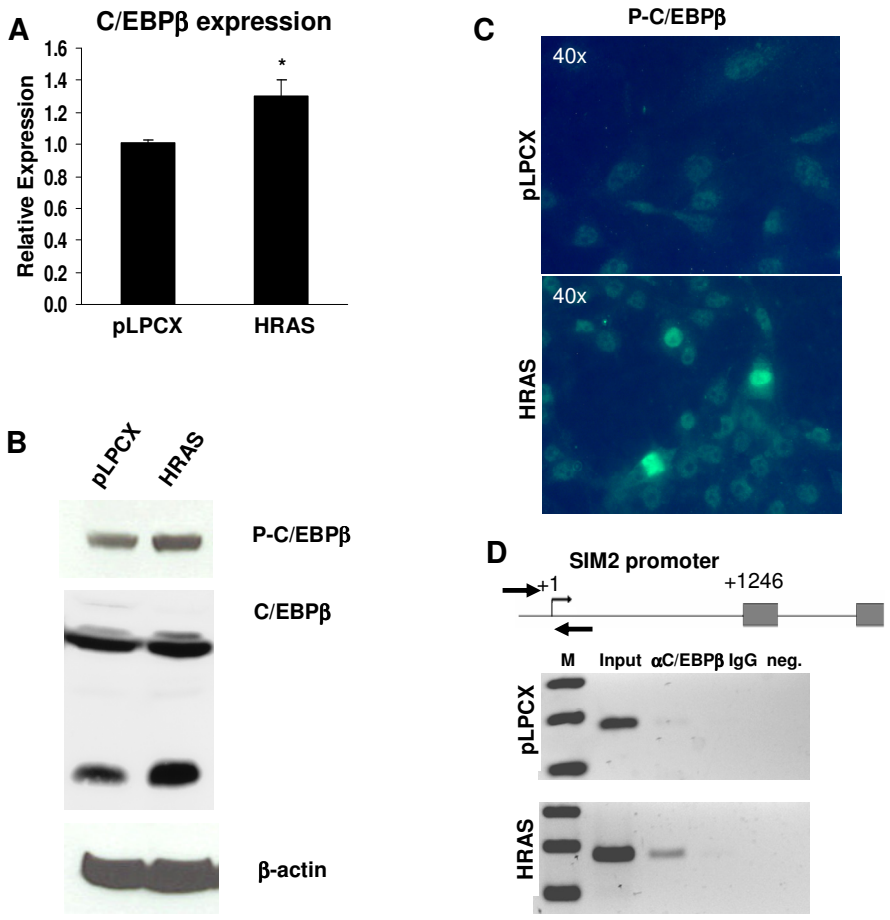

Figure 17
C/EBPβ is activated in HRAS-overexpressing MCF10A cells. (A) C/EBPβ expression in HRAS-overexpressing and control (pLPCX) MCF10A cells by real time RT-PCR. *Asterisk*, C/EBPβ levels were significantly higher in HRAS-overexpressing cells compared to control (p = 0.02). (B) Western blot for phosphorylated C/EBPβ and total C/EBPβ in MCF10A cells stably transduced with HRAS or vector control.
(C) Immunofluorescence for phospho-C/EBPβ in HRAS-overexpressing MCF10A cells and control cells. (D) ChIP analysis for C/EBPβ on the SIM2 promoter in HRAS-overexpressing cells compared to control (pLPCX).

repressed SIM2 promoter activity while LIP had little effect (Figure 18A). Western blot confirmed successful expression of each isoform (Figure 18B).

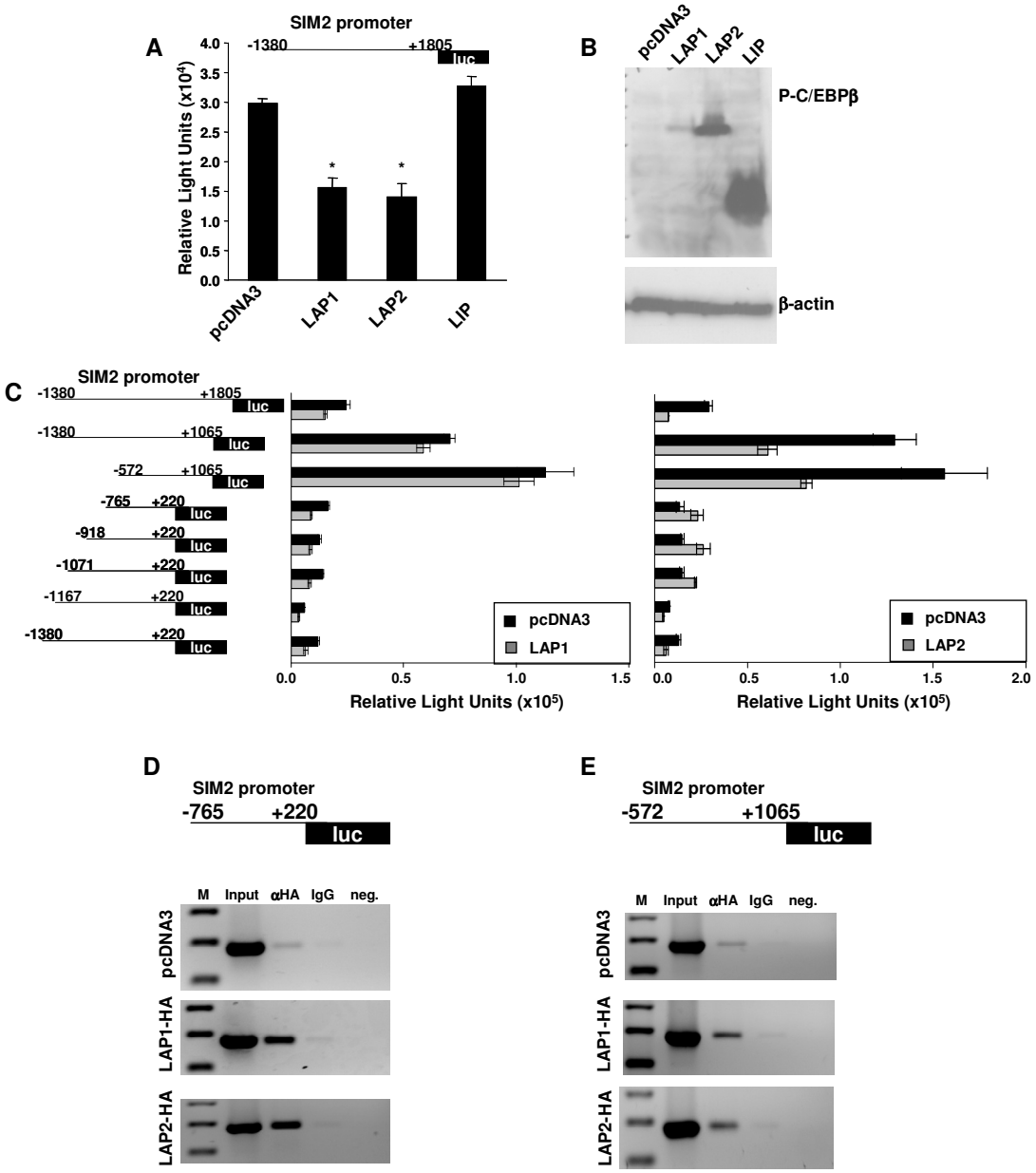

Figure 18

C/EBPβ binds and represses SIM2 promoter. (A) Luciferase activity after transient transfection of three C/EBPβ isoforms on full length SIM2 promoter construct compared to pcDNA3 control. *Asterisk*, SIM2 promoter activity is significantly reduced by LAP1 and LAP2 compared to control ($p \leq 0.001$). (B) Western blot for phospho-C/EBPβ and β-actin in cells transiently transfected with C/EBPβ isoforms. (C) Luciferase activities after transient transfections of LAP1 and LAP2 on various SIM2 promoter constructs. (D-E) ChIP for transfected HA-tagged C/EBPβ isoforms on co-transfected SIM2 promoter constructs diagrammed above.

Further investigation found differing activities of LAP1 and LAP2 on the SIM2 promoter truncations (Figure 18C). LAP1 was able to repress the SIM2 promoter, except when the region from -765 to -572 was deleted (Figure 18C). LAP2 activated the promoter truncations containing sequence only between -1071 to +220 but repressed the promoter constructs which extended either further 5′ or 3′ (Figure 18C). This suggests that C/EBPβ isoforms have different activities on the SIM2 promoter, which may involve interactions with different cofactors. To explore these differences further, we performed ChIP analyses of transfected promoter constructs. On the -765 to +220 promoter construct, LAP1 repressed while LAP2 activated reporter activity. However, both C/EBPβ isoforms were able to bind to this construct (Figure 18D). On the -572 to +1065 promoter construct, LAP2 repressed reporter activity and LAP1 had no effect. Despite this difference, both isoforms showed reduced binding to the -572 to +1065 promoter construct (Figure 18E). These studies demonstrate that both of these C/EBPβ isoforms repress the SIM2 promoter but operate through distinct mechanisms.

Stable overexpression of C/EBPβ isoforms represses SIM2 expression in MCF10A cells

To confirm the effect of C/EBPβ on endogenous SIM2, we generated MCF10A cell lines stably overexpressing LAP1 and LAP2 (Figure 19A and 19C). SIM2 expression was reduced in both cell lines compared to vector control as determined by real time RT-PCR and Western blot (Figure 19B and 19C). We also performed ChIP analysis of the SIM2 promoter in the LAP1 and LAP2 overexpressing MCF10A cell

lines compared to the vector only control. LAP1 was able to bind to the endogenous SIM2 promoter, while LAP2 binding was undetectable (Figure 19D). This was not due to experimental error since we observed LAP2 on the c-FOS promoter as a positive control (Figure 19E).

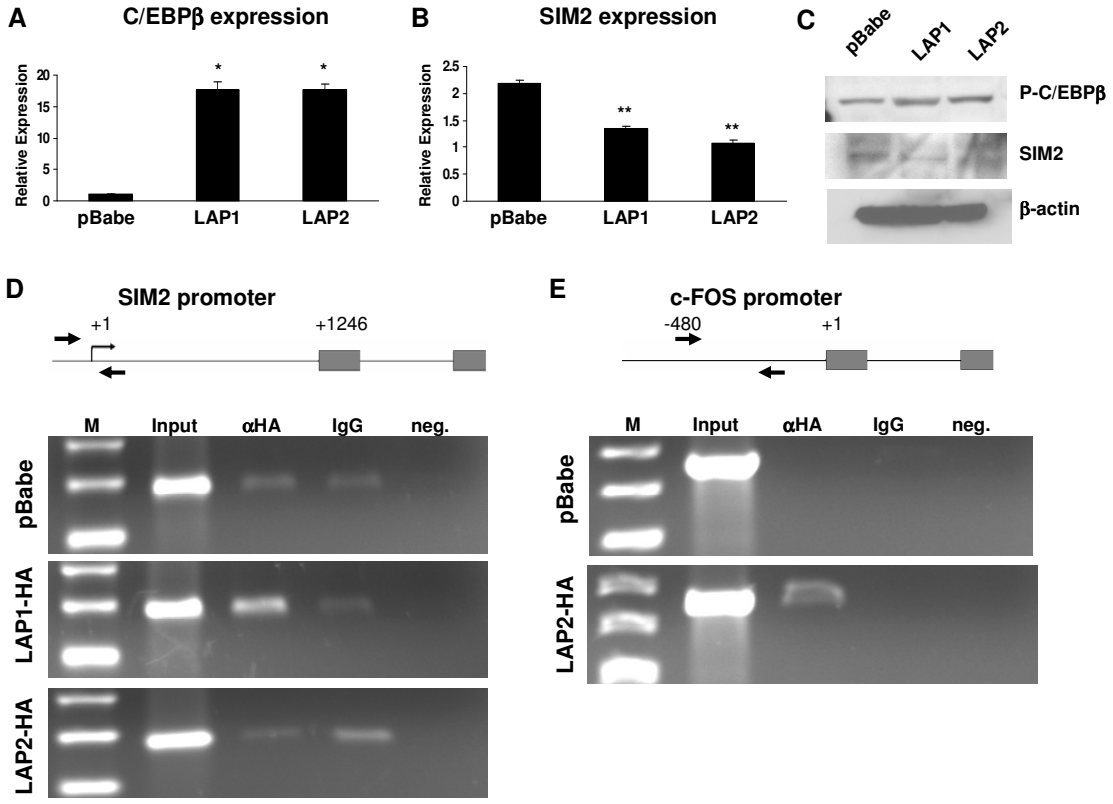

Figure 19
LAP1 and LAP2 repress SIM2 expression when overexpressed in MCF10A cells.
(A-B) Expression by real time RT-PCR in MCF10A cells stably transduced with LAP1, LAP2 or pBabe vector control. *Asterisk*, C/EBPβ expression is significantly elevated in LAP1- and LAP2-transduced cells compared to control ($p \leq 0.0002$). *Double asterisk*, SIM2 levels are significantly reduced in LAP1- and LAP2-transduced cells compared to control ($p \leq 0.0002$). (C) Western blot for SIM2 and phospho-C/EBPβ isoforms in stably transduced MCF10A cells. (D) ChIP analysis for C/EBPβ on endogenous SIM2 promoter in MCF10A cells stably overexpressing LAP1 or LAP2 (HA-tagged) versus control MCF10A cells (pBabe). (E) ChIP analysis for LAP2 on c-FOS promoter as positive control. Diagrams above show promoters and primer positions for reference.

C/ebpβ represses Sim2 *in vivo*

C/ebpβ$^{-/-}$ mice are viable but display immune system defects, abnormal brown adipose tissue function, skin irregularities and female infertility (59). Lack of C/ebpβ in the mammary gland leads to impaired ductal morphogenesis, resulting in enlarged ducts with decreased branching (62). We found that Sim2 is overexpressed in C/ebpβ$^{-/-}$ mouse mammary glands (Figure 20A). Immunostaining for Sim2 demonstrated that Sim2 is expressed in a punctate pattern within the luminal epithelium in wild-type glands, while its expression is higher and more uniform in C/ebpβ$^{-/-}$ glands (Figure 20B). Two cell lines were established from C/ebpβ$^{-/-}$ mouse mammary epithelial cells based on their phenotype in culture. One line is morphologically similar to normal mammary epithelial (flat) cells in culture; the second line forms foci in culture (unpublished data). Sim2 levels were found to be extremely elevated in the C/ebpβ$^{-/-}$ flat cells compared to the foci-forming cells (Figure 20C). The effect of reintroducing each of the three C/ebpβ isoforms on Sim2 expression in the C/ebpβ$^{-/-}$ flat cells was analyzed. Real time RT-PCR and Western blot confirmed that each isoform of C/ebpβ was being expressed in the cells (Figure 20D and 20F). However, there was some mLIP detected by Western blot in each of these cell lines. This could be due to cleavage either *in vivo* or *in vitro* during protein preparation (116). Sim2 expression was reduced in each of the cell lines in which C/ebpβ expression had been re-established at the RNA and protein levels (Figure 20E and 20F). It was surprising that the murine LIP isoform repressed Sim2 expression and was the most effective isoform as no Sim2 protein was detected in the C/ebpβ$^{-/-}$ cell

line overexpressing mLIP. This is in contrast to the human cell lines, in which the dominant negative LIP had no effect on SIM2 promoter activity.

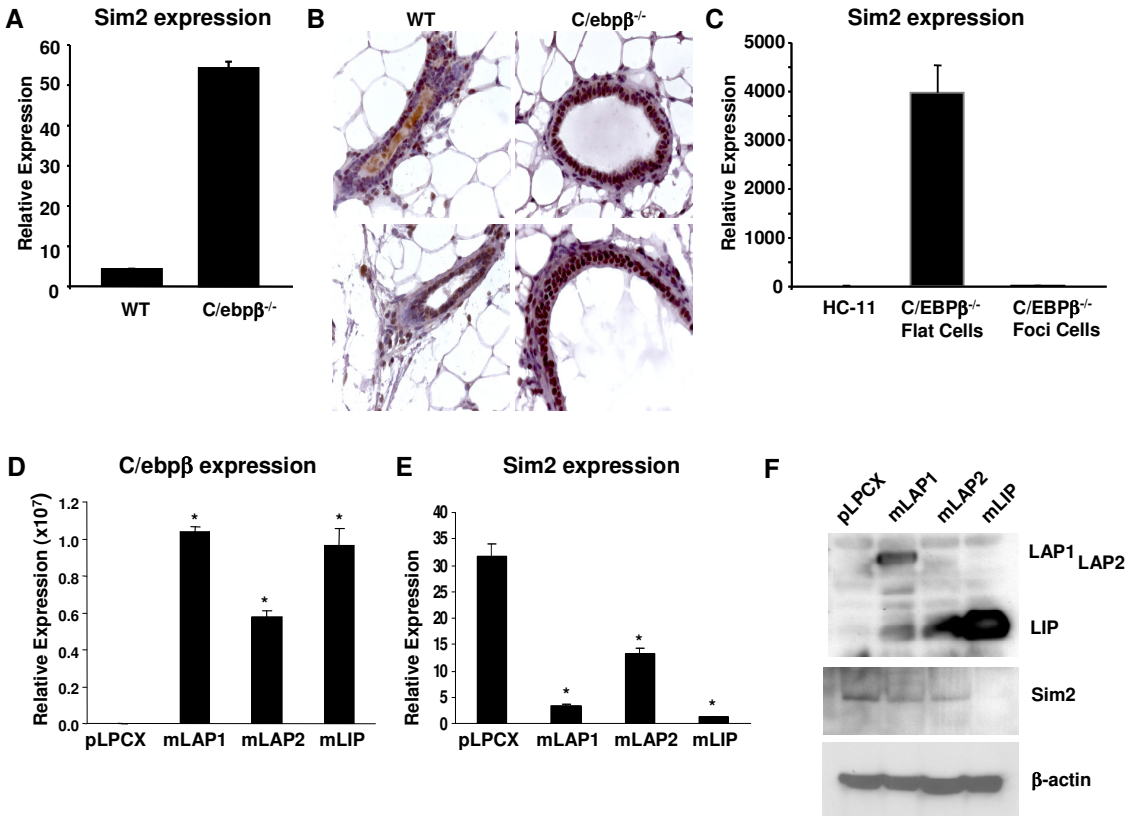

Figure 20
C/ebpβ represses Sim2 in a mouse model. (A) Sim2 expression in C/ebpβ$^{-/-}$ mammary glands by real time RT-PCR. (B) Immunohistochemistry for Sim2 expression in C/ebpβ-/- mammary glands compared to wild-type glands. (C) Expression of Sim2 in flat cells and foci-forming cells derived from C/ebpβ-/- mammary glands by real time RT-PCR. (D) Expression of C/ebpβ in C/ebpβ$^{-/-}$ flat cells in which mLAP1, mLAP2 or mLIP has been stably transduced by real time RT-PCR. *Asterisk*, C/ebpβ levels are significantly higher in flat cells transduced with mLAP1, mLAP2 and mLIP ($p \leq 0.001$). (E) Expression of Sim2 in C/ebpβ$^{-/-}$ flat cells in which mLAP1, mLAP2 or mLIP has been stably transduced by real time RT-PCR. *Asterisk*, Sim2 levels are significantly lower in flat cells transduced with mLAP1, mLAP2 and mLIP ($p \leq 0.001$). (F) Western blot for C/ebpβ isoforms and Sim2 in C/ebpβ$^{-/-}$ flat cells in which mLAP1, mLAP2 or mLIP has been stably transduced.

CHAPTER V

RESULTS: INTERACTIONS BETWEEN NFκB AND SIM2

SIM2s-overexpressing MDA435 cells show increased drug sensitivity

We have identified SIM2 as a tumor suppressor gene, actively down-regulated by several mechanisms in breast cancer. We thus sought to better characterize the biological impact of loss/gain of SIM2 on cancer cells. Chemoresistance is a major barrier to successful tumor treatment, causing failure in as many as 90% of cases of metastatic cancer (88). To explore the effect of expression of SIM2 on chemoresistance, MDA435 cells overexpressing SIM2s or vector control were treated with 1.5 mM 5-fluoruracil (5-FU) or 1 μM doxorubicin (DOX). Cells were counted on the day of treatment (day 0) and for three days thereafter. SIM2s-overexpressing MDA435 cells were significantly more sensitive to 5-FU after two days ($p = 0.01$) and by the third day SIM2s-overexpressing cells had half the number of control cells ($p = 0.0004$) (Figure 21A). Similarly, SIM2s-overexpressing MDA435 cells showed increased sensitivity to DOX after two days ($p = 0.03$). By the third day, SIM2s-overexpressing and control cells were all dead, so cell counts were not done. To confirm these results, an MTT cell viability assay was conducted. After 24 hours of doxorubicin treatment, MDA435 SIM2s-overexpressing cells were significantly less viable compared to control cells ($p < 0.0007$) (Figure 21B). 5-Fluorouracil treatment resulted in decreased viability in MDA435 SIM2s-overexpressing cells compared to control cells after 36 hours ($p < 0.002$).

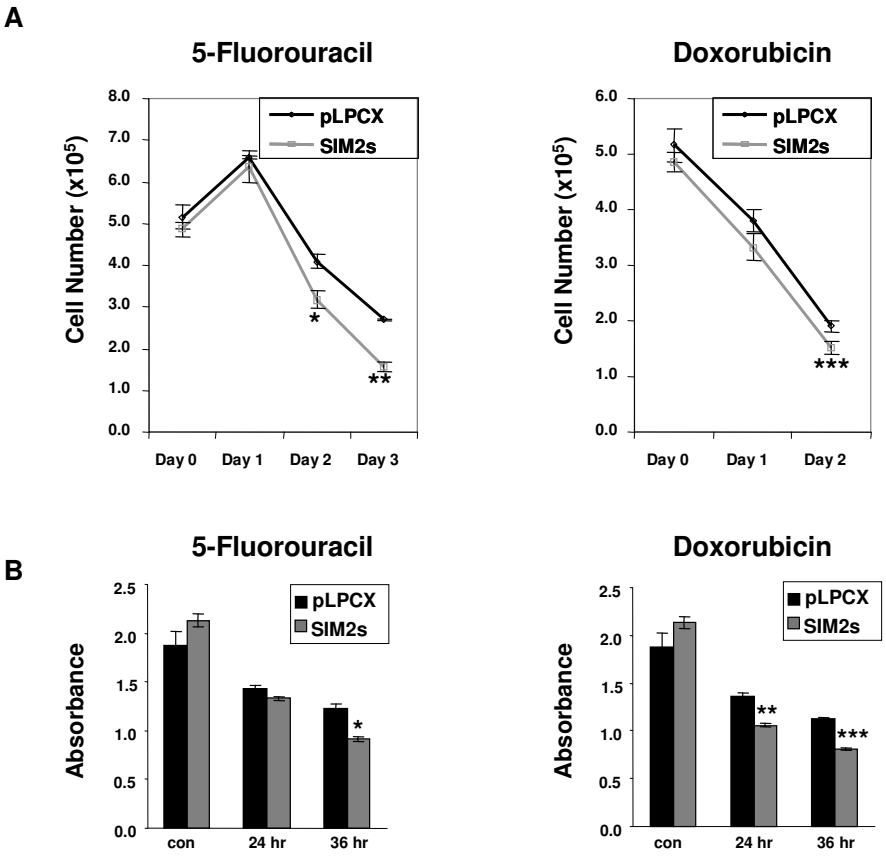

Figure 21

MDA435 cells overexpressing SIM2s show increased sensitivity to antineoplastic drugs. (A) Cell counts in MDA435 control cells and cells overexpressing SIM2s treated with 1.5 mM 5-fluorouracil or 1 μM doxorubicin on the day of treatment (day 0) and each day thereafter indicated. *Asterisk*, Cell number was significantly lower in SIM2s-overexpressing cells compared to control after 2 days of treatment with 5-fluorouracil ($p = 0.01$). *Double asterisk*, Cell number was significantly lower in SIM2s-overexpressing cells compared to control cells on day 3 of treatment with 5-fluorouracil ($p = 0.0004$). *Triple asterisk*, Cell number was significantly lower in SIM2s-overexpressing cells compared to control on day 2 of treatment with doxorubicin ($p = 0.03$). (B) MTT cell viability assay in control MDA435 cells and MDA435 SIM2s-overexpressing cells after treatment with 1.5 mM 5-fluorouracil or 1 μM doxorubicin. *Asterisk*, Cell viability is significantly reduced in SIM2s-overexpressing cells compared to control cells treated with 5-fluorouracil after 36 hours ($p < 0.002$). *Double asterisk,* Cell viability is significantly reduced in SIM2s-overexpressing cells compared to control cells treated with doxorubicin after 24 hours ($p < 0.0007$) and, *triple asterisk*, after 36 hours ($p = 0.00002$).

SIM2s inhibits ABCB5 expression

Inflammation was linked to cancer formation as early as 1863 by Rudolf Virchow (117). More recently, alterations in drug metabolism and chemoresistance have been linked to inflammatory processes (105). Particularly, the ABC family of transporters plays a significant role in drug resistance. To identify whether ABC transporters were contributing to the increased chemosensitivity observed in SIM2s-overexpressing MDA435 cells, expression of a selection of ABC genes known to be involved in drug resistance was evaluated in control and SIM2s-overexpressing cells (Figure 22A). ABCB5 expression was found to be reduced by SIM2s expression in MDA435 cells. ABCB5 expression has recently been shown to contribute to chemoresistance to 5-fluorouracil and doxorubicin in human malignant melanoma cell lines (94, 95). Because NFκB is a major link between inflammation, chemoresistance and regulation of xenobiotic metabolism genes, we explored the regulation of the ABCB5 promoter by NFκB and SIM2. A region of the ABCB5 promoter from -2486 to +513 was cloned upstream of the luciferase reporter gene and co-transfected with NFκB p65, SIM2s or both (Figure 22B). NFκB activated this promoter construct ($p = 0.04$), whereas SIM2s had no effect by itself but did prevent activation by NFκB ($p = 0.01$). To explore the interaction between SIM2 and the ABCB5 promoter, we performed ChIP analysis of the ABCB5 promoter in MDA435 control cells and SIM2s-overexpressing cells. SIM2 was found to be present at the ABCB5 promoter and present at much higher levels in the cells overexpressing SIM2s (Figure 22C).

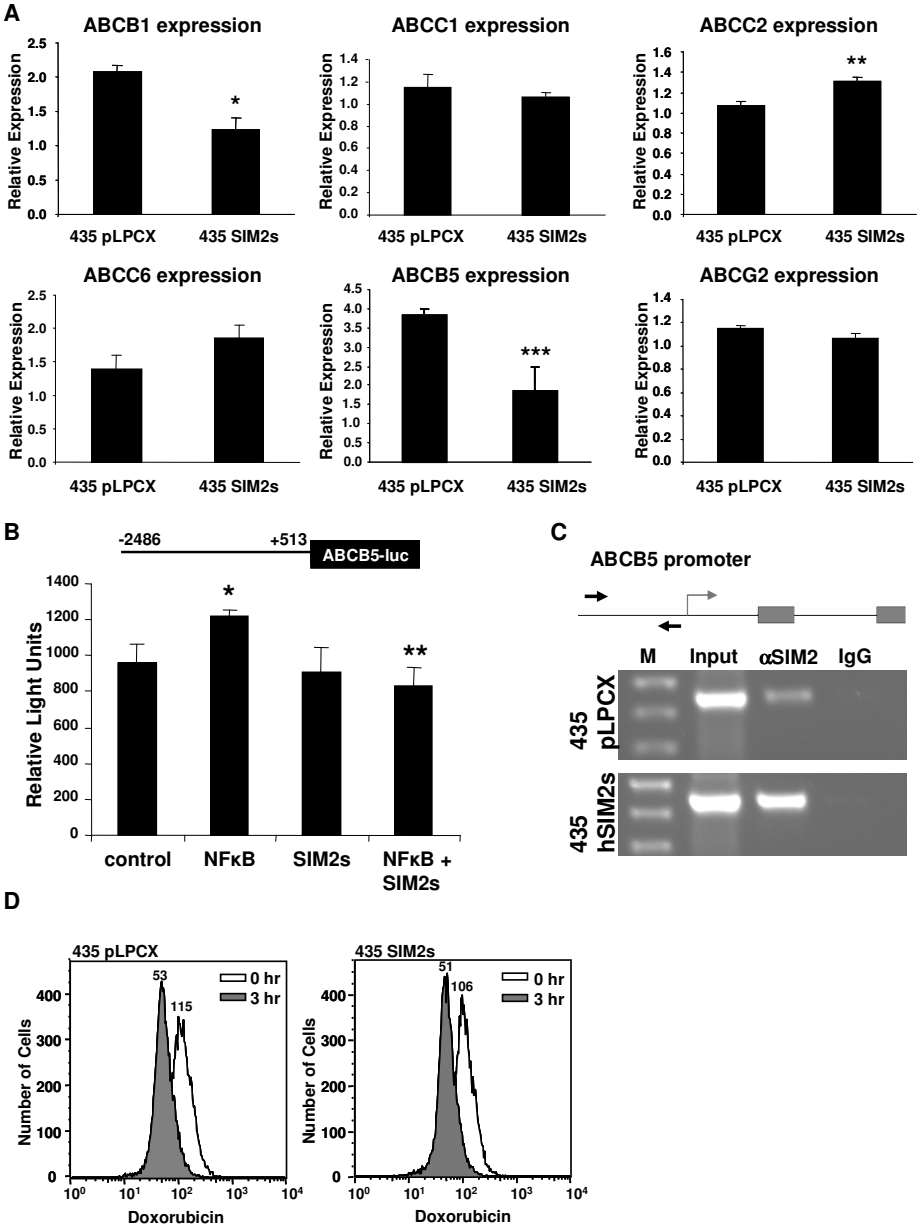

Figure 22

SIM2s inhibits ABCB5 expression. (A) Expression in MDA435 control cells and cells overexpressing SIM2s by real time RT-PCR. *Asterisk,* ABCB1 expression is significantly reduced in MDA435 cells overexpressing SIM2s compared to control (*$p < 0.02$). *Double asterisk,* ABCC2 expression is significantly elevated in the MDA435 cells overexpressing SIM2s compared to control (**$p < 0.02$). *Triple asterisk,* ABCB5 expression is significantly reduced in MDA435 cells overexpressing SIM2s compared to control (***$p < 0.04$). (B) ABCB5 promoter activity in MDA435 cells co-transfected with the ABCB5 promoter cloned upstream of the luciferase gene and NFκB p65 and/or SIM2s. Diagram of ABCB5 promoter construct shown above for reference. *Asterisk*, NFκB significantly activates ABCB5 promoter activity compared to control ($p < 0.04$). *Double asterisk*, SIM2s significantly reduces activation of the ABCB5 promoter by NFκB compared to ABCB5 promoter activity in the presence of NFκB alone ($p = 0.01$). (C) ChIP for SIM2 on ABCB5 promoter in MDA435 control cells and SIM2s-overexpressing cells. (D) Flow cytometry for doxorubicin fluorescence of MDA435 control (pLPCX) cells and SIM2s-overexpressing cells treated with 10 μM doxorubicin for 30 minutes, washed and incubated for 0 or 3 hours to allow doxorubicin efflux. Median fluorescence is labeled above each peak.

To determine the role of SIM2s-mediated repression of ABCB5 in the observed increase in sensitivity to doxorubicin, MDA435 cells were dosed with 10 μM doxorubicin for 30 minutes and then incubated for 0 or 3 hours to allow for doxorubicin efflux. Flow cytometry was used to measure doxorubicin content after no efflux and 3 hours of efflux (Figure 22D); however, no difference was observed between MDA435 control cells and SIM2s-overexpressing cells, suggesting that other mechanisms were involved in the increased chemosensitivity to doxorubicin.

NFκB signaling activates ABCB5 expression

Since NFκB activated the ABCB5 promoter in transient transfection assays, MDA435 cells were stably transduced with the inhibitor of kappaB superrepressor (IκB-SR), and ABCB5 expression was analyzed by real time RT-PCR (Figure 23A). ABCB5 expression was decreased in MDA435 cells overexpressing IκB-SR. Inhibition of NFκB signaling was confirmed by immunofluorescent staining for NFκB p50, which showed reduced nuclear staining in MDA435 cells overexpressing IκB-SR compared to control MDA435 cells (Figure 23B). NFκB was bound to the ABCB5 promoter in control MDA435 cells by ChIP and was lost when NFκB signaling was inhibited by IκB-SR overexpression (Figure 23C). Interestingly, SIM2 overexpression resulted in an equal loss of NFκB from the ABCB5 promoter (Figure 23C).

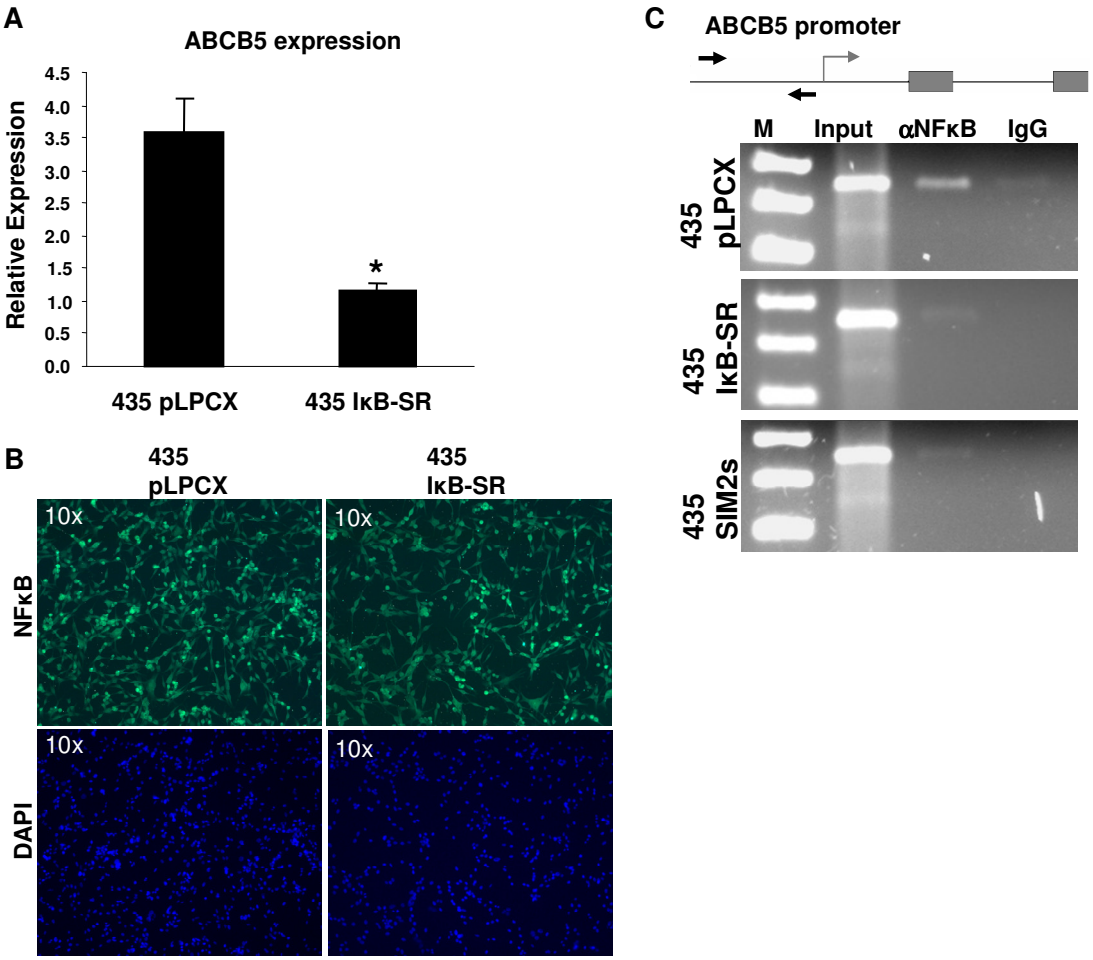

Figure 23
NFκB activates ABCB5 expression. (A) ABCB5 expression in MDA435 control cells and cells overexpressing IκB-SR by real time RT-PCR. *Asterisk*, ABCB5 expression is significantly reduced by overexpression of IκB-SR compared to control ($p < 0.005$). (B) Immunofluorescence for NFκB in MDA435 cells stably transduced with control vector (pLPCX) or IκB-SR. (C) ChIP for NFκB on ABCB5 promoter in MDA435 control cells, IκB-SR-overexpressing cells and SIM2s-overexpressing cells.

NFκB represses SIM2 expression

To explore this possible relationship between SIM2 and NFκB, MDA435 cells were treated with the metal chelator and antioxidant pyrollidine dithiocarbamate (PDTC), which is a potent inhibitor of NFκB activation. PDTC treatment reduced nuclear NFκB levels by immunofluorescence (Figure 24A), and, at the same time, expression of SIM2 increased approximately 20-fold ($p = 0.0003$) (Figure 24B). To study the ability of NFκB to regulate SIM2 more specifically, the SIM2 promoter upstream of the luciferase gene was co-transfected with increasing amounts of NFκB p65. A dose-dependent repression of promoter activity was observed (Figure 24C). This was not a dominant negative effect as co-transfection of IκB-SR reversed the effect (Figure 24D). By chromatin immunoprecipitation analysis, NFκB p65 was found to bind to the SIM2 promoter around the transcriptional start site (Figure 24E).

We also assayed SIM2 levels in the MDA435 cells overexpressing IκB-SR and, as expected, found them to be elevated compared to control cells (Figure 25B). MCF10A cells are a normal immortalized breast epithelial cell line and express high levels of SIM2. The NFκB pathway was activated in MCF10A cells by stable transduction of inhibitor of kappa kinase beta (IKKβ) and increased nuclear staining for NFκB p50 was observed (Figure 25A). SIM2 levels were depressed in MCF10A cells overexpressing IKKβ compared to control cells by real time RT-PCR (Figure 25C). Decreased SIM2 protein levels were also verified in the MCF10A IKKβ-overexpressing cells by Western blot and immunofluorescence (Figure 25D and 25E).

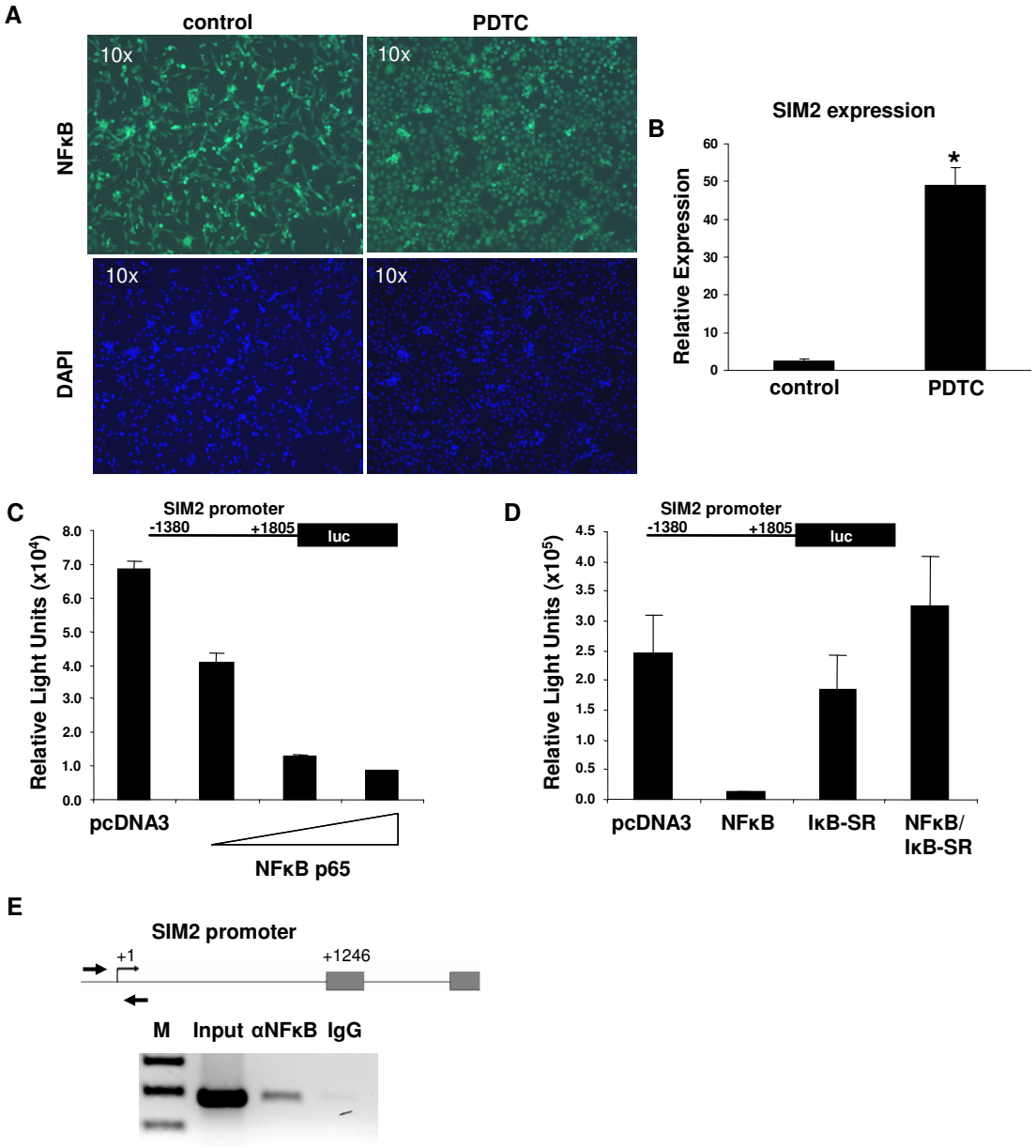

Figure 24

NFκB represses SIM2 promoter activity. (A) Immunofluorescence for NFκB with or without treatment of MDA435 cells with pyrollidine dithiocarbamate (PDTC). (B) SIM2 expression in MDA435 cells treated with PDTC compared to untreated cells. *Asterisk*, SIM2 expression is significantly elevated in cells treated with PDTC compared to control (p = 0.0003). (C) SIM2 promoter activity in HEK293T cells co-transfected with SIM2 promoter upstream of the luciferase gene and increasing amounts of NFκB p65. (D) SIM2 promoter activity after co-transfection of promoter with control vector (pcDNA3), NFκB p65, and/or IκB-SR. (E) ChIP assay for NFκB binding after transient transfection of SIM2 promoter with NFκB p65 in HEK293T cells.

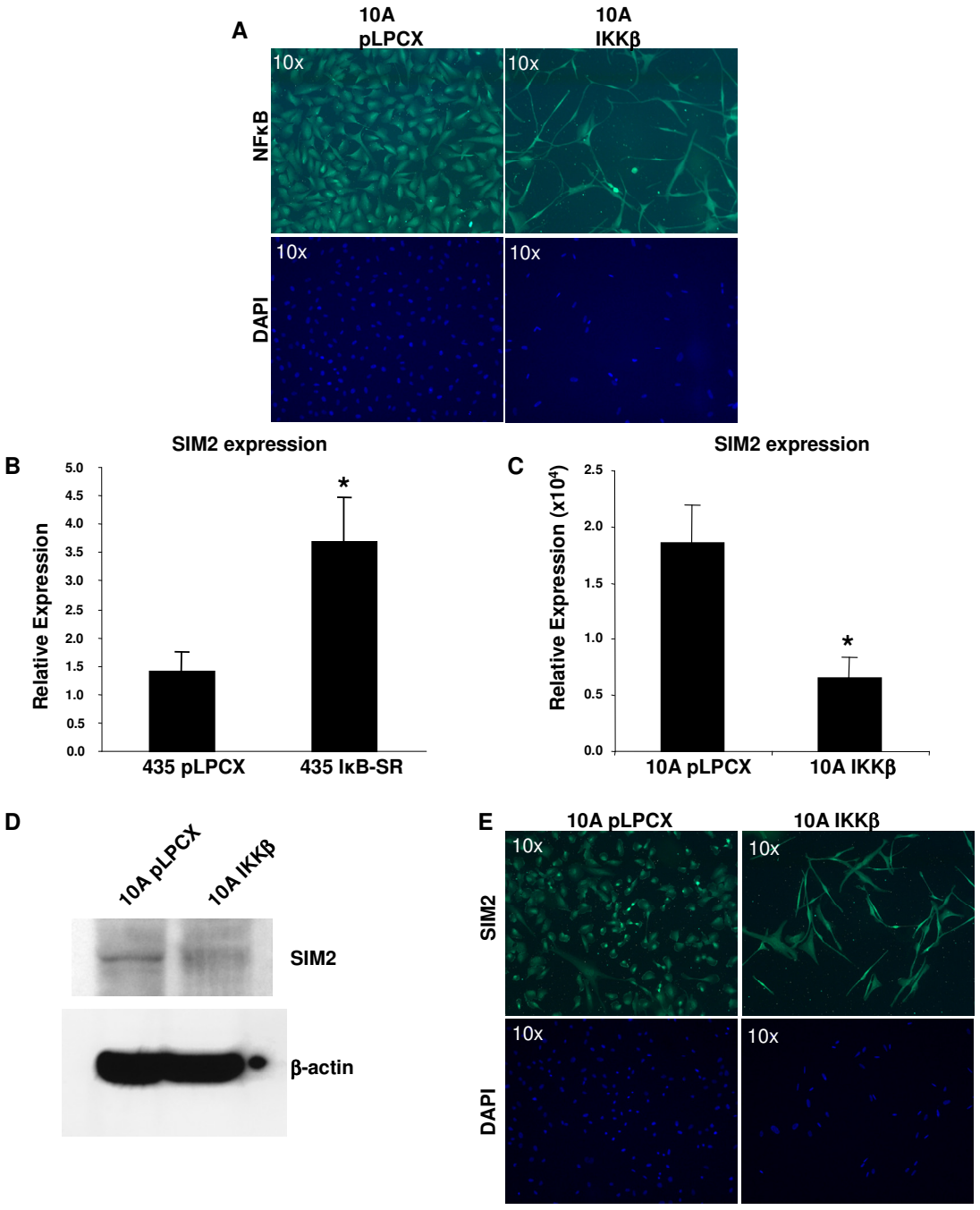

Figure 25

NFκB regulates SIM2 expression in MDA435 and MCF10A cell lines. (A) Immunofluorescence for NFκB in MCF10A cells stably transduced with control vector (pLPCX) or IKKβ. (B) SIM2 expression in MDA435 cells overexpressing IκB-SR compared to control by real time RT-PCR. *Asterisk*, SIM2 expression is significantly higher in MDA435 cells overexpressing IκB-SR compared to control ($p < 0.03$). (C) SIM2 expression in MCF10A cells overexpressing IKKβ compared to control by real time RT-PCR. *Asterisk*, SIM2 expression is significantly reduced in MCF10A cells overexpressing IKKβ compared to control ($p < 0.02$). (D) Western blot for SIM2 and β-actin in control MCF10A cells and MCF10A IKKβ-overexpressing cells. (E) Immunofluorescence for SIM2 in control MCF10A cells and MCF10A IKKβ-overexpressing cells.

NFκB binds to endogenous SIM2 promoter

To verify that the binding of NFκB observed on the transiently transfected SIM2 promoter was biologically relevant, ChIP analysis for NFκB p50 was performed on the SIM2 promoter in MDA435 cells treated with PDTC compared to untreated cells (Figure 26A). NFκB was present on the SIM2 promoter in untreated MDA435 cells but not detectable above normal IgG in cells treated with the NFκB inhibitor PDTC. In addition, NFκB p50 binding was assessed in the MDA435 IκB-SR-overexpressing cells and the MCF10A IKKβ-overexpressing cells compared to control cells (Figure 26B and 26C). Binding was again present in the MDA435 control cells but absent after inhibition of NFκB by IκB-SR. In contrast, no binding was observed in control MCF10A cells but was present in cells overexpressing IKKβ.

NFκB activation leads to deacetylation of the SIM2 promoter

NFκB has previously been shown to interact with HDAC1 to regulate target genes (102). Therefore, to determine if deacetylation was playing a role in the NFκB-mediated repression of SIM2, we determined relative levels of acetylated histone 3 at the SIM2 promoter in MDA435 cells treated with PDTC compared to control cells, and, at the same time, we assayed binding of HDAC1 to the SIM2 promoter (Figure 27A). Acetylation of histone 3 was undetectable in MDA435 cells with or without PDTC treatment; however, HDAC1 was observed bound to the SIM2 promoter in control cells and was lost from the promoter after PDTC treatment. This suggests that activation of NFκB contributes to the recruitment of HDAC1 to the SIM2 promoter. To study this

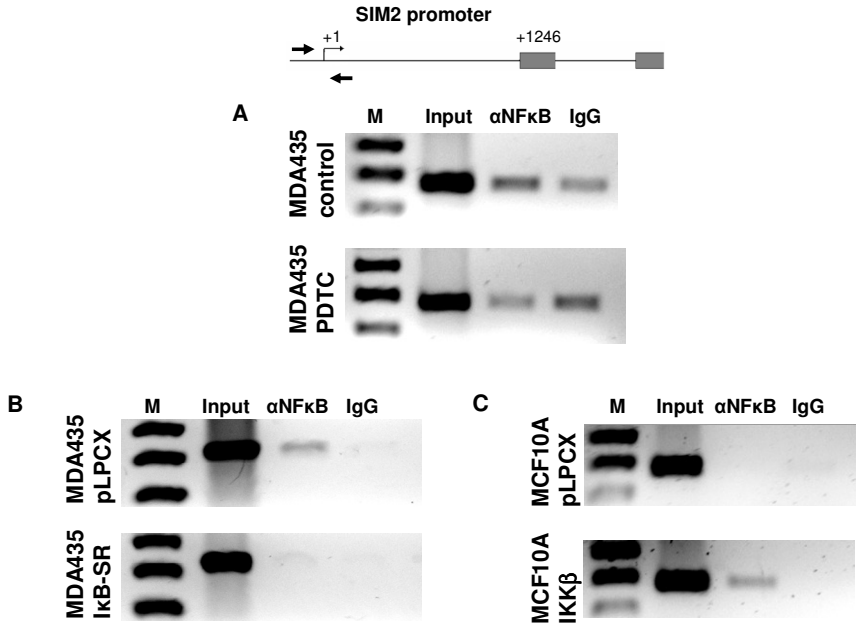

Figure 26
NFκB binds to endogenous SIM2 promoter. (A) ChIP for NFκB on SIM2 promoter in MDA435 control cells or cells treated with PDTC. (B) ChIP for NFκB on SIM2 promoter in MDA435 control cells or cells overexpressing IκB-SR. (C) ChIP for NFκB on SIM2 promoter in MCF10A control cells or cells overexpressing IKKβ.

effect more specifically, we again assayed acetylated histone 3 levels and HDAC1 binding in the MDA435 and MCF10A stable cell lines (Figure 27B and 27C). In the MDA435 IκB-SR-overexpressing cell line, increased acetylation of histone 3 was observed accompanied by a loss of HDAC1 on the SIM2 promoter compared to control cells. In the MCF10A IKKβ-overexpressing cells, acetylation of histone 3 was reduced but HDAC1 was difficult to detect above background. These data show that deacetylation of the SIM2 promoter plays a role in the mechanism of NFκB-mediated repression.

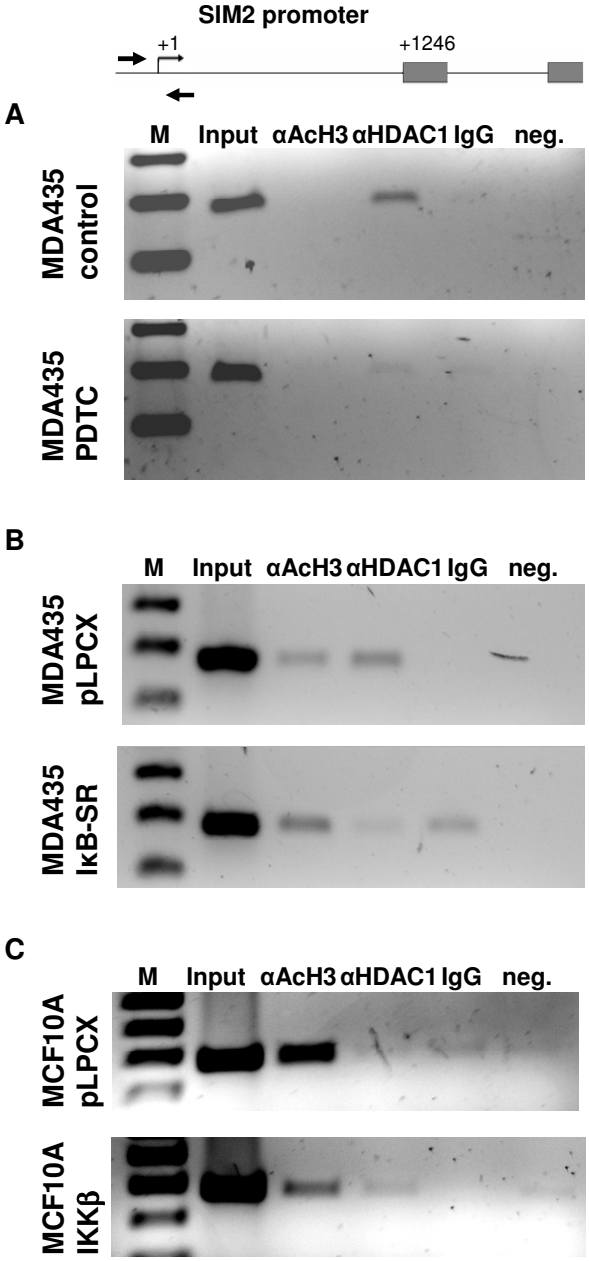

Figure 27
Mechanism of NFκB-mediated repression involves deacetylation of SIM2 promoter and recruitment of HDAC1. (A) ChIP for acetylated histone 3 (AcH3) and histone deacetylase 1 (HDAC1) on SIM2 promoter in MDA435 control cells or cells treated with PDTC. (B) ChIP for AcH3 and HDAC1 on SIM2 promoter in MDA435 control cells or cells overexpressing IκB-SR. (C) ChIP for AcH3 and HDAC1 on SIM2 promoter in MCF10A control cells or cells overexpressing IKKβ.

SIM2s antagonizes NFκB activity through a direct interaction

We have found that NFκB transcriptionally represses SIM2 expression, but SIM2 also inhibits binding of NFκB to the ABCB5 promoter. To investigate whether this was a specific effect for the ABCB5 gene or a general antagonism between NFκB and SIM2, we co-transfected a 5X NFκB binding site upstream of the luciferase gene (5X NFκB-luc) with NFκB p65 and SIM2s (Figure 28A). As expected, NFκB strongly activated the reporter construct ($p < 0.01$). SIM2s attenuated activation by NFκB ($p = 0.03$), indicating a more general inhibition of NFκB by SIM2. To determine the mechanism of this inhibition, the transfection was repeated with a SIM2s expression construct with the repression domain deleted (SIM2sΔR) (Figure 28B). This construct still attenuated the activation of the 5X NFκB-luc construct by NFκB, demonstrating that the inhibition of NFκB signaling is independent of the C-terminal repression domain of SIM2. To determine whether binding to the 5X NFκB-luc construct was involved, cells were co-transfected with SIM2s and NFκB p65, and a ChIP assay was performed (Figure 28C). Interestingly, both NFκB p65 and SIM2s were found to interact with the construct. To further explore this interaction, a ChIP assay was performed after transfection of SIM2s and the 5X NFκB-luc construct into MDA435 control and IκB-SR-overexpressing cells (Figure 28D). SIM2s was found to bind to the 5X NFκB-luc construct in the control cells but not in the cells in which NFκB activity was inhibited. This suggests that SIM2s requires NFκB p65 to interact with NFκB binding sites to prevent their activation. To demonstrate whether there was an interaction between SIM2s and NFκB p65, co-

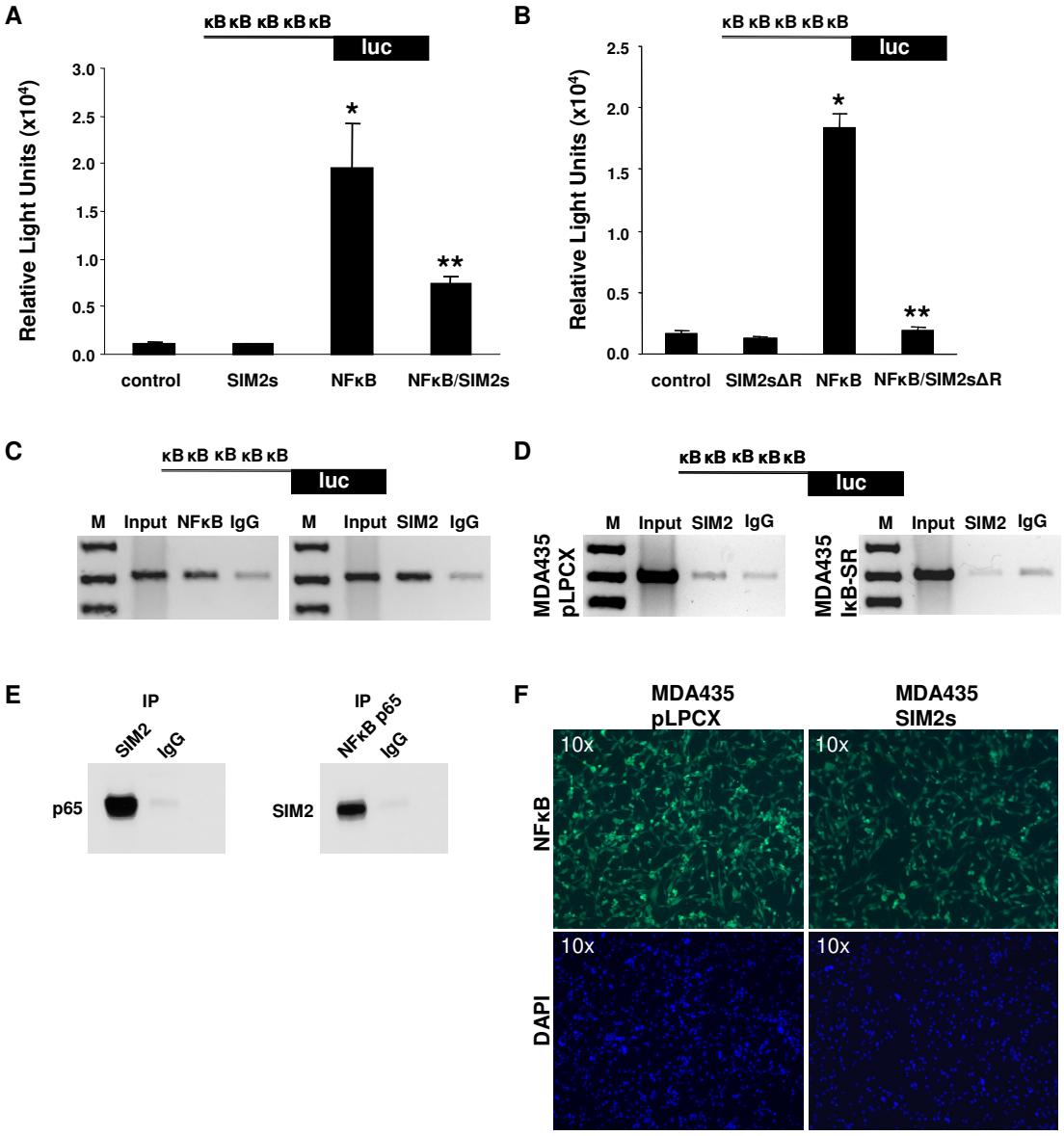

Figure 28

SIM2s antagonizes NFκB activity through direct interaction. (A) Luciferase activity in HEK293T cells co-transfected with 5X NFκB binding site upstream of the luciferase gene (5X NFκB-luc) and NFκB p65 and/or SIM2s. Diagram of promoter construct is shown above for reference. *Asterisk*, NFκB significantly increases promoter activity compared to control (p = 0.0006). *Double asterisk*, SIM2s significantly attenuates the activation of the promoter construct by NFκB (p = 0.04). (B) Luciferase activity in HEK293T cells co-transfected with 5X NFκB-luc and NFκB p65 and/or SIM2s with its repression domain deleted (SIM2sΔR). *Asterisk*, NFκB significantly increases promoter activity compared to control (p = 0.00007). *Double asterisk*, SIM2sΔR significantly attenuates the activation of the promoter construct by NFκB (p < 0.00008). (C) ChIP analysis of binding of NFκB p65 and SIM2 to NFκB binding sites after co-transfection of the 5X NFκB-luc construct, NFκB p65 and SIM2s into HEK293T cells. (D) ChIP analysis of binding of SIM2 to NFκB binding sites after co-transfection of the 5X NFκB-luc construct and SIM2s into MDA435 control (pLPCX) and IκB-SR-overexpressing cells. (E) Co-immunoprecipitation analysis of NFκB p65 and SIM2 after co-transfection of NFκB p65 and SIM2s into HEK293T cells. (F) Immunofluorescence for NFκB in control MDA435 cells and MDA435 SIM2s-overexpressing cells.

immunoprecipitation analysis was utilized, which confirmed the interaction (Figure 28E).

If SIM2s could interact with NFκB p65, then we hypothesized that this might alter localization of NFκB. Immunofluorescent staining was utilized to explore localization of NFκB in MDA435 control and SIM2s-overexpressing cells. Results showed reduced NFκB p50 nuclear staining in MDA435 cells overexpressing SIM2s compared to control MDA435 cells (Figure 28F). This suggests another means by which SIM2 inhibits NFκB signaling by preventing its nuclear translocation, likely through binding and sequestration in the cytoplasm.

NFκB necessary for repression by C/EBPβ but not Notch

It is interesting to note that both NOTCH1 and C/EBPβ have been shown to directly interact with NFκB. The NICD interacts with NFκB p50 to increase its nuclear retention in activated peripheral T cells (50). Also, through complexes formed with p50 and c-Rel, the NICD directly regulates interferon-γ expression (50). In addition, C/EBPβ interacts with NFκB p50 and p65 (118, 119). The Rel homology domain of p50 and the leucine zipper motif of C/EBPβ are important for this interaction (119). The inflammatory Mediterranean fever gene promoter is regulated by NFκB p65 and C/EBPβ binding at separate sites, but their interaction synergistically activates the promoter (118). To identify cooperation among C/EBPβ, NICD and NFκB p65 on the SIM2 promoter, MDA435 control (pLPCX) cells and IκB-SR-overexpressing cells were co-transfected with the SIM2 promoter, C/EBPβ and NICD. As expected the SIM2

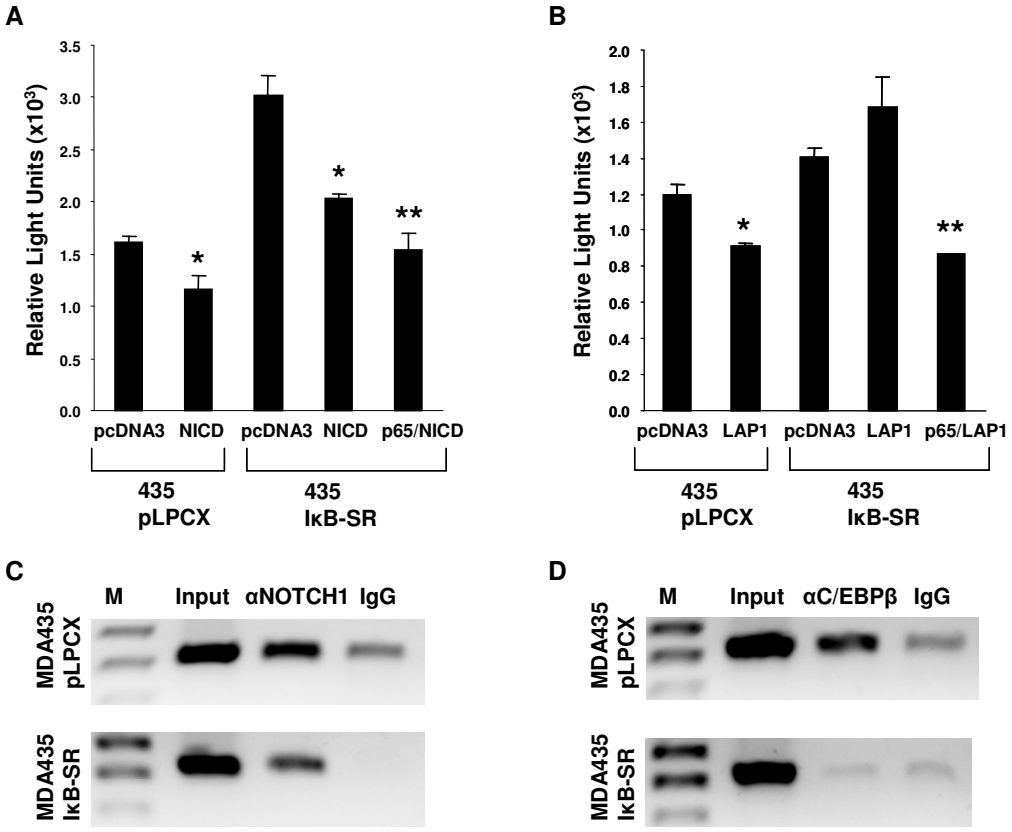

Figure 29
Interactions of repressors on SIM2 promoter. (A) Luciferase activity in MDA435 control (pLPCX) cells and IκB-SR-overexpressing cells co-transfected with the SIM2 promoter and vector control (pcDNA3), NICD or NFκB p65. *Asterisk,* SIM2 promoter activity is significantly reduced by NICD compared to vector control in MDA435 control cells and IκB-SR-overexpressing cells ($p < 0.03$). *Double asterisk,* SIM2 promoter activity is significantly reduced by p65 and NICD compared to NICD alone ($p = 0.04$). (B) Luciferase activity in MDA435 control and IκB-SR-overexpressing cells co-transfected with the SIM2 promoter and control vector, LAP1 or NFκB p65. *Asterisk,* SIM2 promoter activity is significantly reduced by LAP1 compared to vector control in MDA435 control cells ($p < 0.009$). *Double asterisk,* SIM2 promoter activity is significantly reduced by p65 and LAP1 compared to LAP1 alone ($p < 0.04$). (C) ChIP for NOTCH1 in MDA435 control and IκB-SR-overexpressing cells on co-transfected SIM2 promoter. (D) ChIP for C/EBPβ in MDA435 control and IκB-SR-overexpressing cells on co-transfected SIM2 promoter.

promoter showed greater activity in the cells overexpressing IκB-SR (Figure 29A and 29B). NICD was able to repress the SIM2 promoter in both cell lines, although increased repression was observed when NFκB p65 was added to the IκB-SR-overexpressing cells (Figure 29A). C/EBPβ, however, did not repress the SIM2

promoter in the IκB-SR-overexpressing cells, but repression was rescued by co-transfection of NFκB p65 (Figure 29B). These data show that NFκB is necessary for repression of SIM2 by C/EBPβ but not NICD. ChIP analysis after transient transfection showed that NICD was bound to the SIM2 promoter in MDA435 control cells and cells overexpressing IκB-SR (Figure 29C), but C/EBPβ was bound only in the control MDA435 cells with normal NFκB activity (Figure 29D). Therefore, NFκB facilitates repression of SIM2 by C/EBPβ by mediating its binding to the SIM2 promoter.

Mammalian homologues of snail do not repress SIM2

In *Drosophila* sim is regulated by dorsal, twist, snail and notch signals to narrow its expression to a single row of cells in the embryo (108). *Drosophila* sim then activates CNS midline gene expression and activates repressive factors to inhibit lateral CNS gene expression in midline cells (120). The mammalian homolog of dorsal, NFκB, was found to regulate SIM2, and NOTCH1 also plays a role in SIM2 repression. However, the mammalian homologues of snail, SNAI1 and SNAI2, did not repress SIM2 promoter activity in transient transfections (Figure 30).

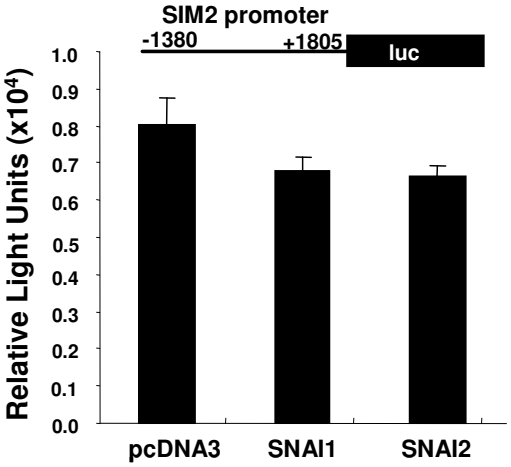

Figure 30
Mammalian homologues of *Drosophila* snail do not repress SIM2. Luciferase activity in HEK293T cells co-transfected with SIM2 promoter and SNAI1 or SNAI2 expression constructs. No significant difference was observed in SIM2 promoter activity after SNAI1 transfection or SNAI2 transfection compared to vector control (pcDNA3) transfection ($p > 0.08$). Diagram of promoter construct is shown above for reference. Difference between promoter activity in the presence of SNAI1/SNAI2 and control (pcDNA3) was not significant ($p > 0.08$).

CHAPTER VI

CONCLUSIONS

Metastatic breast cancer is currently treated with combination chemotherapy, including anthracyclines followed by cyclophosphamide, methotrexate and 5-fluorouracil. Taxanes may also be used in combination with anthracyclines in some protocols (121). These treatments are often limited by their severe side effects, including suppression of the bone marrow, causing increased risk of infection. Therapies targeted to an individual's cancer biology have improved patient survival in recent years. Hormonal therapy with tamoxifen or aromatase inhibitors improves efficacy and disease-free survival in women with high risk estrogen receptor positive cancer (121). Herceptin (trastuzumab), which targets growth factor receptor HER2, is the first molecular targeting agent approved for treatment of metastatic breast cancer (122). HER2 is overexpressed in about 20% of breast cancers, and trastuzumab is now a common component of treatment protocols for women whose tumors overexpress HER2 (121). Further progress in elucidation of specific pathways altered during breast cancer may allow for more patient-tailored medicine to maximize therapeutic efficacy while minimizing toxicity on an individual basis.

HRAS and c-MYC lead to SIM2 silencing

Since Single-minded 2 expression is lost in a large percentage of breast cancers and has tumor suppressive activity in mammary tissues (21), we sought to elucidate

pathways targeting it for down-regulation during carcinogenesis. By transforming normal immortalized MCF10A breast epithelial cells with HRAS and c-MYC, we identified these oncogenic signals as mechanisms of SIM2 silencing. HRAS-overexpression led to a greater decrease in SIM2 mRNA levels, but both oncogenes decreased SIM2 protein levels. Although HRAS gene amplification is not associated with breast cancer, the oncogene plays an important role in 50% of breast cancer due to its relation to kinase signaling pathways (30). c-MYC contributes to normal mammary gland development (42) and is amplified in 15-20% and overexpressed in approximately 70% of breast cancers (43). These percentages are consistent with the observed frequency of loss of SIM2 in breast cancers (21).

Notch is a transcriptional repressor of SIM2

Recently, Ras transformation of mouse mammary glands has been shown to require Notch (57). Ras activates Notch signaling by increasing γ-secretase activity, which leads to increased release of the active NICD (46). Given that notch signaling also regulates sim expression in *Drosophila*, we postulated that NICD may be a repressor of SIM2. The NICD was demonstrated to bind to the SIM2 promoter following HRAS overexpression and function as a transcriptional repressor of SIM2.

The NICD interacts with CBF1 to activate target genes like HES1 in canonical Notch signaling (48). However, the NICD has been shown to interact with other transcription factors including MEF2C (49), NFκB (50) and HIF-1α (51), and there is significant evidence for the importance of CBF1-independent Notch function for

maintaining cell fate (52). This study, however, is the first to demonstrate a direct tumor suppressor gene target of CBF1-independent Notch signaling. The relationship between SIM2 and Notch also suggests a role for SIM2 in assigning cell fate. In the mammary gland, Notch signaling regulates stem cell self-renewal (123). This implies that SIM2 plays a role in directing cells away from "stemness."

C/EBPβ transcriptionally represses SIM2

All three isoforms of C/EBPβ have been shown to be overexpressed in breast cancer (124-126), and C/ebpβ was identified as an important mediator of Hras-induced tumorigenesis in a mouse skin carcinogenesis model known to cause Hras mutations (47). This study is the first report to identify a direct tumor suppressor gene target of C/EBPβ. Although both of the longer isoforms of C/EBPβ have an intact transactivation domain, there is increasing evidence for functional differences between the LAP1 and LAP2 isoforms (60, 66, 127, 128). For example, human LAP1 and LAP2 differ by 23 amino acids at the N-terminus, which allow LAP1, but not LAP2, to interact with the SWI/SNF complex and effect chromatin remodeling (60). In the studies presented here, both LAP1 and LAP2 were able to repress SIM2 when both transiently and stably introduced into MCF10A cells; however, it is interesting that only the full length LAP1 was found to repress SIM2 expression through binding to the SIM2 promoter. Binding of C/EBPβ to the SIM2 promoter also occurred in the HRAS-overexpressing cells. Binding of LAP1 was found to be mediated by NFκB, which was necessary for repression of SIM2 expression. Repression by LAP2 more likely involves sequestration

of specific coactivators, as binding to the SIM2 promoter was not required for it to repress SIM2 expression. The role of C/EBPβ in SIM2 repression was well corroborated by our *in vivo* mouse studies, which also demonstrated a role for C/ebpβ in mediating Sim2 repression. The murine LIP isoform was a strong suppressor of Sim2 expression, consistent with its role in mammary proliferation in mouse models (67). Human LIP, however, did not repress SIM2 promoter activity. Since human and mouse LIP share significant sequence homology at the DNA and protein levels, this difference is more likely due to differences in the mouse and human Sim2 promoters, which show greater sequence divergence.

In the liver, LAP functions primarily as a transcriptional activator, and LIP functions as an antagonist of LAP activity by competing for DNA binding sites as a homodimer or a LAP/LIP heterodimer (61). In other cases, LAP and LIP show different relationships. In thyrocytes, LAP has been shown to repress the sodium iodide symporter (NIS) promoter activity, while LIP had no effect (129). In contrast, in human endometrial stromal cells LIP cooperates with progesterone receptor B to enhance activation of a progesterone response element, but LAP does not and instead interacts cooperatively with progesterone receptor A on C/EBPβ response elements (130). Since human SIM2 expression is repressed by the activating forms of C/EBPβ, which do not interact with a C/EBPβ binding site directly to mediate repression, perhaps it is not surprising that LIP does not function in its traditional role on the SIM2 promoter.

Data suggests that C/EBPβ also plays a role in cell fate determination, based on altered expression of a number of molecular markers in C/ebpβ$^{-/-}$ mammary glands

(131). It is of interest that two proteins involved in cell fate decisions independently regulate SIM2. This suggests that SIM2 plays a role in cell fate, probably directing cells toward differentiation. Future studies utilizing a $Sim2^{-/-}$ mouse mammary gland model should better elucidate the function of SIM2 in cell fate determination.

NFκB is a transcriptional repressor of SIM2

Inflammation is linked to cancers in various tissues, including hepatocellular carcinoma associated with hepatitis B and hepatitis C viral infection, colorectal cancer linked to chronic inflammatory bowel disease, and mesothelioma associated with chronic injury caused by asbestos fibers (99, 132). It is now known that NFκB is a major contributor to the underlying mechanism for this link. NFκB not only contributes to cancer progression by stimulating proliferation and preventing apoptosis but also contributes to drug resistance by activating transcription of members of the ABC family of transporters, like MDR1 (99, 104, 107). In addition to proinflammatory cytokines or pathogen-associated molecules, deregulation of Ras signaling, PI3K signaling and MAPK activity can participate in the activation of NFκB (109).

In *Drosophila*, dorsal, the NFκB homolog, contributes to regulation of sim expression in the central midline. These studies have demonstrated SIM2 is also regulated, specifically repressed, by NFκB. Inhibiting NFκB signaling in MDA435 cancer cells through overexpression of IκB-SR led to increased expression of SIM2; whereas, activation of the NFκB pathway by overexpression of IKKβ subunit in the

MCF10A cells led to repression of SIM2 expression. The mechanism of NFκB-mediated repression involves deacetylation of the SIM2 promoter by HDAC1.

SIM2 is epigenetically regulated

These studies demonstrate that epigenetic changes to SIM2 occur during tumor progression, but these mechanisms are only partially responsible for silencing SIM2. In the cancer cell line model, loss of expression of SIM2 was associated with increased DNA methylation within exon 1. In contrast, methylation was prevalent around the transcriptional start site, irrespective of expression level. While this was somewhat unexpected, CpG islands often extend into the first exon and methylation within exon 1 has been associated with silencing of other tumor suppressor genes, including RASSF1A and RB1 (133, 134). In gastric cancer cell lines, ERα is hypermethylated near its ATG start codon and silenced (135). In our cell line model, methylation at the ATG start site was predictive of expression and, since 5-aza-dC partially reactivated SIM2 expression in the MDA435 cells, contributed to some extent to silencing.

Analysis of the chromatin structure of the 5′ SIM2 gene also showed epigenetic modifications. The normal breast epithelial cell line MCF10A maintains an open, acetylated chromatin structure which is consistent with its high level of SIM2 expression. The MCF7 cells represent an intermediate stage in the silencing of SIM2, with expression being approximately 7-fold lower than that in the MCF10A cells. The chromatin is more compacted as shown by *MspI* accessibility, and these modifications are further advanced within exon 1 than at the transcriptional start site, since

deacetylation of histone 3 has occurred within exon 1, while the promoter region remains acetylated. The MDA435 cells display a completely epigenetically silenced SIM2 gene, with high levels of DNA methylation, complete deacetylation of exon 1 and the promoter region and greatly compacted, inaccessible chromatin. Overall epigenetic modifications at the ATG start region better correlate with SIM2 expression in cancer cell lines. However, even the combination of 5-aza-dC and TSA only increased SIM2 levels by 14-fold in the MDA435 cells, compared to the 3500-fold higher levels in the normal breast epithelial MCF10A cells, and had no effect in the MCF7 cells (data not shown). These results suggest a high level of complexity in the regulation of SIM2.

We modeled the specific role of DNA methylation in silencing the SIM2 tumor suppressor gene by overexpression of DNMT1 in the MCF10A cell line. Overexpression of DNMT1 did lead to approximately 50% repression of the SIM2 mRNA accompanied by a doubling of methylation with exon 1. Acetylation, however, was not affected. Therefore, this increase in methylation is insufficient to cause further epigenetic modification and complete silencing. Similar to this result, a recent publication has shown that demethylation was insufficient for reestablishing a euchromatic environment for silenced tumor suppressor genes, including MLH1, in colorectal cancer (136). These data support a role for transcriptional repressors in promoting histone modifications that contribute to a completely epigenetically silenced locus, as represented by the MDA435 cells. One such repressor has been identified as NFκB. NFκB regulates SIM2 expression through recruitment of HDAC1 and changes in promoter acetylation, demonstrated in both normal immortalized breast epithelial

MCF10A cells and highly invasive MDA435 cancer cells. In contrast to direct methylation of the SIM2 promoter, activation of NFκB leads to histone modification of the SIM2 promoter. These combined data suggest that specific transcriptional repressors play the major role in silencing SIM2 expression.

To determine how well the cell line model reflected human cancer, breast tumor tissue was analyzed for SIM2 methylation and expression. In the breast tumor samples studied, 53% showed partial methylation in the first exon of SIM2. Interestingly, methylation did not correlate with protein expression of SIM2 in these breast tumor samples. This supports the complexity of the regulation of SIM2, consistent with the modest effect of overexpression of DNMT1 in MCF-10A cells. This suggests that methylation contributes to regulation of SIM2 but other factors, such as the activation of specific oncogenes, like HRAS, C/EBPβ and NOTCH1, can play a major role in determining SIM2 expression independently of epigenetic changes. For example, MCF10A cells overexpressing HRAS show no change in acetylation of histone 3 in the SIM2 promoter despite the observed repression (Figure 31).

Methylation is thought to be an early event in cancer progression. Support for this model comes from key epigenetic changes, such as hypermethylation of p16, that occur early in mammary tumorigenesis (137). DNA methyltransferase activity also increases incrementally during colon cancer progression (138). The data presented here demonstrate that methylation does contribute to tumor suppressor gene silencing, but was insufficient to initiate heterochromatin formation and lead to complete silencing. One possibility is that a greater level of methylation, such as that seen in MDA435 cells,

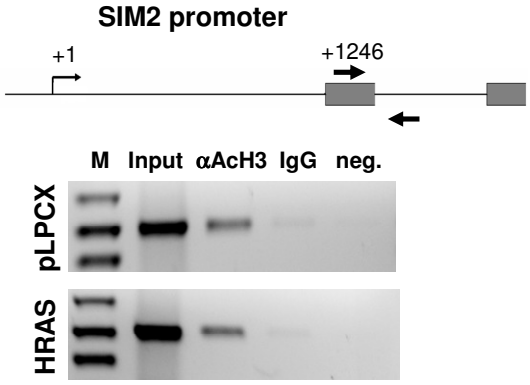

Figure 31
Repression of SIM2 by HRAS does not involve deacetylation of the SIM2 promoter. ChIP assay for acetylated histone 3 (AcH3) at SIM2 promoter in HRAS-overexpressing MCF10A cells compared to control (pLPCX). Diagram of promoter and primer position is shown above for reference.

is necessary for complete silencing. Targeted, rather than global, methylation and demethylation strategies would be extremely useful in elucidating the exact role of methylation in gene silencing and heterochromatin formation.

The benefit of epigenetic silencing to cancer treatment is its reversibility, and these studies suggest it may be possible to target SIM2 for reactivation in breast cancer. A strong caveat to this possibility, however, is that altering the epigenetic status of the SIM2 locus changed expression very little (14-fold) in comparison to the difference in expression between normal epithelial cells and cancer cells (3500-fold). Complete reactivation cannot be assumed by targeting epigenetic processes alone for tumor suppressor genes such as SIM2 which are also heavily regulated by specific transcriptional repressors.

Implications of SIM2 expression for chemoresistance

Resistance to chemotherapeutic agents is a leading cause of treatment failure, affecting up to 90% of patients with metastatic cancer (88). In 1973 it was recognized that reduced drug accumulation was a major factor in chemoresistance, and this led to the discovery of the ABC family of transporters (89). NFκB plays a major role in mediating chemoresistance, as inhibition of NFκB signaling has been shown to enhance antineoplastic-induced apoptosis (97). These studies have identified ABCB5 as an additional drug metabolism gene regulated by NFκB. We have also identified a novel role of SIM2 in inhibiting NFκB activity and, thus, increasing sensitivity to the antineoplastics doxorubicin and 5-fluorouracil. SIM2 can interact directly with NFκB, preventing activation of NFκB enhancer elements and preventing NFκB nuclear translocation. SIM2 also binds to specific promoters, like ABCB5, and antagonizes NFκB binding. ABCB5 has recently been shown to have an important role in 5-fluorouracil and doxorubicin resistance in human melanoma (94, 95). However, no difference in doxorubicin efflux was observed between control MDA435 cells and cells overexpressing SIM2s. In the MDA435 cell model, it is apparent that antagonism of NFκB signaling by SIM2 plays a greater role in increasing chemosensitivity than the repression of certain ABC-transporters. The NFκB targets contributing to the increased chemosensitivity remain to be elucidated. We expect that the relationship between NFκB and SIM2 may be exploited to develop new treatment strategies targeting NFκB and countering antineoplastic drug resistance.

Model of SIM2 silencing in breast cancer

In these studies we have characterized epigenetic mechanisms, oncogenic transformation and transcriptional repressors, NFκB, NOTCH1 and C/EBPβ, which contribute to silencing SIM2 in cancer cells (Figure 32). Ras activation has previously been shown to increase cleavage of Notch, releasing the active NICD (46). At the same time, Ras-initiated MAPK signaling leads to phosphorylation of C/EBPβ (68). Ras can also activate NFκB by triggering MAPK or PI3K activity in certain cell types (109).

The NICD interacts with CBF1 to activate certain target genes, like HES1, but also acts through a CBF1-independent mechanism to target SIM2 for silencing. Since NICD cannot directly interact with DNA and does not require NFκB for repression of SIM2, in contrast to C/EBPβ, it is assumed that the NICD is interacting with as yet undetermined cofactors to bind to the SIM2 promoter. C/EBPβ binds to the SIM2 promoter through interaction with NFκB p65 in order to repress SIM2 expression, as repression and binding were prevented by inhibition of NFκB activity.

NFκB binds to the SIM2 promoter around the transcriptional start site to mediate repression, which involves deacetylation of histone 3. SIM2, however, if expressed, inhibits NFκB signaling by a direct interaction which prevents activation of NFκB enhancer elements and NFκB nuclear translocation. SIM2 can also bind to the promoter of NFκB target ABCB5, which may also play a role in inhibiting binding of NFκB. We do not suggest that these are the only mediators of SIM2 repression in breast cancer. By evaluating SIM2 expression in other oncogene-driven models of breast cancer, such as HER2 and WNT1, it is likely that other signaling pathways mediating SIM2 repression

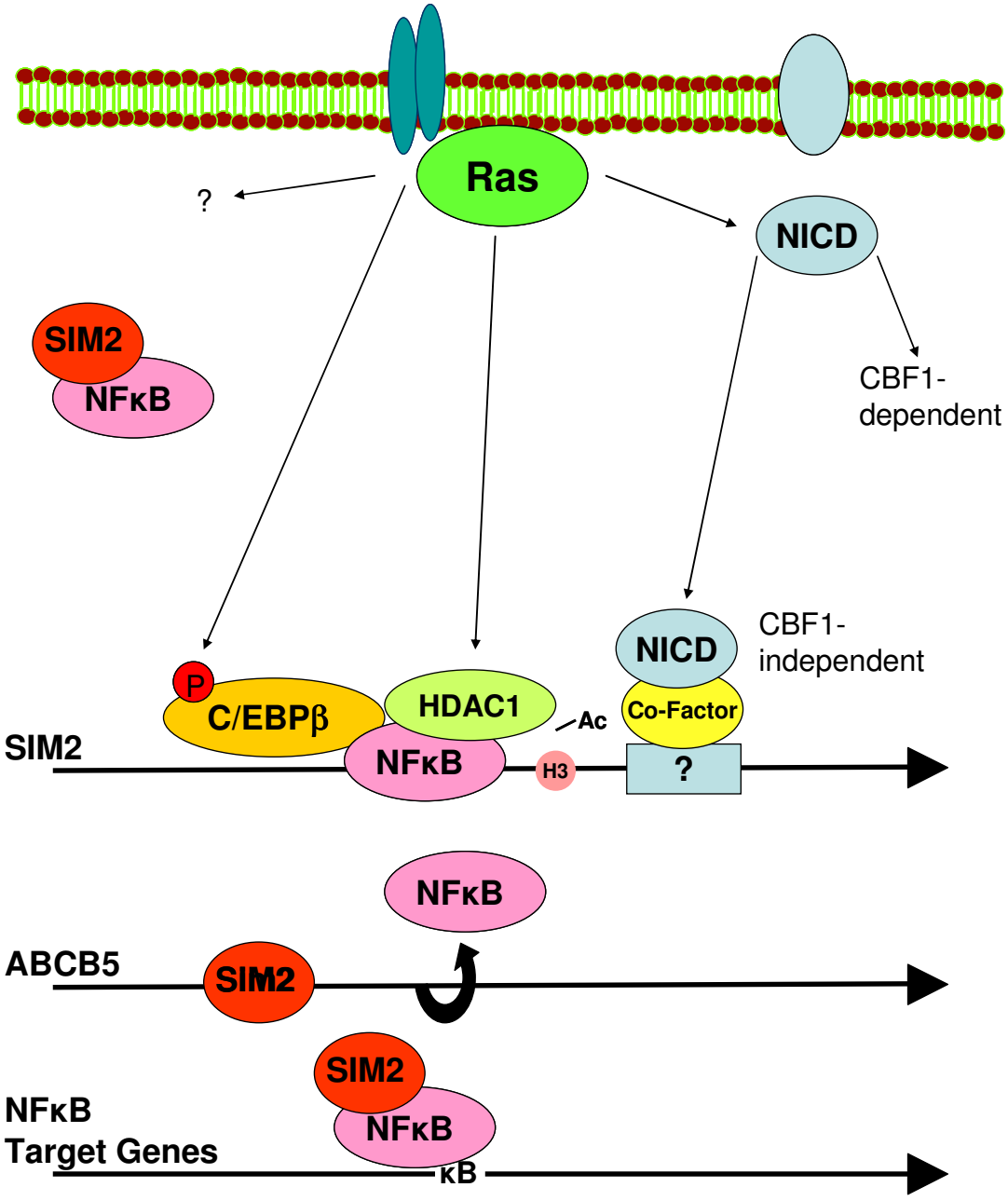

Figure 32
Model of SIM2 silencing in breast cancer. Ras activation leads to increased cleavage of NOTCH1. The NICD then acts through CBF1-dependent mechanisms on some targets like HES1 and through a CBF1-independent mechanism to bind to and repress SIM2 promoter activity. At the same time, Ras activation leads to increased phosphorylation of C/EBPβ, and the LAP1 isoform binds to and represses SIM2 promoter activity. In some cell types, Ras activates NFκB, which binds to and represses the SIM2 promoter, which involves recruitment of HDAC1 and deacetylation of histone 3. NFκB also facilitates repression by C/EBPβ. It is likely that other factors, as yet unidentified, cooperate to repress SIM2 expression as well. SIM2, when expressed, antagonizes NFκB signaling by direct interaction with p65, preventing its nuclear localization and its activity on NFκB binding sites. Also, SIM2 directly binds to the promoter of the NFκB target ABCB5 and antagonizes NFκB binding.

will be revealed. We expect that SIM2 silencing plays an important role in progression of a subset of human breast cancer, which is supported by analysis of SIM2 expression by immunohistochemistry (21). Elucidating oncogenic pathways and transcriptional repressors involved in SIM2 silencing contributes to the characterization of the molecular basis for specific subsets of cancer and thus aids the development of targeted therapies for human breast cancer.

REFERENCES

1. Sporn, M.B., Dunlop, N.M., Newton, D.L., and Smith, J.M. Prevention of chemical carcinogenesis by vitamin A and its synthetic analogs (retinoids). Fed. Proc., *35*: 1332-1338, 1976.
2. Wang, H., Han, H., Mousses, S., and Von Hoff, D.D. Targeting loss-of-function mutations in tumor-suppressor genes as a strategy for development of cancer therapeutic agents. Semin. Oncol., *33*: 513-520, 2006.
3. Tamura, G. Alterations of tumor suppressor and tumor-related genes in the development and progression of gastric cancer. World J. Gastroenterol., *12*: 192-198, 2006.
4. Oliveira, A.M., Ross, J.S., and Fletcher, J.A. Tumor suppressor genes in breast cancer: the gatekeepers and the caretakers. Am. J. Clin. Pathol., *124 Suppl*: S16-28, 2005.
5. Segditsas, S., and Tomlinson, I. Colorectal cancer and genetic alterations in the Wnt pathway. Oncogene, *25*: 7531-7537, 2006.
6. Kewley, R.J., Whitelaw, M.L., and Chapman-Smith, A. The mammalian basic helix-loop-helix/PAS family of transcriptional regulators. Int. J. Biochem. Cell Biol., *36*: 189-204, 2004.
7. Ema, M., Morita, M., Ikawa, S., Tanaka, M., Matsuda, Y., Gotoh, O., Saijoh, Y., Fujii, H., Hamada, H., Kikuchi, Y., and Fujii-Kuriyama, Y. Two new members of the murine Sim gene family are transcriptional repressors and show different

expression patterns during mouse embryogenesis. Mol. Cell Biol., *16*: 5865-5875, 1996.

8. Crews, S., Franks, R., Hu, S., Matthews, B., and Nambu, J. Drosophila single-minded gene and the molecular genetics of CNS midline development. J. Exp. Zool., *261*: 234-244, 1992.
9. Thomas, J.B., Crews, S.T., and Goodman, C.S. Molecular genetics of the single-minded locus: a gene involved in the development of the Drosophila nervous system. Cell, *52*: 133-141, 1988.
10. Nambu, J.R., Lewis, J.O., Wharton, K.A., Jr., and Crews, S.T. The Drosophila single-minded gene encodes a helix-loop-helix protein that acts as a master regulator of CNS midline development. Cell, *67*: 1157-1167, 1991.
11. Crews, S.T. Control of cell lineage-specific development and transcription by bHLH-PAS proteins. Genes Dev., *12*: 607-620, 1998.
12. Dickson, B.J., and Gilestro, G.F. Regulation of commissural axon pathfinding by slit and its Robo receptors. Annu. Rev. Cell Dev. Biol., *22*: 651-675, 2006.
13. Stemerdink, C., and Jacobs, J.R. Argos and Spitz group genes function to regulate midline glial cell number in Drosophila embryos. Development, *124*: 3787-3796, 1997.
14. Goshu, E., Jin, H., Fasnacht, R., Sepenski, M., Michaud, J.L., and Fan, C.M. Sim2 mutants have developmental defects not overlapping with those of Sim1 mutants. Mol. Cell Biol., *22*: 4147-4157, 2002.

15. Probst, M.R., Fan, C.M., Tessier-Lavigne, M., and Hankinson, O. Two murine homologs of the Drosophila single-minded protein that interact with the mouse aryl hydrocarbon receptor nuclear translocator protein. J. Biol. Chem., *272*: 4451-4457, 1997.

16. Michaud, J.L., DeRossi, C., May, N.R., Holdener, B.C., and Fan, C.M. ARNT2 acts as the dimerization partner of SIM1 for the development of the hypothalamus. Mech. Dev., *90*: 253-261, 2000.

17. Rachidi, M., Lopes, C., Charron, G., Delezoide, A.L., Paly, E., Bloch, B., and Delabar, J.M. Spatial and temporal localization during embryonic and fetal human development of the transcription factor SIM2 in brain regions altered in Down syndrome. Int. J. Dev. Neurosci., *23*: 475-484, 2005.

18. Ema, M., Ikegami, S., Hosoya, T., Mimura, J., Ohtani, H., Nakao, K., Inokuchi, K., Katsuki, M., and Fujii-Kuriyama, Y. Mild impairment of learning and memory in mice overexpressing the mSim2 gene located on chromosome 16: an animal model of Down's syndrome. Hum. Mol. Genet., *8*: 1409-1415, 1999.

19. Metz, R.P., Kwak, H.I., Gustafson, T., Laffin, B., and Porter, W.W. Differential transcriptional regulation by mouse single-minded 2s. J. Biol. Chem., *281*: 10839-10848, 2006.

20. Shamblott, M.J., Bugg, E.M., Lawler, A.M., and Gearhart, J.D. Craniofacial abnormalities resulting from targeted disruption of the murine Sim2 gene. Dev. Dyn., *224*: 373-380, 2002.

21. Kwak, H.I., Gustafson, T., Metz, R.P., Laffin, B., Schedin, P., and Porter, W.W. Inhibition of breast cancer growth and invasion by single-minded 2s. Carcinogenesis, *28*: 259-266, 2007.

22. Satge, D., Sasco, A.J., Pujol, H., and Rethore, M.O. [Breast cancer in women with trisomy 21]. Bull. Acad. Natl. Med., *185*: 1239-1252, discussion 52-54, 2001.

23. Scholl, T., Stein, Z., and Hansen, H. Leukemia and other cancers, anomalies and infections as causes of death in Down's syndrome in the United States during 1976. Dev. Med. Child Neurol., *24*: 817-829, 1982.

24. Hasle, H., Clemmensen, I.H., and Mikkelsen, M. Risks of leukaemia and solid tumours in individuals with Down's syndrome. Lancet, *355*: 165-169, 2000.

25. Mendes, O., Kim, H.T., and Stoica, G. Expression of MMP2, MMP9 and MMP3 in breast cancer brain metastasis in a rat model. Clin. Exp. Metastasis, *22*: 237-246, 2005.

26. Bodey, B., Bodey, B., Jr., Siegel, S.E., and Kaiser, H.E. Matrix metalloproteinases in neoplasm-induced extracellular matrix remodeling in breast carcinomas. Anticancer Res., *21*: 2021-2028, 2001.

27. Parmar, H., and Cunha, G.R. Epithelial-stromal interactions in the mouse and human mammary gland *in vivo*. Endocr. Relat. Cancer, *11*: 437-458, 2004.

28. Robinson, G.W. Identification of signaling pathways in early mammary gland development by mouse genetics. Breast Cancer Res., *6*: 105-108, 2004.

29. National Institutes of Health. Biology of the Mammary Gland. [cited June 2007]; Available from: http://mammary.nih.gov

30. Shen, Q., and Brown, P.H. Transgenic mouse models for the prevention of breast cancer. Mutat. Res., *576*: 93-110, 2005.

31. McGill, M.A., and McGlade, C.J. Cellular Signaling. *In:* I. F. Tannock, R. P. Hill, R. G. Bristow, and L. Harrington (eds.), The Basic Science of Oncology, pp. 142-151. New York, NY: McGraw-Hill Medical Publishing Division, 2005.

32. Davis, R.J. Transcriptional regulation by MAP kinases. Mol. Reprod. Dev., *42*: 459-467, 1995.

33. Luscher, B. Function and regulation of the transcription factors of the Myc/Max/Mad network. Gene, *277*: 1-14, 2001.

34. Khleif, S.N., Abrams, S.I., Hamilton, J.M., Bergmann-Leitner, E., Chen, A., Bastian, A., Bernstein, S., Chung, Y., Allegra, C.J., and Schlom, J. A phase I vaccine trial with peptides reflecting ras oncogene mutations of solid tumors. J. Immunother., *22*: 155-165, 1999.

35. von Lintig, F.C., Dreilinger, A.D., Varki, N.M., Wallace, A.M., Casteel, D.E., and Boss, G.R. Ras activation in human breast cancer. Breast Cancer Res. Treat., *62*: 51-62, 2000.

36. Slamon, D.J., Godolphin, W., Jones, L.A., Holt, J.A., Wong, S.G., Keith, D.E., Levin, W.J., Stuart, S.G., Udove, J., Ullrich, A., et al. Studies of the HER-2/neu proto-oncogene in human breast and ovarian cancer. Science, *244*: 707-712, 1989.

37. Yu, Q., Geng, Y., and Sicinski, P. Specific protection against breast cancers by cyclin D1 ablation. Nature, *411*: 1017-1021, 2001.

38. Dunn, K.L., Espino, P.S., Drobic, B., He, S., and Davie, J.R. The Ras-MAPK signal transduction pathway, cancer and chromatin remodeling. Biochem. Cell Biol., *83*: 1-14, 2005.

39. Nielsen, L.L., Discafani, C.M., Gurnani, M., and Tyler, R.D. Histopathology of salivary and mammary gland tumors in transgenic mice expressing a human Ha-ras oncogene. Cancer Res., *51*: 3762-3767, 1991.

40. Sinn, E., Muller, W., Pattengale, P., Tepler, I., Wallace, R., and Leder, P. Coexpression of MMTV/v-Ha-ras and MMTV/c-myc genes in transgenic mice: synergistic action of oncogenes *in vivo*. Cell, *49*: 465-475, 1987.

41. Cardiff, R.D., and Wellings, S.R. The comparative pathology of human and mouse mammary glands. J. Mammary Gland Biol. Neoplasia, *4*: 105-122, 1999.

42. Strange, R., Li, F., Saurer, S., Burkhardt, A., and Friis, R.R. Apoptotic cell death and tissue remodelling during mouse mammary gland involution. Development, *115*: 49-58, 1992.

43. Nass, S.J., and Dickson, R.B. Defining a role for c-Myc in breast tumorigenesis. Breast Cancer Res. Treat., *44*: 1-22, 1997.

44. Boxer, R.B., Jang, J.W., Sintasath, L., and Chodosh, L.A. Lack of sustained regression of c-MYC-induced mammary adenocarcinomas following brief or prolonged MYC inactivation. Cancer Cell, *6*: 577-586, 2004.

45. Chin, L., Tam, A., Pomerantz, J., Wong, M., Holash, J., Bardeesy, N., Shen, Q., O'Hagan, R., Pantginis, J., Zhou, H., Horner, J.W., Cordon-Cardo, C., Yancopoulos, G.D., and DePinho, R.A. Essential role for oncogenic Ras in tumour maintenance. Nature, *400*: 468-472, 1999.

46. Weijzen, S., Rizzo, P., Braid, M., Vaishnav, R., Jonkheer, S.M., Zlobin, A., Osborne, B.A., Gottipati, S., Aster, J.C., Hahn, W.C., Rudolf, M., Siziopikou, K., Kast, W.M., and Miele, L. Activation of Notch-1 signaling maintains the neoplastic phenotype in human Ras-transformed cells. Nat. Med., *8*: 979-986, 2002.

47. Zhu, S., Yoon, K., Sterneck, E., Johnson, P.F., and Smart, R.C. CCAAT/enhancer binding protein-beta is a mediator of keratinocyte survival and skin tumorigenesis involving oncogenic Ras signaling. Proc. Natl. Acad. Sci. U.S.A., *99*: 207-212, 2002.

48. Wilson, A., and Radtke, F. Multiple functions of Notch signaling in self-renewing organs and cancer. FEBS Lett., *580*: 2860-2868, 2006.

49. Wilson-Rawls, J., Molkentin, J.D., Black, B.L., and Olson, E.N. Activated notch inhibits myogenic activity of the MADS-Box transcription factor myocyte enhancer factor 2C. Mol. Cell. Biol., *19*: 2853-2862, 1999.

50. Shin, H.M., Minter, L.M., Cho, O.H., Gottipati, S., Fauq, A.H., Golde, T.E., Sonenshein, G.E., and Osborne, B.A. Notch1 augments NF-kappaB activity by facilitating its nuclear retention. EMBO J., *25*: 129-138, 2006.

51. Gustafsson, M.V., Zheng, X., Pereira, T., Gradin, K., Jin, S., Lundkvist, J., Ruas, J.L., Poellinger, L., Lendahl, U., and Bondesson, M. Hypoxia requires notch signaling to maintain the undifferentiated cell state. Dev. Cell, *9*: 617-628, 2005.

52. Martinez-Arias, A., Zecchini, V., and Brennan, K. CSL-independent Notch signalling: a checkpoint in cell fate decisions during development? Curr. Opin. Genet. Dev., *12*: 524-533, 2002.

53. Shirayoshi, Y., Yuasa, Y., Suzuki, T., Sugaya, K., Kawase, E., Ikemura, T., and Nakatsuji, N. Proto-oncogene of int-3, a mouse Notch homologue, is expressed in endothelial cells during early embryogenesis. Genes Cells, *2*: 213-224, 1997.

54. Grabher, C., von Boehmer, H., and Look, A.T. Notch 1 activation in the molecular pathogenesis of T-cell acute lymphoblastic leukaemia. Nat. Rev. Cancer, *6*: 347-359, 2006.

55. Stylianou, S., Clarke, R.B., and Brennan, K. Aberrant activation of notch signaling in human breast cancer. Cancer Res., *66*: 1517-1525, 2006.

56. Lefort, K., and Dotto, G.P. Notch signaling in the integrated control of keratinocyte growth/differentiation and tumor suppression. Semin. Cancer Biol., *14*: 374-386, 2004.

57. Kiaris, H., Politi, K., Grimm, L.M., Szabolcs, M., Fisher, P., Efstratiadis, A., and Artavanis-Tsakonas, S. Modulation of notch signaling elicits signature tumors and inhibits hras1-induced oncogenesis in the mouse mammary epithelium. Am. J. Pathol., *165*: 695-705, 2004.

58. Mungamuri, S.K., Yang, X., Thor, A.D., and Somasundaram, K. Survival signaling by Notch1: mammalian target of rapamycin (mTOR)-dependent inhibition of p53. Cancer Res., *66*: 4715-4724, 2006.

59. Grimm, S.L., and Rosen, J.M. The role of C/EBPbeta in mammary gland development and breast cancer. J. Mammary Gland Biol. Neoplasia, *8*: 191-204, 2003.

60. Kowenz-Leutz, E., and Leutz, A. A C/EBP beta isoform recruits the SWI/SNF complex to activate myeloid genes. Mol. Cell, *4*: 735-743, 1999.

61. Zahnow, C.A. CCAAT/enhancer binding proteins in normal mammary development and breast cancer. Breast Cancer Res., *4*: 113-121, 2002.

62. Seagroves, T.N., Krnacik, S., Raught, B., Gay, J., Burgess-Beusse, B., Darlington, G.J., and Rosen, J.M. C/EBPbeta, but not C/EBPalpha, is essential for ductal morphogenesis, lobuloalveolar proliferation, and functional differentiation in the mouse mammary gland. Genes Dev., *12*: 1917-1928, 1998.

63. Jensen, L.E., and Whitehead, A.S. Regulation of serum amyloid A protein expression during the acute-phase response. Biochem. J., *334*: 489-503, 1998.

64. Fajas, L., Fruchart, J.C., and Auwerx, J. Transcriptional control of adipogenesis. Curr. Opin. Cell Biol., *10*: 165-173, 1998.

65. Raught, B., Liao, W.S., and Rosen, J.M. Developmentally and hormonally regulated CCAAT/enhancer-binding protein isoforms influence beta-casein gene expression. Mol. Endocrinol., *9*: 1223-1232, 1995.

66. Bundy, L.M., and Sealy, L. CCAAT/enhancer binding protein beta (C/EBPbeta)-2 transforms normal mammary epithelial cells and induces epithelial to mesenchymal transition in culture. Oncogene, *22*: 869-883, 2003.

67. Zahnow, C.A., Cardiff, R.D., Laucirica, R., Medina, D., and Rosen, J.M. A role for CCAAT/enhancer binding protein beta-liver-enriched inhibitory protein in mammary epithelial cell proliferation. Cancer Res., *61*: 261-269, 2001.

68. Nakajima, T., Kinoshita, S., Sasagawa, T., Sasaki, K., Naruto, M., Kishimoto, T., and Akira, S. Phosphorylation at threonine-235 by a ras-dependent mitogen-activated protein kinase cascade is essential for transcription factor NF-IL6. Proc. Natl. Acad. Sci. U.S.A., *90*: 2207-2211, 1993.

69. Lamb, J., Ramaswamy, S., Ford, H.L., Contreras, B., Martinez, R.V., Kittrell, F.S., Zahnow, C.A., Patterson, N., Golub, T.R., and Ewen, M.E. A mechanism of cyclin D1 action encoded in the patterns of gene expression in human cancer. Cell, *114*: 323-334, 2003.

70. Feinberg, A.P., Ohlsson, R., and Henikoff, S. The epigenetic progenitor origin of human cancer. Nat. Rev. Genet., *7*: 21-33, 2006.

71. Robertson, K.D. DNA methylation and human disease. Nat. Rev. Genet., *6*: 597-610, 2005.

72. Bird, A. DNA methylation patterns and epigenetic memory. Genes Dev., *16*: 6-21, 2002.

73. Buryanov, Y.I., and Shevchuk, T.V. DNA methyltransferases and structural-functional specificity of eukaryotic DNA modification. Biochemistry (Mosc.), *70*: 730-742, 2005.

74. Agoston, A.T., Argani, P., Yegnasubramanian, S., De Marzo, A.M., Ansari-Lari, M.A., Hicks, J.L., Davidson, N.E., and Nelson, W.G. Increased protein stability causes DNA methyltransferase 1 dysregulation in breast cancer. J. Biol. Chem., *280*: 18302-18310, 2005.

75. Girault, I., Tozlu, S., Lidereau, R., and Bieche, I. Expression analysis of DNA methyltransferases 1, 3A, and 3B in sporadic breast carcinomas. Clin. Cancer Res., *9*: 4415-4422, 2003.

76. Beaulieu, N., Morin, S., Chute, I.C., Robert, M.F., Nguyen, H., and MacLeod, A.R. An essential role for DNA methyltransferase DNMT3B in cancer cell survival. J. Biol. Chem., *277*: 28176-28181, 2002.

77. Jenuwein, T., and Allis, C.D. Translating the histone code. Science, *293*: 1074-1080, 2001.

78. Kouzarides, T. Chromatin modifications and their function. Cell, *128*: 693-705, 2007.

79. Berger, S.L. The complex language of chromatin regulation during transcription. Nature, *447*: 407-412, 2007.

80. Craig, J.M. Heterochromatin--many flavours, common themes. Bioessays, *27*: 17-28, 2005.

81. Bi, G., and Jiang, G. The molecular mechanism of HDAC inhibitors in anticancer effects. Cell. Mol. Immunol., *3*: 285-290, 2006.

82. Kouzarides, T. Histone acetylases and deacetylases in cell proliferation. Curr. Opin. Genet. Dev., *9*: 40-48, 1999.

83. National Institutes of Health. ClinicalTrials.gov. [cited June 2007]; Available from: http://clinicaltrials.gov

84. Graff, J.R., Gabrielson, E., Fujii, H., Baylin, S.B., and Herman, J.G. Methylation patterns of the E-cadherin 5' CpG island are unstable and reflect the dynamic, heterogeneous loss of E-cadherin expression during metastatic progression. J. Biol. Chem., *275*: 2727-2732, 2000.

85. Herman, J.G., Merlo, A., Mao, L., Lapidus, R.G., Issa, J.P., Davidson, N.E., Sidransky, D., and Baylin, S.B. Inactivation of the CDKN2/p16/MTS1 gene is frequently associated with aberrant DNA methylation in all common human cancers. Cancer Res., *55*: 4525-4530, 1995.

86. Kopelovich, L., Crowell, J.A., and Fay, J.R. The epigenome as a target for cancer chemoprevention. J. Natl. Cancer Inst., *95*: 1747-1757, 2003.

87. Szyf, M., Pakneshan, P., and Rabbani, S.A. DNA methylation and breast cancer. Biochem. Pharmacol., *68*: 1187-1197, 2004.

88. Longley, D.B., and Johnston, P.G. Molecular mechanisms of drug resistance. J. Pathol., *205*: 275-292, 2005.

89. Modok, S., Mellor, H.R., and Callaghan, R. Modulation of multidrug resistance efflux pump activity to overcome chemoresistance in cancer. Curr. Opin. Pharmacol., *6*: 350-354, 2006.

90. Leonard, G.D., Fojo, T., and Bates, S.E. The role of ABC transporters in clinical practice. Oncologist, *8*: 411-424, 2003.

91. Huang, Y., and Sadee, W. Membrane transporters and channels in chemoresistance and -sensitivity of tumor cells. Cancer Lett., *239*: 168-182, 2006.

92. Smalley, M.J., and Clarke, R.B. The mammary gland "side population": a putative stem/progenitor cell marker? J. Mammary Gland Biol. Neoplasia, *10*: 37-47, 2005.

93. Frank, N.Y., Pendse, S.S., Lapchak, P.H., Margaryan, A., Shlain, D., Doeing, C., Sayegh, M.H., and Frank, M.H. Regulation of progenitor cell fusion by ABCB5 P-glycoprotein, a novel human ATP-binding cassette transporter. J. Biol. Chem., *278*: 47156-47165, 2003.

94. Frank, N.Y., Margaryan, A., Huang, Y., Schatton, T., Waaga-Gasser, A.M., Gasser, M., Sayegh, M.H., Sadee, W., and Frank, M.H. ABCB5-mediated doxorubicin transport and chemoresistance in human malignant melanoma. Cancer Res., *65*: 4320-4333, 2005.

95. Huang, Y., Anderle, P., Bussey, K.J., Barbacioru, C., Shankavaram, U., Dai, Z., Reinhold, W.C., Papp, A., Weinstein, J.N., and Sadée, W. Membrane

transporters and channels: role of the transportome in cancer chemosensitivity and chemoresistance. Cancer Res., *64*: 4294-4301, 2004.

96. Houghton, P.J., Germain, G.S., Harwood, F.C., Schuetz, J.D., Stewart, C.F., Buchdunger, E., and Traxler, P. Imatinib mesylate is a potent inhibitor of the ABCG2 (BCRP) transporter and reverses resistance to topotecan and SN-38 in vitro. Cancer Res., *64*: 2333-2337, 2004.

97. Arlt, A., and Schafer, H. NFkappaB-dependent chemoresistance in solid tumors. Int. J. Clin. Pharmacol. Ther., *40*: 336-347, 2002.

98. Xiao, W. Advances in NF-kappaB signaling transduction and transcription. Cell. Mol. Immunol., *1*: 425-435, 2004.

99. Karin, M. Nuclear factor-kappaB in cancer development and progression. Nature, *441*: 431-436, 2006.

100. Baldwin, A.S., Jr. The NF-kappa B and I kappa B proteins: new discoveries and insights. Annu. Rev. Immunol., *14*: 649-683, 1996.

101. Perkins, N.D. Integrating cell-signalling pathways with NF-kappaB and IKK function. Nat. Rev. Mol. Cell. Biol., *8*: 49-62, 2007.

102. Ashburner, B.P., Westerheide, S.D., and Baldwin, A.S., Jr. The p65 (RelA) subunit of NF-kappaB interacts with the histone deacetylase (HDAC) corepressors HDAC1 and HDAC2 to negatively regulate gene expression. Mol. Cell. Biol., *21*: 7065-7077, 2001.

103. Graham, B., and Gibson, S.B. The two faces of NFkappaB in cell survival responses. Cell Cycle, *4*: 1342-1345, 2005.

104. Piva, R., Belardo, G., and Santoro, M.G. NF-kappaB: a stress-regulated switch for cell survival. Antioxid. Redox Signal., *8*: 478-486, 2006.

105. Aitken, A.E., Richardson, T.A., and Morgan, E.T. Regulation of drug-metabolizing enzymes and transporters in inflammation. Annu. Rev. Pharmacol. Toxicol., *46*: 123-149, 2006.

106. Gerbod-Giannone, M.C., Li, Y., Holleboom, A., Han, S., Hsu, L.C., Tabas, I., and Tall, A.R. TNFalpha induces ABCA1 through NF-kappaB in macrophages and in phagocytes ingesting apoptotic cells. Proc. Natl. Acad. Sci. U.S.A., *103*: 3112-3117, 2006.

107. Bentires-Alj, M., Barbu, V., Fillet, M., Chariot, A., Relic, B., Jacobs, N., Gielen, J., Merville, M.P., and Bours, V. NF-kappaB transcription factor induces drug resistance through MDR1 expression in cancer cells. Oncogene, *22*: 90-97, 2003.

108. Morel, V., and Schweisguth, F. Repression by suppressor of hairless and activation by Notch are required to define a single row of single-minded expressing cells in the Drosophila embryo. Genes Dev., *14*: 377-388, 2000.

109. Amiri, K.I., and Richmond, A. Role of nuclear factor-kappa B in melanoma. Cancer Metastasis Rev., *24*: 301-313, 2005.

110. Futscher, B.W., Oshiro, M.M., Wozniak, R.J., Holtan, N., Hanigan, C.L., Duan, H., and Domann, F.E. Role for DNA methylation in the control of cell type specific maspin expression. Nat. Genet., *31*: 175-179, 2002.

111. Gorisch, S.M., Wachsmuth, M., Toth, K.F., Lichter, P., and Rippe, K. Histone acetylation increases chromatin accessibility. J. Cell Sci., *118*: 5825-5834, 2005.

112. Jarriault, S., Brou, C., Logeat, F., Schroeter, E.H., Kopan, R., and Israel, A. Signalling downstream of activated mammalian Notch. Nature, *377*: 355-358, 1995.

113. Rao, P., and Kadesch, T. The intracellular form of notch blocks transforming growth factor beta-mediated growth arrest in Mv1Lu epithelial cells. Mol. Cell. Biol., *23*: 6694-6701, 2003.

114. Bray, S.J. Notch signalling: a simple pathway becomes complex. Nat. Rev. Mol. Cell. Biol., *7*: 678-689, 2006.

115. Ehebauer, M., Hayward, P., and Martinez-Arias, A. Notch signaling pathway. Sci. STKE, *2006*: cm7, 2006.

116. Baer, M., and Johnson, P.F. Generation of truncated C/EBPbeta isoforms by in vitro proteolysis. J. Biol. Chem., *275*: 26582-26590, 2000.

117. Balkwill, F., and Mantovani, A. Inflammation and cancer: back to Virchow? Lancet, *357*: 539-545, 2001.

118. Papin, S., Cazeneuve, C., Duquesnoy, P., Jeru, I., Sahali, D., and Amselem, S. The tumor necrosis factor alpha-dependent activation of the human mediterranean fever (MEFV) promoter is mediated by a synergistic interaction between C/EBP beta and NF kappaB p65. J. Biol. Chem., *278*: 48839-48847, 2003.

119. LeClair, K.P., Blanar, M.A., and Sharp, P.A. The p50 subunit of NF-kappa B associates with the NF-IL6 transcription factor. Proc. Natl. Acad. Sci. U.S.A., *89*: 8145-8149, 1992.

120. Estes, P., Mosher, J., and Crews, S.T. Drosophila single-minded represses gene transcription by activating the expression of repressive factors. Dev. Biol., *232*: 157-175, 2001.

121. Smith, I., and Chua, S. Medical treatment of early breast cancer. III: chemotherapy. BMJ, *332*: 161-162, 2006.

122. Longo, R., Torino, F., and Gasparini, G. Targeted therapy of breast cancer. Curr. Pharm. Des., *13*: 497-517, 2007.

123. Liu, S., Dontu, G., and Wicha, M.S. Mammary stem cells, self-renewal pathways, and carcinogenesis. Breast Cancer Res., *7*: 86-95, 2005.

124. Eaton, E.M., Hanlon, M., Bundy, L., and Sealy, L. Characterization of C/EBPbeta isoforms in normal versus neoplastic mammary epithelial cells. J. Cell. Physiol., *189*: 91-105, 2001.

125. Zahnow, C.A., Younes, P., Laucirica, R., and Rosen, J.M. Overexpression of C/EBPbeta-LIP, a naturally occurring, dominant-negative transcription factor, in human breast cancer. J. Natl. Cancer Inst., *89*: 1887-1891, 1997.

126. Milde-Langosch, K., Loning, T., and Bamberger, A.M. Expression of the CCAAT/enhancer-binding proteins C/EBPalpha, C/EBPbeta and C/EBPdelta in breast cancer: correlations with clinicopathologic parameters and cell-cycle regulatory proteins. Breast Cancer Res. Treat., *79*: 175-185, 2003.

127. Su, W.C., Chou, H.Y., Chang, C.J., Lee, Y.M., Chen, W.H., Huang, K.H., Lee, M.Y., and Lee, S.C. Differential activation of a C/EBP beta isoform by a novel

redox switch may confer the lipopolysaccharide-inducible expression of interleukin-6 gene. J. Biol. Chem., *278*: 51150-51158, 2003.

128. Eaton, E.M., and Sealy, L. Modification of CCAAT/enhancer-binding protein-beta by the small ubiquitin-like modifier (SUMO) family members, SUMO-2 and SUMO-3. J. Biol. Chem., *278*: 33416-33421, 2003.

129. Pomerance, M., Mockey, M., Young, J., Quillard, J., and Blondeau, J.P. Expression, hormonal regulation, and subcellular localization of CCAAT/enhancer-binding protein-beta in rat and human thyrocytes. Thyroid, *15*: 197-204, 2005.

130. Christian, M., Pohnke, Y., Kempf, R., Gellersen, B., and Brosens, J.J. Functional association of PR and CCAAT/enhancer-binding protein beta isoforms: promoter-dependent cooperation between PR-B and liver-enriched inhibitory protein, or liver-enriched activatory protein and PR-A in human endometrial stromal cells. Mol. Endocrinol., *16*: 141-154, 2002.

131. Seagroves, T.N., Lydon, J.P., Hovey, R.C., Vonderhaar, B.K., and Rosen, J.M. C/EBPbeta (CCAAT/enhancer binding protein) controls cell fate determination during mammary gland development. Mol. Endocrinol., *14*: 359-368, 2000.

132. Manning, C.B., Vallyathan, V., and Mossman, B.T. Diseases caused by asbestos: mechanisms of injury and disease development. Int. Immunopharmacol., *2*: 191-200, 2002.

133. Yan, P.S., Shi, H., Rahmatpanah, F., Hsiau, T.H., Hsiau, A.H., Leu, Y.W., Liu, J.C., and Huang, T.H. Differential distribution of DNA methylation within the RASSF1A CpG island in breast cancer. Cancer Res., *63*: 6178-6186, 2003.

134. Greger, V., Debus, N., Lohmann, D., Hopping, W., Passarge, E., and Horsthemke, B. Frequency and parental origin of hypermethylated RB1 alleles in retinoblastoma. Hum. Genet., *94*: 491-496, 1994.

135. Woo, I.S., Park, M.J., Choi, S.W., Kim, S.J., Lee, M.A., Kang, J.H., Hong, Y.S., and Lee, K.S. Loss of estrogen receptor-alpha expression is associated with hypermethylation near its ATG start codon in gastric cancer cell lines. Oncol. Rep., *11*: 617-622, 2004.

136. McGarvey, K.M., Fahrner, J.A., Greene, E., Martens, J., Jenuwein, T., and Baylin, S.B. Silenced tumor suppressor genes reactivated by DNA demethylation do not return to a fully euchromatic chromatin state. Cancer Res., *66*: 3541-3549, 2006.

137. Tlsty, T.D., Crawford, Y.G., Holst, C.R., Fordyce, C.A., Zhang, J., McDermott, K., Kozakiewicz, K., and Gauthier, M.L. Genetic and epigenetic changes in mammary epithelial cells may mimic early events in carcinogenesis. J. Mammary Gland Biol. Neoplasia, *9*: 263-274, 2004.

138. Issa, J.P., Vertino, P.M., Wu, J., Sazawal, S., Celano, P., Nelkin, B.D., Hamilton, S.R., and Baylin, S.B. Increased cytosine DNA-methyltransferase activity during colon cancer progression. J. Natl. Cancer Inst., *85*: 1235-1240, 1993.

VITA

Name: Tanya Gustafson

Address: Texas A&M College of Veterinary Medicine, VMA Bldg Rm 107, College Station, TX 77843-4458

Email Address: tlgustafson@cvm.tamu.edu

Education: B.A., Biochemistry, Tufts University, 2002
Ph.D., Toxicology, Texas A&M University, 2009

Honors:

Spring '03	Howard Hughes Medical Institute Predoctoral Fellowship in Biological Sciences
Spring '03	Dr. William F. Egan '43 Memorial Award
Spring '07	George T. Edds Award in Toxicology

Publications:

Gustafson, T., Laffin, B., Metz, R.P., Zahnow, C., and Porter, W. HRAS overexpression leads to repression of Single-minded 2 through Notch1 and C/EBPβ in breast cancer. Submitted to J. Biol. Chem.

Kwak, H.I., Gustafson, T., Metz, R.P., Laffin, B., Schedin, P., and Porter, W.W. Inhibition of breast cancer growth and invasion by single-minded 2s. Carcinogenesis, *28*: 259-266, 2007.

Metz, R.P., Kwak, H., Gustafson, T., Laffin, B., and Porter, W.W. Differential transcriptional regulation by mouse single-minded 2s. J. Biol. Chem., *281*: 10839-10848, 2006.

Lahiri, M., Gustafson, T.L., Majors, E.R., and Freudenreich, C.H. Expanded CAG repeats activate the DNA damage checkpoint pathway. Mol. Cell, *15*: 287-293, 2004.